Organochlorine pesticide and mercury bioaccumulation in shark species from the South African coastline

DJ Coetsee

orcid.org 0000-0003-4057-7704

Dissertation accepted in fulfilment of the requirements for the degree *Master of Science in Environmental Sciences* at the North-West University

Supervisor: Prof V Wepener

Co-supervisor: Prof NJ Smit

DECLARATION

ACKNOWLEDGEMENTS

I would like to acknowledge the following people and organisations and express sincere gratitude for assisting with the final completion of this project:

- My supervisors, Prof. Victor Wepener and Prof. Nico Smit, for their endless support, guidance, motivation, and the many hours of hard work they dedicated to me and this project. I greatly appreciate all you have done during my time as your student.
- I would like to acknowledge the Laboratory of Toxicology, Department of Environmental and Veterinary Sciences, Faculty of Veterinary Medicine, Hokkaido University, Japan for the training I received to extract and analyse the OCPs in the shark tissues. I would like to thank Dr. Yared Beyene and Prof. Yoshinori Ikenaka specifically who assisted in the training. Funding for the analyses was made available through the Africa-Japan Collaborative Research (AJ-CORE) project entitled: “Field and Mechanism-Based Toxicity Research on Pesticides in Africa; PIs Maymi Ishizuka and Victor Wepener) jointly funded by the South African National Research Foundation (Grant number UID: 132805) and the Japanese Science Programme (JST AJ-CORE, Grant/Award Number: PJ36210002).
- To the KwaZulu-Natal Sharks Board and South African Sharks Conservancy for the samples used in the study.
- To Danielle Fourie for the assistance with the lab work required for the selenium chapter of this study.
- To Dr Hannes Erasmus for the assistance with of the lab work required for a large portion of the mercury chapter of this study.
- To Dr Suranie Horn for the assistance and guided troubleshooting in the laboratory for effective extractions methods for OCPs.
- To my friends for providing all the support needed for the journey of this study.
- My family for all the love and support during this journey.

SUMMARY

Organochlorine pesticide (OCP), selenium (Se) and mercury (Hg) contamination of South Africa's marine waters potentially has deleterious effects on sharks, rays, and skates. These contaminants are released into the marine environment through numerous diffuse sources. Elasmobranchs are long-lived predators that occupy high trophic positions and are therefore prone to bioaccumulating these pollutants via food webs. However, there is still minimal research done on the levels of OCPs, Hg and Se in elasmobranchs around the coast of South Africa.

The research hypotheses that were tested in this project were: 1) the OCP, Se and Hg levels in elasmobranch species along the South African coastline are due to factors such as sex, size, migratory habits, trophic position (intrinsic traits) and geographical location (extrinsic trait); 2) that the OCP, Hg and levels in elasmobranch tissues pose a health risk to humans who consume them; 3) there is an antagonistic relationship between Se and Hg concentrations in elasmobranch muscle tissue, thereby protecting elasmobranchs from Hg toxicity.

Muscle tissue from 22 elasmobranch species were prepared for OCP and element (Se and Hg) analyses. The OCPs concentrations were analysed with a Shimadzu triple quadrupole GC-MS-TQ8050 NX following a QuECHERS extraction method. The Hg concentrations were determined using a flow injection mercury system (PerkinElmer FIMS 400) and the Se element concentrations were determined using an Agilent inductively coupled plasma mass spectrometry (ICP-MS) techniques.

There was a statistically significant ($p<0.05$) correlations between levels of OCPs, especially DDxs and trace element Hg, and the trophic positions within the elasmobranchs from the coast of South Africa. However, Se was not significantly correlated with the trophic position of the species sampled. There were limited correlations between OCPs profiles in elasmobranchs and geographical regions, i.e., the east and south coasts. There were significant DDxs correlations with female elasmobranchs and increasing trophic position. There were similar significant correlations of Hg with trophic positions in all of the elasmobranchs analysed in the current study. Based on the human health risks assessment there were potential health risks associated with the consumption of elasmobranch contaminated with OCPs (notably p,p'-DDE) and Hg. Consumption of elasmobranch tissue contaminated with p,p'-DDE displayed unacceptable carcinogenic adverse health effects for *M. mustelus* (smoothhound shark), *N. cepedianus* (broadnose sevengill shark), and *C. carcharias* (white shark). All east coast elasmobranchs posed a possible long-term non-carcinogenic health risk based on the consumption of Hg-contaminated muscle tissue. Health risks posed by both DDxs, and Hg are

of special concern in the houndsharks (*M. mustelus*) and dogsharks as these species are targeted for commercial harvesting purposes. The health value benefit of Se (HVB_{Se}) was calculated to determine whether Se levels in elasmobranchs were high enough to counteract the toxic effects of Hg. With exception of *N. cepedianus* (broadnose sevengill shark), all elasmobranchs from the south coast had positive HVB_{Se} values. Species from the east coast [*G. cuvier* (tiger shark), *S. lewini* (scalloped hammerhead shark), *C. leucas* (bull shark), and *C. taurus* (ragged tooth shark)], had negative HVB_{Se} values that indicate the potential toxicity of Hg to these species and the humans that consume them. The data obtained support the first two hypotheses, with only the hypothesis that all elasmobranchs are protected due to the high Se content not being supported for four of the 22 species studied. This study makes an important contribution to providing much needed baseline information on OCPs, Hg and Se in the studied species.

Keywords: bioaccumulation, DDT, mercury, selenium, toxicity, elasmobranchs, South Africa

Table of Contents

LIST OF TABLES

LIST OF FIGURES

0.043, p = 0.424) (B), Female elasmobranchs (r^2 = 0.546, p = 0.003) (C). Number with corresponding species are presented in the footnote of Table 2.4.

Figure 2.16: Correlation of the log of the sum of DDxs and Chlors concentrations against the trophic position (TP) of male and female elasmobranch species collected from the east- and south coast of South Africa (r^2 = 0.203, p = 0.036) (A), (r^2 = 0.036, p = 0.396) (B); Male elasmobranchs (r^2 = 0.056, p = 0.360) (C), (r^2 = 0.109, p = 0.195) (D); Female elasmobranchs (r^2 – 0.551, p – 0.002) (E), (r^2 = 0.140, p = 0.207) (F). Number with corresponding species are presented in the footnote of Table 2.4.

Figure 2.17: Principal component analysis (PCA) biplot graph using the mean organochlorine pesticide concentrations from the muscle samples of the elasmobranch species. Fist two axes explained 82.24% of the variation in OCP levels in elasmobranchs from the east and south coasts of South Africa.

Figure 3.1: Mercury and selenium concentrations (mean ± standard error expressed in mg/kg dry weight) in muscle tissue of different elasmobranch species collected from the east and south coast of South Africa.

Figure 3.2: Percentage contribution of mercury and selenium concentrations analysed in sampled shark species.

Figure 3.3: Percentage contribution of mercury and selenium concentrations analysed in sampled ray and skate species.

Figure 3.4: Percentage contribution of mercury and selenium concentrations analysed in sampled male shark species.

Figure 3.5: Percentage contribution of mercury and selenium concentrations analysed in sampled male ray and skate species.

Figure 3.6: Percentage contribution of mercury and selenium concentrations analysed in sampled female shark species.

Figure 3.7: Percentage contribution of mercury and selenium concentrations analysed in sampled female ray and skate species.

Figure 3.8: Correlation of the log of the sum of mercury and selenium concentrations against the trophic position of male and female elasmobranch collected from the east- and south coast of South Africa (r^2 = 0.633, p = 0.002) (A), (r^2 = 0.205, p = 0.360) (B); Male elasmobranchs (r^2 = 0.551, p = 0.022) (C), (r^2 = 0.510, p = 0.036) (D); Female elasmobranchs (r^2 = 0.683, p = 0.007) (E), (r^2 = 0.308, p = 0.283) (F). Number with corresponding species are presented in the footnote of Table 3.1.

Figure 3.9: Principal component analysis (PCA) biplot graph based on the mean mercury and selenium concentrations in muscle tissue of the elasmobranch species. First two axes explained 100% of the variation in elasmobranchs from the east and south coasts of South Africa.

Chapter 1: General Introduction

1.1 Background information

Organochlorine pesticides (OCPs) have been widely used worldwide for crop protection and disease vector control; a practice well-documented in studies such as Kumar *et al.* (2008). However, it is crucial to recognise that these pesticides come with a range of adverse health effects, leading to many being either banned or restricted for use, primarily focusing on disease vector control (Quinn *et al.,* 2011).

Organic Chemicals of Environmental Concern (OCEC) can be classified into two categories. First, natural organic chemicals are present in the environment and used for various human activities like fossil fuels. Recent studies, such as those conducted by Farrington & Takada (2014), have shown an alarming increase in the introduction of these compounds into marine environments over the past few centuries. Secondly, the presence of organic chemicals that do not occur naturally but need to be synthesised for use, like Dichlorodiphenyltrichloroethane (DDT), which raise environmental concerns upon release. These synthesised chemicals, often referred to as xenobiotic chemicals, indicate a changing chemistry in marine ecosystems (Farrington & Takada, 2014). It is essential to note that these xenobiotics and contaminants degrade slowly due to the covalent bonds between their molecules (Wang *et al.,* 2016). Legacy contaminants such as polychlorinated biphenyls (PCBs) and DDTs are recognised for their persistence in the environment and ease of bioaccumulation within organisms. These OCPs can also be classified as persistent organic pollutants (POPs) and contribute to water and soil contamination.

These contaminants compromise the health of organisms, particularly those found at higher trophic levels (Boldrocchi *et al.,* 2019). Organochlorine pesticides are organic compounds with highly toxic, refractory, and easily residual characteristics (Han & Sapozhnikova, 2020). Organochlorine pesticides display characteristics such as resistance to degradation, e.g., metabolic activity, ultraviolet radiation, or extreme temperatures (Quinn *et al.,* 2011). Research by Dallaire *et al.* (2013) highlighted that when these contaminants are introduced into the environment due to improper disposal or use, they persist within the environment and its associated organisms. These lipophilic compounds are part of the larger group of hydrocarbons widely used in various industries and agricultural applications worldwide (Gerber *et al.,* 2016). Furthermore, these compounds can be transported over considerable distances through wind, water, or soil (Buccini, 2003; Fitzgerald & Wikoff, 2014).

In-depth research on the persistence of organochlorine pesticides (OCPs) in the environment has revealed that these contaminants are absorbed by sediments or soils to varying degrees.

They can form stable bonds with these sediment and soil particles, significantly extending their persistence in the environment (Dorsey, 2005). While some OCPs exhibit stability in both salt and freshwater, they are not as stable as they are in sediment and soil. They are also resistant to photodegradation, posing a considerable risk to aquatic environments such as lakes and estuaries (Kartalović *et al.,* 2016; Zhou *et al.,* 2006). This can result in OCPs being magnified up the food web, a point highlighted in earlier studies by Dallaire *et al.* (2013), Gerber *et al.* (2016), Boldrocchi *et al.* (2019), and Li & Liu (2018). These OCPs are insoluble in water due to their persistent nature, but highly soluble in fat tissues due to their lipophilic properties, making them prone to easy bioaccumulation within organisms (Gerber *et al.,* 2016).

Although organochlorine pesticide use in South Africa was banned in 2002 under the regulations of the Stockholm Convention (Bouwman, 2004), DDT is still used in South Africa's efforts to combat malaria. The primary method of using DDT for malaria control is indoor residual spraying (IRS) (Blumberg *et al.,* 2014). Recently, Buah-Kowfie *et al.* (2018) and Erasmus *et al*. (2020) found that OCPs enter marine environments through runoff into the ocean and aerial depositions as the result of land-based activities. The focus on sharks, rays and skates, to a lesser extent, stems from their status as apex predators, which tend to accumulate OCPs through biomagnification. Factors such as diet and feeding regions are also crucial when considering potential exposure to these chemicals, especially given the higher prevalence of DDT along the eastern coast of South Africa.

1.2 Organochlorine pesticides under investigation

1.2.1 Dichlorodiphenyltrichloroethane (DDT)

Dichlorodiphenyltrichloroethane is a chemical compound consisting of two molecules: p,p'-dichlorodiphenyltrichloroethane (p,p'-DDT) and o,p'-dichlorodiphenyltrichloroethane (o,p'-DDT). These two isomers are differentiated by the positions of the substituted chlorine atoms on the carbon rings of the diphenylethane rings (ATSDR, 2019). DDT can degrade into two forms: dichlorodiphenyldichloroethane (DDD) and dichlorodiphenyldichloroethylene (DDE) (ATSDR, 2019). Both DDT and DDD were used as insecticides in agriculture, with DDD being used to a lesser extent (ATSDR, 2019). Dehydrochlorination is the process by which DDT is transformed into DDE, which is produced commercially but is often found in higher concentrations in the environment than DDT (ATSDR, 2019). Reductive dichlorination is also a process whereby DDT is degraded into DDD (Kitamura *et al.,* 2002).

The DDTs are known for their slow breakdown and excretion, which means that DDD and DDE can persist in the body for decades after initial exposure (ATSDR, 2019). Research by Morgan and Roan (1971) ranked these compounds by biological half-lives from longest to shortest as DDE > DDT > DDD. These chemicals can remain within the body for many years, primarily stored in fat deposits (Morgan & Roan, 1971). Research by Binelli & Provini (2003) suggested a half-life of about eight months for p,p'-DDT in fish, while the half-life of p,p'-DDD and p,p'-DDE is estimated to be around seven years. This supports the idea that DDD and DDE can persist within an organism for extended periods and can be indicators of recent exposure to DDT (Buah-Kwofie *et al.,* 2018).

Organochlorine pesticides, particularly DDT, have demonstrated ecological toxic effects, including disruption of functions within the endocrine systems of the biota. DDT is recognised as one of the 12 persistent organic pollutants (POPs) regulated by the Stockholm Convention. Due to its persistence, long-range transport from the source of origin, and potential environmental and human health impacts, the use of DDT is restricted until an effective alternative control method is developed.

1.2.2 Hexachlorobenzene (HCB)

Hexachlorobenzene (HCB), used as a fungicide in industry and agriculture, was banned in South Africa in 1983 (Bouwman, 2003). Hexachlorobenzene has been found in treated and background soils, sediments, and marine systems (Taylor & Wilson, 2002). Although almost insoluble in water, HCB is highly soluble in fats, oils, and organic solvents (Taylor & Wilson, 2002). This highly persistent environmental pollutant has been shown to bioaccumulate, even being found in human breast milk (Taylor & Wilson, 2002). While large-scale projects in the USA have revealed biomagnification in aquatic fish species, more research is needed to

confirm this in other ecosystems (Taylor & Wilson, 2002). The chemical stability of hexachlorobenzene makes it highly resistant to biodegradation (Taylor & Wilson, 2002).

Hexachlorobenzene is released into the environment as a by-product during the manufacturing of other chemicals, solvents, and pesticides. Improper use and disposal of HCB from coal, cement, biomass, and medical waste combustion processes also contribute to its introduction into the environment despite its official ban (Taylor & Wilson, 2002).

1.2.3 Chlordane (CHL)

Chlordane (CHL) is present in various isomers, including cis-, trans-chlordane, and cis-, trans-nonachlor. It was used in termite control applications and as an agro-insecticide (Bouwman, 2004). Although less persistent in the environment than DDT, some traces of chlordane have been found in aquatic ecosystems around Kruger National Park, where intensive agricultural activities such as citrus fruits still occur, suggesting continued use despite its ban (Gerber *et al.,* 2021). Research has shown that chlordane compounds tend to accumulate in the liver and kidneys at high concentrations initially and then spread to fat deposits, where they can persist for extended periods (ATSDR, 2018). The strong lipophilicity and hydrophobicity of the compound suggest that elimination occurs through passive diffusion (ATSDR, 2018). Excretion can occur through bile, urine, and lactation (ATSDR, 2018). Muir *et al.* (1988) discovered chlordane compounds and heptachlor epoxide in various arctic species, indicating long-range transport and contamination of diverse ecosystems not yet diagnosed (Muir *et al.,* 1988).

1.2.4 Hexachlorocyclohexane (HCH)

Hexachlorocyclohexane (HCH) encompasses four commercially relevant isomers, namely alpha, beta, delta, and gamma, with their distinction hinging on the positioning of chlorine atoms on the cyclohexane ring carbon atoms (Luek *et al.,* 2017). Notably, γ-HCH, also known as lindane, can transform into α-HCH (Luek *et al.,* 2017). Lindane serves as an insecticide for diverse applications, including on fruits, vegetables, forest crops, and animal premises (Przybyla *et al.*, 2023). Studies on zebrafish have demonstrated the accumulation of α-HCH and β-HCH within organisms, with β-HCH exhibiting the highest bioaccumulation among isomers (Przybyla *et al.*, 2023). Biodegradation has emerged as the most effective process for eliminating γ-HCH from aquatic systems (Przybyla *et al.*, 2023).

HCH isomers appear as white solids capable of volatilising into the gas or particulate phase. When released into the environment, HCH can volatilise from, or partition to, the soil, potentially leaching into the groundwater. The general population may experience low-level exposure to HCH by inhaling contaminated ambient air, ingesting contaminated water, or

coming into contact with polluted soils (Przybyla *et al.*, 2023). The toxicological profile outlined by Przybyla *et al.* (2023) for HCH isomers revealed that oral exposure to α-HCH leads to liver toxicity as a sensitive effect and endpoint. When animals are orally exposed to β-HCH, it causes liver toxicity and adverse neurological effects. Similarly, the presumed hepatic and neurological effects identified in animals is also a potential health concern for humans (Przybyla *et al.*, 2023). γ-HCH, in animals, shows sensitivity to developmental toxicity and immune system effects, with hepatic and neurological effects presumed to be health concerns for humans (Przybyla *et al.*, 2023).

1.2.5 Heptachlor (HPT)

Heptachlor (HPT) is a product of chlordane breakdown and is also part of the components used in chlordane pesticides (ATSDR, 2007). Heptachlor was used as an insecticide to kill insects, especially termites, in homes, buildings, and food crops (ATSDR, 2007). Because of the large-scale use of heptachlor, it has been found in areas near the origin of exposure, such as water bodies and nearby soil and sediment areas. Heptachlor and heptachlor epoxide have been documented to adhere to soil very strongly and slowly evaporate into the air over an extended period (ATSDR, 2007). Heptachlor is degraded to heptachlor epoxide in the bodies of organisms through metabolism (ATSDR, 2007).

Research completed by Lyman *et al.* (1990) revealed that heptachlor separates quickly from surface water into the atmosphere and that volatilisation plays a significant role. Humidity has also been shown to increase the persistence of these contaminants in the environment (ATSDR, 2007). Because of the persistent nature of heptachlor epoxide within the bodies of organisms, it has been documented to bio-magnify at higher trophic levels in aquatic and terrestrial organisms (ATSDR, 2007). Although heptachlor is still being used in South Africa, although in smaller quantities, the study by Buah-Kwofie *et al.* (2018) still found the compound and its metabolite present within fish tissue.

1.2.6 Cyclodienes (Drins)

According to Akan *et al.* (2013), endrin stands out as the only chemical on the United Nations Environmental Programme (UNEP) list that does not significantly biomagnify. Although several POPs on the UNEP list, such as aldrin, dieldrin, and endrin, are acutely toxic, most others are listed primarily due to their biomagnification potential, with low acute toxicity (Norstrom, 2002). Once used worldwide as a DDT substitute, aldrin is highly toxic and despite its ban as an insecticide in South Africa in 1992, various uses continued until a complete prohibition in 2013 (National Gazette of South Africa, Notice 1116 of 3123). Aldrin undergoes conversion to dieldrin in living systems through the process of epoxidation (Norstrom, 2002; Haper *et al.*, 2022), and dieldrin exhibits resistance to bacterial and chemical breakdown

outside living systems (Afful *et al.,* 2010). Additionally, there is a stereoisomer of dieldrin called endrin, known for its stationary nature, soil particle absorption, and hydrophobic properties, widely used as an avicide, rodenticide, and insecticide (Haper *et al.*, 2022).

Both aldrin and dieldrin are semi-volatile and biodegrade slowly, with low soil mobility indicated by large soil adsorption coefficients, suggesting a propensity to partition to sediments and suspended solids in the water column (Haper *et al.*, 2022). Low levels of aldrin and dieldrin have been detected in various environmental compartments, including soil, sediments, surface water, groundwater, public water, crops, dairy products, and meat (Haper *et al.*, 2022).

High-level exposure to aldrin or dieldrin in humans can result in central nervous system excitation, convulsions, and death, especially in acute cases (Haper *et al.*, 2022). Long-term occupational exposure has been linked to adverse effects on the central nervous system, although liver and kidney toxicity and haemolytic anaemia, reported in some cases of oral exposure, were not consistently observed in more extensive occupational studies. Animal studies indicate that hepatic, neurological, and reproductive endpoints, body weight, and developmental endpoints are sensitive targets of aldrin and/or dieldrin toxicity (Haper *et al.*, 2022).

The primary route of exposure to endrin is likely through the ingestion of imported foods contaminated with the compounds. However, localised risks may also arise from exposure near waste disposal sites or groundwater contaminated with endrin (Haper *et al.*, 2022). Case reports of endrin toxicity in humans suggest steady absorption following ingestion, with evidence from occupational settings indicating potential dermal exposure. Limited animal data also suggest rapid metabolism and excretion through urine and faeces, but low concentrations can persist in adipose tissue after high exposure (Haper *et al.*, 2022).

Studies on the noncancer toxicity of endrin are based on oral studies in animals, revealing that the most sensitive effects in laboratory animals involve neurological effects (e.g., altered activity, convulsions) and hepatic toxicity (Haper *et al.*, 2022). Other noncancer toxicity effects are typically observed at doses associated with lethality, including diffuse organ damage (lungs, heart, kidney, endocrine glands) and body weight effects. Apart from altered locomotor activity in the offspring, developmental effects were observed only at doses that caused significant maternal mortality and/or toxicity (Haper *et al.*, 2022).

1.3 Mercury and Selenium

Mercury (Hg) is known to occur in the natural environment and increases in levels due to input from anthropogenic sources (Lim *et al.,* 2022; Chen *et al.,* 2022). Many industries are responsible for dumping this contaminant and other related contaminants into the aquatic environment (Chen *et al.,* 2022; Lim *et al.,* 2022). Long-range deposition of these contaminants has been recorded both within the ocean surface water and on the land surface (AMAP/UNEP, 2019). The aerial deposition pathway opens up the potential for Hg input to both the ocean surface and deep ocean water (Amezcua *et al.,* 2022). This is supported by the findings of Barone et al. (2021), who found that, generally, benthic dwelling organisms are exposed to higher concentrations of Hg, which accumulates in sediment. This further raises the question of the importance of Hg sedimentation, or feeding patterns in fish, in Hg accumulation (Barone *et al.,* 2021).

Furthermore, due to its high mobility within the marine ecosystem, Hg efficiently undergoes biomagnification as it moves up the food chain, ultimately accumulating in substantial quantities within apex predators (Barone *et al.,* 2021). When introduced into an aquatic environment, Hg is transformed into methylmercury (MeHg) through various species of bacteria (Dallaire *et al.,* 2013; Jeremiason *et al.,* 2006). Methylmercury is subsequently adsorbed and absorbed by aquatic organisms such as phytoplankton (Lee & Fisher, 2016; Lim *et al*., 2022; Chen *et al.,* 2022). Methylmercury is known to be highly lipophilic and known to biomagnify up the food web ending up in predatory fish (Quinn *et al.,* 2011; Watras & Bloom, 1992). Mercury is also considered one of the main toxic substances of concern according to the priorities of the Agency for Toxic Substances and Disease Registry (ATSDR, 2015). Methylmercury also shows very strong characteristics of a dangerous neurotoxin and can also affects pregnant women due to the ability of the compound to cross the placental barrier (Caserta *et al.,* 2013; Rice *et al.,* 2014).

Research on sharks have consistently shown to have Hg levels far above the maximum safe consumption limit set for humans, and this can be attributed to the slow maturation, growth rate, trophic position, and reproductive abilities (Tiktak *et al.,* 2020; Adams, 2004; Branco *et al.,* 2004). To date, relatively limited research studies have been conducted on the possible antagonistic relationship that selenium (Se) may play with the powerful neurotoxin Hg (Raymond & Ralston, 2009; Ralston *et al.,* 2008; Takahashi *et al.,* 2021). However, studies by Ralston *et al.* (2016) and Rayman (2000) showed that there can be health benefits associated with the consumption of fish with high Se levels. Storelli *et al.* (2022), however, cautioned against thinking that, although Se can have a potential health, that it is safe to consume fish with high level.

Selenium is regarded as an essential trace element for almost all biological organisms, especially in the form of the amino acid selenocysteine (Gelslichter & Walker, 2010). Selenium also undergoes homeostatic regulation within organisms (Ralston *et al., 2016*), and as such, variability of Se concentration within organisms and between species differ less than Hg concentrations (Barone *et al.,* 2021). However, which fish species show the highest concentrations of Se according to their ecological traits is still unknown (Ulusoy *et al.,* 2018; Olmedo *et al.,* 2013).

Understanding the relationship between environmental geochemistry and health is crucial for selenium due to its derivation from natural and anthropogenic sources, with rocks as the primary origin in terrestrial systems (Fordyce, 2012). Fordyce (2012) highlighted that the natural presence of selenium is predominantly found in the earth's crust (0.05 mg/kg), volcanic rocks (0.35 mg/kg), sedimentary rocks such as limestone (0.03-0.08 mg/kg) and sandstone (<0.05 mg/kg), as well as in soils worldwide (0.4 mg/kg). Oceans play a significant role as an environmental reservoir for Se as well as being a major flux for selenium cycling through the environment, second only to anthropogenic activities, which release 76000 to 88000 tonnes of selenium per year globally (Fordyce, 2012).

Simply estimating Se intake alone may not adequately assess the health risks or benefits of Se if its interaction with Hg is not carefully considered (Cabañero *et al.,* 2007). Numerous studies have shown that Se moderates Hg uptake and mitigates its toxicity in various animal species, including fish and humans. The exact mechanisms involved are not fully defined, but many of them center around the formation of Hg-Se compounds, which are typically poorly bioavailable and aid in the removal and excretion of MeHg through demethylation processes (Zhang *et al.,* 2014; Khan & Wang, 2010). Therefore, when investigating health issues related to Hg exposure, primarily through fish consumption, a primary focus should be understanding the interactions between these two elements (Ralston *et al.,* 2016). Generally, an excess of Se compared to Hg serves as a potential protective barrier against the adverse effects of Hg. Specifically, a molar Se:Hg ratio that exceeds one is associated with the protective effect of Se against Hg toxicity (Peterson *et al.,* 2009).

1.4 Elasmobranchs as target species

Elasmobranchs, belonging to the class Chondrichthyans, represent one of the most ancient and ecologically diverse lineages in the animal kingdom, with a history spanning over 420 million years. These cartilaginous fish are distributed throughout all the world's oceans and occupy key positions at the upper levels of aquatic food webs. Many elasmobranch species play an important role in the regulation of coastal and oceanic ecosystems, as highlighted by Ebert *et al*. (2013) and Dulvy *et al*. (2014).

The South African coastline is known to have a diverse range of fauna and flora, with over 200 species of chondrichthyans inhabiting its waters (Ebert & van Hees, 2015). However, much of the attention from scientific studies has been directed toward larger shark species, such as the great white shark, leaving many other diverse shark species relatively understudied. Of the 185 species of cartilaginous fish in South African waters, 47 are classified as threatened. To address this, the government launched the South African Shark Biodiversity Management Plan, designed to enhance our understanding of these species, and implement protective measures (South Africa, 2015). A significant objective of this plan is to investigate the specific impacts of pollution on sharks through comprehensive research and monitoring programs.

Many pollutants have the capacity to accumulate and magnify within ecosystems, disproportionately affecting apex predators with concentrations of pollutants higher than those found in the environment. Extensive research has been conducted in teleost fish, molluscs, and marine mammals, as evidenced by studies by Blocksom *et al*. (2010), Sharma *et al*. (2014), Jepson *et al*. (2016), Barone *et al*. (2018). These studies illustrated the adverse health effects of such pollutants, including suppressed reproductive development, immunosuppression, endocrine disruption, and oxidative stress (Letcher *et al*., 2010).

However, elasmobranchs have received relatively less attention in pollutant research compared to other vertebrate groups, which is particularly concerning given their high trophic position in marine food webs and the ongoing population declines they are experiencing (Dulvy *et al*., 2014). Elasmobranchs share biological and ecological traits with large-bodied mammals, including late maturation, slow reproductive rates, and the production of relatively few offspring (García *et al*., 2007; Dulvy *et al*., 2014). This combination of traits and their prominent position in marine food webs place elasmobranchs at a higher risk of exposure to pollutants and associated adverse effects.

Sharks, being apex predators at the top of various aquatic food webs, are highly susceptible to bioaccumulation of organic compounds due to biomagnification processes. Their longevity,

low metabolic rates, and large livers rich in lipids (Boldrocchi *et al*., 2019) further increase their vulnerability to contaminants. In addition to this, various other factors, such as commercial fishing and the shark fin trade (Worm *et al*., 2013), climate change (Rosa *et al*., 2014), and habitat degradation (Knip *et al.*, 2010), contribute to the global decline of shark populations. As a result, sharks can experience a significant bioaccumulation of pollutants in their tissues throughout their lifetime. Currently, there is no established baseline for the contaminant load present within elasmobranchs or the potential physiological effects of these pollutants (Boldrocchi *et al*., 2019). Amin & Hashem (2012) have suggested that exposure to these pollutants may lead to adverse effects due to increased tissue burden resulting from acute and chronic exposure.

Existing research suggests that the dietary habits of these predators play a substantial role in the accumulation of OCPs, as emphasised by Beaudry *et al*. (2015). Notably, Beaudry *et al*. (2015) revealed that the age of these organisms was not the most critical indicator of OCP accumulation. Instead, various factors exert more significant influences, including the trophic level occupied by elasmobranchs, growth rate, the aquatic environment, and the food web within their habitat. Other factors, such as feeding rates, metabolic capacity, and ontogenetic diet shifts, should also be considered (Cortés, 2000).

Skates and rays, belonging to the order Rajiformes and Myliobatidae respectively, are demersal elasmobranchs found in a wide range of shelf seas and deep-water habitats (Nicolaus *et al*., 2017). They occupy various trophic positions within their order, with many species functioning as benthic predators, while others have a more piscivorous diet, even preying on other elasmobranchs. Skates and rays are of significant commercial importance in many parts of the world, including Europe, even though some species may have a low market value. Their demersal habitat and potentially long lifespans make them susceptible to bioaccumulation of different contaminants, including substances such as mercury and persistent organic contaminants (Nicolaus *et al*., 2016; Lyons & Adams, 2017).

Several studies have investigated the presence of contaminants in skates and rays from the inner continental shelf of European seas (Dixon & Jones, 1994; De Gieter et al., 2002), and other regions such as the USA (Weijs *et al.,* 2015) and Australia (Cagnazzi *et al.,* 2019). However, data on skates and rays living in deeper waters are limited (Mormede & Davies, 2001), despite some evidence suggesting that mercury concentrations in marine fish can increase with greater water depth (Choy *et al*., 2009).

1.5 Elasmobranch species included in this study

A summary of the biological traits and characteristics of the preferred prey of the species selected for this study are presented in Tables 1.1 and 1.2, respectively. The diverse world of sharks, especially within the order Carcharhiniformes, encompasses a wide array of species with distinct characteristics, foraging behaviours, and reproductive strategies, with examples of the species researched in the current study discussed below (Last *et al.,* 2016; Ebert *et al.,* 2021; Froese & Pauly, 2022).

- **Extended foraging range:**
  - **Tiger shark (*Galeocerdo cuvier*):** Are often known for their extensive and often unpredictable movements. They cover long distances and inhabit various habitats, ranging from turbid areas with high freshwater runoff, estuaries, and harbours to clear-water coral atolls and lagoons. Their irregular movements may be a tactic to surprise local young and inexperienced prey populations.
  - **Scalloped hammerhead shark (*Sphyrna lewini*):** Exhibits seasonally migratory behaviour, forming large schools primarily composed of females around seamounts and offshore islands during the day. They disperse alone or in small groups to feed at night. Females tend to have more localised dispersion, whereas males undertake longer-distance dispersions.
  - **Spinner shark (*Carcharhinus brevipinna*):** These are highly migratory, often moving inshore during spring and summer for feeding and breeding. They then head south and into deeper waters in winter. They are known for their active schooling behaviour, primarily feeding on fish, especially migrating mackerel.
- **Largest and longest lifespan:**
  - **White shark (*Carcharodon carcharias*)**: Among the largest sharks, they can reach impressive sizes, with mature females reaching lengths of 600-640 cm. They are also known for their longevity, with a maximum age of 30-73 years. *Carcharodon carcharias* have a wide-ranging habitat, tolerating temperatures from 5 - 25°C.
  - **Bull shark (*Carcharhinus leucas*):** These are known for their ability to inhabit freshwater and are among the largest requiem sharks. They can reach lengths of up to 366 cm. *Carcharhinus leucas* has a wide distribution, from coastal waters to freshwater lakes and rivers. Their maximum age is estimated to be up to 50 years.
  - **Dusky shark (*Carcharhinus obscurus*):** Large sharks with a maximum length of 420 cm. They are highly migratory, moving into higher latitudes during warmer months and retreating as the waters cool. Dusky sharks have a slow reproduction rate (2–3 years), making them vulnerable to exploitation.

- **Reproductive strategies:**
  - **Ragged tooth shark (*Carcharias taurus*):** This species has one of the lowest reproductive rates among chondrichthyans. It adopts an oophagus reproductive strategy, in which the developing offspring feed in utero on eggs the mother produces during the 9–12 month gestation. Additionally, intrauterine cannibalism occurs, where the embryos consume smaller embryos, including their siblings and half-siblings. This process continues until only one pup survives in each uterus. Males reach maturity at 6-7 years, females at 9-10 years. Although the maximum observed age in the wild is 15-17 years, *Carcharias taurus* has been known to live for more than 30 years in aquariums.
  - **Broadnose sevengill shark (*Notorynchus cepedianus*):** Viviparous with a one-year gestation followed by a year of recovery. *Notorynchus cepedianus* gives birth to 67–104 pups in shallow nursery bays each spring. Males mature at 4-5 years, females at 11-21 years, with a longevity of 30-50 years.
  - **Spinner shark (*Carcharhinus brevipinna*):** Viviparous with an 11-15 month gestation. *Carcharhinus brevipinna* has a 2-year reproductive cycle. They are fast-growing, with females reaching maturity at 8–10 years. The maximum age is 17–19 years.

Rays and skate form part of the taxonomic orders Rajiformes, Myliobatiformes, and Mobulidae. Within these taxonomic classifications there are a variety of species with distinct characteristics, foraging behaviours, and reproductive strategies, with examples for the current study mentioned below: (Last *et al.,* 2016; Ebert *et al.,* 2021; Froese & Pauly, 2022)

- **Extended Foraging range:**
  - **Cownose rays (Rhinopteridae):** These are mostly benthopelagic and are found in various locations such as continental shelves, offshore islands, bays, and estuaries. They often occur in large congregations and may migrate over substantial distances. The Shorttail cownose ray (*Rhinoptera jayakari*) is widespread in the Indo-West Pacific, ranging from South Africa to eastern Indonesia and the Ryukyu Islands. Their benthopelagic nature allows them to move freely in the open ocean and often aggregate in large shoals.
  - **Devil rays (Mobulidae):** These are predominantly pelagic, covering extensive areas over continental shelves and near offshore islands. The Kuhl's devil ray (*Mobula kuhlii*) in the Indo-West Pacific, from South Africa to eastern Australia, is pelagic, mainly in coastal waters or inshore. The migratory behaviour and large distances covered contribute to their role in open ocean ecosystems. Devil rays,

being highly mobile, showcase significant movements, especially during migrations.

- **Spotted skate (Rajidae):** The Spotted skate (*Raja straeleni*) demonstrates a regular migration pattern, moving toward the coast in warm seasons and transitioning to deeper waters in winter. This oceanodromous behaviour indicates a dynamic range of movement, allowing them to adapt to different environments throughout the year.

- **Largest and longest lifespan:**
  - **Bull ray (*Aetomylaeus bovinus*):** Among the rays discussed, *A. bovinus* from the family Myliobatidae stands out for its large size, reaching up to 294 cm in length. While not as big as some sharks, its critical endangered status highlights the vulnerability of larger rays to various threats.
  - **Devil rays:** The Longhorned devil ray (*Mobula eregoodootenkee*) and Shortfin devil ray (*M. kuhlii*) exhibit a degree of variability in size, but they fall within the category of medium to very large rays. However, they are still considerably smaller than *A. bovinus.*
  - **Spotted skate (*Raja straeleni*):** Attains a maximum length of 90 cm, representing a notable size among skates, but is the smallest of the rays and skates within the study. While not as large as some sharks or rays, its presence in shallow enclosed bays and slopes underscores the diverse ecological niches occupied by skates.
- **Reproductive strategies:**
  - **Bull ray (*Aetomylaeus bovinus*):** Is viviparous, giving birth to litters of 3-6 pups with gestation periods ranging from 5-6 months (off Senegal) to 12 months (off South Africa). This reproduction strategy aligns with the larger trend among rays, where most are livebearers.
  - **Devil rays:** Viviparous, giving birth to a single pup per litter. The reproductive strategies of *M. kuhlii* and *M. eregootenkee* are not fully specified, emphasising the need for further research on the reproductive biology of these species.
  - **Spotted skate (*Raja straeleni*):** Oviparous, with females laying their eggs in cases. The slow development of embryos, which can take up to 2 years to hatch, reflects the complex reproductive strategies within the Rajidae family.

Table 1.1. General information on sampled elasmobranchs with biometrics, geographical distribution range (GDR), (endemic to South Africa (EZA); endemic to Africa (EA), and Mediterranean (EAM); endemic to Indian Ocean (EIO); global (G)), and IUCN Red List category (least concern (LC); near threatened (NR); vulnerable (VU); endangered (EN); critically endangered (CR)) (Erasmus *et al.,* 2022). Feeding characteristics were obtained from Jacobsen & Bennet (2013), and Depth range, Maturity, Max weight, Max age, and Biology from Froese & Pauly (2022). Trophic position obtained from Cortes (1999), Ebert & Bizzarro (2009), Hussey *et al.* (2012), and Jacobsen & Bennet (2013).

Common name (species)	**Geographical distribution range**	**Depth range (m)**	**Maturity (cm)**	**Max weight (kg)**	**Max age**	**Feeding**	**Trophic position**	**Biology**	**IUCN Redlist**
Lamniformes Lamnidae									
Great white shark (*Carcharodon carcharias*)	G	0-1200	475 (450-500)	-	30-73	FISH, ELAS, RNDM, CEPH, CRUS, BIRD	5	Coastal and offshore behaviour along the shelves. Often occupies the surf zone and enter shallow bays. Pelagic nature enables migrations across vast oceanic regions. Oceanodromous. Mostly amphitemperate.	VU
Carcharhiniformes Carcharhinidae									
Java shark (*Carcharhinus amboinensis*)	EIO	0-150	280* (198-223)	-	-	FISH, ELAS, CEPH, CRUS, MOLL, RNDM	4.3	Inshore areas of shelves. Prefers shallow water near coast. Can be found in shallow bays and estuaries. Avoid rivers.	VU
Spinner shark (*Carcharhinus brevipinna*)	G	0-100	304* (170-266)	89.7	17-19	FISH, ELAS, CEPH	4.2	Shelves inshore to offshore. Oceanodromous.	VU
Bull shark (*Carcharhinus leucas*)	G	1-164	366* (180-230)	316.5	32-50	FISH, ELAS, CRUS, RNDM, REPT, CEPH, MOLL	4.3	Coastal and freshwater areas, including shallow waters such as bays, estuaries, rivers, and lakes. Penetrate far into rivers and hypersaline bays. Juveniles can travel long distances from sea.	VU
Blacktip shark (*Carcharhinus limbatus*)	G	0-140	286* (120-194)	122.8	12	FISH, ELAS, CEPH, CRUS	4.2	Shelves, near and far from shore. Near river mouths, estuaries, bays, mangroves, lagoons, coral reefs. Young common near beaches.	VU
Dusky shark (*Carcharhinus obscurus*)	G	0-500	420* (220-300)	346.5	34-53	FISH, ELAS, CEPH, CRUS, MOLL, RNDM	4.2	Shoreline and offshore waters, excluding deep oceans. Young prefer shallower water. Oceanodromous.	EN
Tiger shark (*Galeocerdo cuvier*)	G	0-1136	>500* (210-350)	807.4	27-37	ELAS, FISH, RNDM, MOLL, CRUS, CEPH, REPT	4.1	Around shelves, entering estuaries, lagoons, coral atoll, and harbours. Frequents oceanic waters but not true oceanic species. Oceanodromous.	NR
Carcharhiniformes Pentanchidae									
Puffadder shyshark (*Haploblepharus edwardsii*)	EZA	0-130	59* (M), 60* (F)	-	-	FISH, CRUS, CEPH	3.8	Sandy and rocky bottoms of inshore and offshore continental shelf.	EN
Brown shyshark (*Haploblepharus fuscus*)	EZA	0-35	69*; M (55-60); F (60-63)	-	-	CRUS, FISH	3.8	Inshore over continental shelf, frequents shallow, rocky environments.	VU
Dark shyshark (*Haploblepharus pictus*)	EZA	0-35	70*; M (40-57); F (36-60)	-	-	FISH, CRUS, CEPH	3.8	Common in shallow sandy environments. Inshore waters. Continental shelf.	LC
Carchariniformes Scyliohinidae									
Leopard catshark (*Poroderma pantherinum*)	EZA	0-256	84* (M); 73* (F)	-	-	FISH, CRUS, CEPH, POLY	3.6	Demersal in warm-temperate waters. Prefers rocky reefs.	LC

Table 1.1 (continued)

Carcharhiniformes Sphyrnidae									
Scalloped hammerhead shark (*Sphyrna lewini*)	G	0-1000	370-430* (140-273)	152.4	35	FISH, CEPH, CRUS, ELAS	4.1	Coastal-pelagic, semi-oceanic habitats occur over shelves, deep waters, approach shores, enters bays. Juveniles found in coastal areas.	CR
Smooth hammerhead shark (*Sphyrna zygaena*)	G	0-200	M (256*); F (370-400*), (210-265)	400	24-25	ELAS, FISH, CRUS, CEPH	4.2	Coastal, pelagic, and semi-oceanic. Migrates northward during summer. Oceanodromous.	VU
Carcharhiniformes Triakidae									
Smooth-hound shark (*Mustelus mustelus*)	EAM	5-624	200*; M (70-112); F (80-124)	-	24	CRUS, CEPH, FISH	3.8	Demersal. Continental shelf and uppermost slopes.	EN
Hexanchiformes Hexanchidae									
Broadnose sevengill shark (*Notorynchus cepedianus*)	G	0-570	200 (192-208)	107	49	ELAS, FISH, RNDM, MOLL	4.7	Continental shelf. Shallow water of bays and estuaries. Larger individuals move deeper into offshore water and deep channels in bays.	VU
Lamniformes Odontaspididae									
Ragged tooth shark (*Carcharias taurus*)	G	1-191	225 (220-230)	158.8	30	FISH, ELAS, CEPH, CRUS	4.4	Close to shore in shallow waters, surf zones, shallow bays. Demersal behaviour. Migration in certain areas. Poleward movement in summer and equatorial shifts in autumn and winter, especially in the northern and southern ranges of the species. Oceanodromous.	CR
Myliobatiformes Mobulidae									
Longhorned devil ray (*Mobula eregoodootenkee*)	EIO	0-50	100*	-	-	EUPH	3.3	Coastal and oceanic waters. There are no known cases of occurrence in the epipelagic zone.	EN
Shortfin devil ray (*Mobula kuhlii*)	EIO	0-50	115-134	30	-	EUPH	3.3	Coastal and oceanic water.	EN
Myliobatiformes Myliobatidae									
Bull ray (*Aetomylaeus bovinus*)	EAM	10-150	294*;90 (35-148)	116	-	CRUS, MOLL	3.4	Tropical and warm temperate coastal water, occasionally offshore.	CR
Myliobatiformes Rhinopteridae									
Oman cownose ray (*Rhinoptera jayakari*)	EIO	0-50	90*	-	-	MOLL**	3.4	Benthopelagic in oceanic waters.	EN

Table 1.1 (continued)

Rajiformes Rajidae									
Spotted skate (*Raja straeleni*)	EA	80-800	91*; M (56-68); F (55-71)	1.4	-	INV, FISH	3.7	Shallow enclosed bays and slopes. Regular migration pattern, moving toward the coast in warm seasons and transitioning to deeper waters in winter. Oceanodromous.	NR
Squatiniformes Squatinidae									
African angelshark (*Squatina Africana*)	EA	0-494	M (77-95); F (82-107)	-	-	FISH, CEPH	4.2	Continental shelf and top region of slopes (inshore to 494m).	NR

* – Max length

** – Compared to closely related *Rhinoptera javanica*

Table 1.2. Prey categories from Cortés (1999) and Ebert & Bizzarro (2009) and trophic levels of prey from Jacobsen & Bennet (2013).

Trophic levels of prey	**Prey categories used to calculate standardised diet compositions and trophic levels**	
Prey category	**Inclusions/Exclusions within each Prey Category**	**Trophic level**
MOLL	Molluscs (excluding Cepahlopoda), includes unidentified molluscs	2.1
PROT	Protochordates, includes *Amphioxus* and acorn worms	2.1
EUPH	Euphausiidae, Mysida, and other zooplankton	2.25
CRUS	Crustaceans (other than elsewhere specified), includes Stomatopoda, and unidentified crustaceans	2.4
INV	Invertebrates (other than elsewhere specified), includes unidentified invertebrates and insects	2.5
DECA	Brachyura, Caridae, Penaeidae, Palinura	2.52
POLY	Polychaetes and other marine worms	2.6
AMPH	Amphipoda, Isopoda	3.18
CEPH	Cuttlefish, squid, octopus, and unidentified cephalopods	3.2
FISH	Fishes (other than chondrichthyans)	3.24
ELAS	Sharks, skates and rays	3.65
RNDM	Marine mammals (seals, dolphins, porpoises, whales), mammalian carrion, inorganic objects	-
REPT	Sea turtles, sea snakes	-
BIRD	Seabirds	-

1.6 Human health risk

The consumption of seafood has been considered a healthy addition to the human diet with numerous health benefits (Khalili Tilami & Samples, 2018). Children have been one of the primary focuses of various studies that can permanently improve brain function with the early consumption of omega-3 supplementation (Carwile *et al.,* 2016; Lepping *et al.,* 2019).

Evidence of hepatic effects of OCPs in animals have shown the liver as one of the primary targets of toxicity, due to the lipophilic properties of these organic compounds (Gerber *et al.,* 2016; Hussein *et al.,* 2022). The difference of lipids between the muscle and liver tissue of elasmobranchs is seen in the research completed by Pethybridge *et al.* (2014) wherein the muscle tissue displayed more phospholipids and the liver tissue more triglycerides. Phospholipids are membrane lipids and not readily used as a source of energy compared to triglycerides (Pethybridge *et al.,* 2014). This enables the bioaccumulation of these contaminants within the muscle tissue as these lipids are not as regularly used and regenerated as the triglycerides found in the liver tissue, and as such displaying the potential more chronic exposure to contaminants. Further research is needed to expand on the work by ATSDR (2007, 2018, 2019), Pryzbyla *et al.* (2023), and Harper *et al.* (2022) in order to better understand the specific chemical and physiological interactions of OCPs within the muscle tissue of organisms.

However, toxicological studies completed on the risks of consumption of fish contaminated with chemical pollutants have shown that fish consumption should be regulated due to the potential harmful effects of OCPs (Gerber et al. 2016) and methylmercury (MeHg) (Barone *et al.,* 2021) within fish. As an example of the risks of OCPs to humans, exposure can take place due to direct contact when used in malaria vector control (Quinn *et al.,* 2011) or consumption of contaminated food such as fish (Volschenk *et al*., 2019). This and other pesticides are known to have human health effects ranging from neurotoxicity, disruption of the endocrine system, immune impacts, and carcinogenesis (Hallenbeck and Cunningham-Burns, 2012). Several studies in South Africa have showcased the possible deleterious effects associated with pesticide exposure with effects ranging from endocrine disruption (Aneck-Hahn *et al.,* 2007), and acetyl-choline esterase inhibition (Dalvie & London, 2006).

Methylmercury is known to accumulate within vital organs within the human body, liver, kidneys, and brain, causing numerous deleterious effects (Bjørklund *et al.,* 2017). Harley *et al.* (2015) found that Hg was far more likely to accumulate in muscle tissue than liver tissue. The known interactions of Se with Hg the research by Fernández-Bautista *et al.* (2022) highlights the occurrence of both these elements in muscle tissue of fish species. Research studies completed by (Ralston & Raymond, 2010; Khan and Wang, 2009; Ralston *et al.,* 2008)

have also confirmed the role that Se has in counteracting the effects of MeHg. As previously stated, the toxic potential of consuming certain marine products with high Hg concentrations can be counteracted with high Se concentrations with the calculation of HBVSe established by Storelli *et al.* (2022). However, as mentioned, other external factors may impede the antagonistic nature of Se with studies by Grgec *et al.* 2020 and others (Azad *et al.,* 2019; Mirlean *et al.,* 2019; Olmedo *et al.,* 2013) contributing to better understand the effects of Se intake on the harmful effects of Hg.

More than 80% of shark meat is now sold globally as frozen steaks and fillets. The quantity of shark meat in trade doubled between 1985 and 2001, peaking at about 100,000 tonnes, then declined as catches fell during the past decade. Most of it is destined for South America (Brazil, Uruguay and Peru) and Europe (particularly Spain, Italy, Portugal and France) (Ebert *et al.,* 2021). Regular public warnings regarding the human health risk associated with the consumption of too much shark meat are issued by food standard authorities (Ebert *et al.,* 2021). The use of various body parts/fluids of sharks for medicinal products has also been around since the 14th century and also poses serious health concerns (Ebert *et al.,* 2021).

1.7 Study hypotheses and aims

Currently, there is limited information on OCPs and the relationship between Hg and Se in the elasmobranchs around the South African coastline (South Africa, 2015).

Hypotheses

- The OCP levels in elasmobranch species along the South African coastline are related to different intrinsic (sex, size, migratory and foraging habits) and extrinsic traits (geographical position).
- The OCP and Hg levels in elasmobranch tissues pose a health risk to humans who consume them.
- Similar to OCPs, the Hg and Se levels in elasmobranch species along the South African coastline are related to different intrinsic and extrinsic traits.
- There is an antagonistic relationship between Se and Hg levels in the elasmobranch species studied.

Research aims

To test the formulated hypotheses, the research aims are to determine:

- The levels of OCPs in 22 elasmobranch species.
- Whether the species differences in contaminant concentrations (OCPs, Hg, Se) are due to intrinsic traits such as sex, size, migratory and foraging range, and diet (i.e., trophic position).
- Whether the species differences in contaminant concentrations (OCPs, Hg, Se) are due to extrinsic factors such as the geographical location of where they occur (i.e., along the east coast or south coast of South Africa).
- The human health risks associated with the consumption of OCP and Hg-contaminated elasmobranch muscle tissue.
- If the antagonistic interaction between Hg and Se can counteract the toxic properties of Hg.

Structure of the dissertation

Chapter 1: General Introduction

Provides the background of the study with hypothesis and aims.

Chapter 2: Organochlorine pesticides in elasmobranch tissue from the east and west coasts of South Africa.

Concentrations of various OCPs were determined from 22 elasmobranch species collected from the east and west coast of South Africa. The hypotheses tested in this chapter are that OCP levels in elasmobranch species along the South African coastline are related to different intrinsic and extrinsic traits and that OCP levels present within elasmobranch tissue pose a human health risk upon consumption.

Chapter 3: Mercury and selenium concentrations in elasmobranch tissue from the east and west coasts of South Africa.

Concentrations of Hg and Se were determined from 22 elasmobranch species collected from the east and west coast of South Africa. The hypotheses tested in this chapter are that Hg and Se levels in elasmobranch species along the South African coastline are related to different intrinsic and extrinsic traits, and secondly, that Se is present in all elasmobranch species is enough to offset the levels of Hg in the tissues.

Chapter 4: Conclusions and Recommendations

The general summary of the results obtained, conclusions, and recommendations for future studies are discussed.

Chapter 5: References

List of all references used throughout the dissertation.

Chapter 2: Organochlorine pesticides in elasmobranch tissue from the east and west coasts of South Africa

2.1 Introduction to OCPs

According to Dalvie *et al.* (2009), South Africa is the top pesticide user in sub-Saharan Africa and ranked in the top four importers in Africa (Quinn *et al.,* 2011). This causes concern with the use of not just current pesticides, but also with the use of banned pesticides (Gerber *et al.,* 2016), particularly organochlorine pesticides (OCPs), which are known to be persistent within the environment. This is concerning, because although many of these pesticides have been banned, they are still found present within many aquatic ecosystems (Gerber *et al.,* 2016). Recent studies by Gerber *et al*. (2015), Volschenk *et al.* (2019), and Gerber *et al*. (2021), highlighted that South Africa's freshwater systems are highly contaminated with OCPs such as DDT, DDD and DDE, particularly those flowing eastward into the Indian Ocean. Sereda & Meinhardt (2005) conducted studies on DDDs and DDEs in north-eastern KwaZulu-Natal during the malaria spraying season and found that more than 40% of collected samples from different locations contained these contaminants, irrespective of the fact that safe application measures, such as indoor residual spraying, were applied. Olisah *et al.* (2020) stated that the improper use of these pesticides has caused these contaminants to disperse in large quantities into the atmosphere, water bodies and soils, and thus posing a threat to the health of the ecosystem as well as the human population. Fatoki & Awofolu (2004) detected high levels of hexachlorobenzene and heptachlor in coastal systems of the Eastern Cape due to agricultural runoff. A study on coral reefs along the KwaZulu-Natal Coast of South Africa by Porter *et al.* (2018) showed that OCPs are also present in the marine environment, as they are transported from terrestrial and freshwater systems either by groundwater seepage or adjacent wetlands and freshwater lake systems.

However, there remain limited research studies on OCP concentrations in the marine environments of South Africa. Research by Porter *et al.* (2018), Olisah *et al.* (2019, 2021), and Erasmus *et al.* (2020) has focused on the South African coastline, shedding light on the presence of OCPs in both the marine environment and the organisms within the ecosystems. Porter *et al.* (2018) specifically examined coral reefs along the northeast coast of South Africa, discovering varying degrees of OCPs in all sampled coral reef organisms. This variability suggests that the accumulation of contaminants is influenced by age, reproductive biology, and foraging habits.

Since OCPs are lipophilic, they have the potential to biomagnify within marine food webs (Hussein *et al.,* 2022). Species with specific traits such as chondrichthyans (characterised by longevity, slow metabolic rates, and lipid-rich livers) make them particularly susceptible to the

bioaccumulation of these contaminants (Hussein *et al.,* 2022, Lee *et al.,* 2015). There are limited studies on OCPs of elasmobranchs along the South African coastline. Schlenk *et al.* (2005) measured OCPs, primarily DDTs, in the muscle and liver tissues of *C. carcharias*. More recent studies by Beaudry *et al.* (2015) found levels of ∑Chlordanes and ∑DDTs in *C. obscurus* and *C. carcharias* around the coast of South Africa.

Shipley *et al.* (2021) and Dent & Clarke (2015) indicated that there is a global trend of increased consumption of shark meat and the use of other shark body parts/fluids for medicinal purposes (Ebert *et al.,* 2021). Despite the low economic value of shark meat, associated risks due to consumption remain understudied. Barone *et al.* (2021), Bjørklund *et al.* (2017), Dallaire *et al.* (2013), Hallenbeck & Cunningham-Burns (2011), Aneck-Hahn *et al.* (2007), Dalvie & London (2006), and Ebert *et al.* (2021) highlighted the health risks associated with consuming elasmobranch meat, emphasising the need for increased awareness, and understanding of these risks in the context of human health.

The aims of this chapter are to firstly, determine the levels of OCPs in muscle tissue of 22 shark species from the east and west coasts of South Africa; secondly, to investigate whether species differences in contaminant concentrations can be attributed to intrinsic traits, such as sex, size, migratory patterns, foraging range, and diet (including trophic position); thirdly, to assess whether the geographical location of occurrence, such as along the east or west coast of South Africa, contributes to variations in OCP levels between species; and finally, to conduct a comprehensive assessment of the human health risk associated with the consumption of elasmobranch muscle tissue contaminated with OCPs.

2.2 Materials and methods

2.2.1 Sampling

Elasmobranch samples were collected by the KwaZulu-Natal Sharks Board and the South African Sharks Conservancy (SASC) on the east coast of KwaZulu-Natal and the south coast of the Western Cape Province, respectively. This study makes use of the muscle tissue of the elasmobranchs for contaminant analysis. Although liver tissue would be preferred for contaminant analysis, the extraction and cleanup procedures used proved ineffective to remove all of the lipids from the liver samples without the loss of the majority of OCPs present. As such it was deemed that the muscle tissue samples would be sufficient in analysing for the presence of the OCPs.

A total of 59 muscle tissue samples were collected from 22 elasmobranch species, representing 17 sharks and five skates and rays. From these 59 muscle tissue samples, 25 were female, 29 male, and 5 unidentified (Table S1). Furthermore, 28 muscle tissue samples were from adult elasmobranchs, 21 from juveniles, and 10 unidentified (Table S1). The different muscle tissue samples and number per species were: *Mobula kuhlii* (Shortfin devil ray; n = 2), *Mobula eregoodootenkee* (Longhorned devil ray; n = 3), *Aetomylaeus bovinus* (Bull ray; n = 5), *Rhinoptera jayakari* (Oman cownose ray; n = 3), *Poroderma pantherinum* (Leopard catshark; n = 3), *Raja straeleni* (Spotted skate; n = 1), *Haploblepharus fuscus* (Brown shyshark; n = 2), *Haploblepharus pictus* (Dark shyshark; n = 1), *Haploblepharus edwardsii* (Puffadder shyshark; n = 1), *Mustelus mustelus* (Smoothhound shark; n = 4), *Galeocerdo cuvier* (Tiger shark; n = 3), *Sphyrna lewini* (Scalloped hammerhead shark; n = 6), *Sphyrna zygaena* (Smooth hammerhead shark; n = 1), *Carcharhinus limbatus* (Blacktip shark; n = 1), *Carcharhinus brevipinna* (Spinner shark; n = 4), *Squatina africana* (African angelshark; n = 1), *Carcharhinus obscurus* (Dusky shark; n = 5), *Carcharhinus leucas* (Bull shark; n = 1), *Carcharhinus amboinensis* (Java shark; n = 1), *Carcharhias taurus* (Ragged tooth shark; n = 1), *Notorynchus cepedianus* (Broadnose sevengill shark; n = 1), *Carcharhinus carcharias* (Great white shark; n = 7).

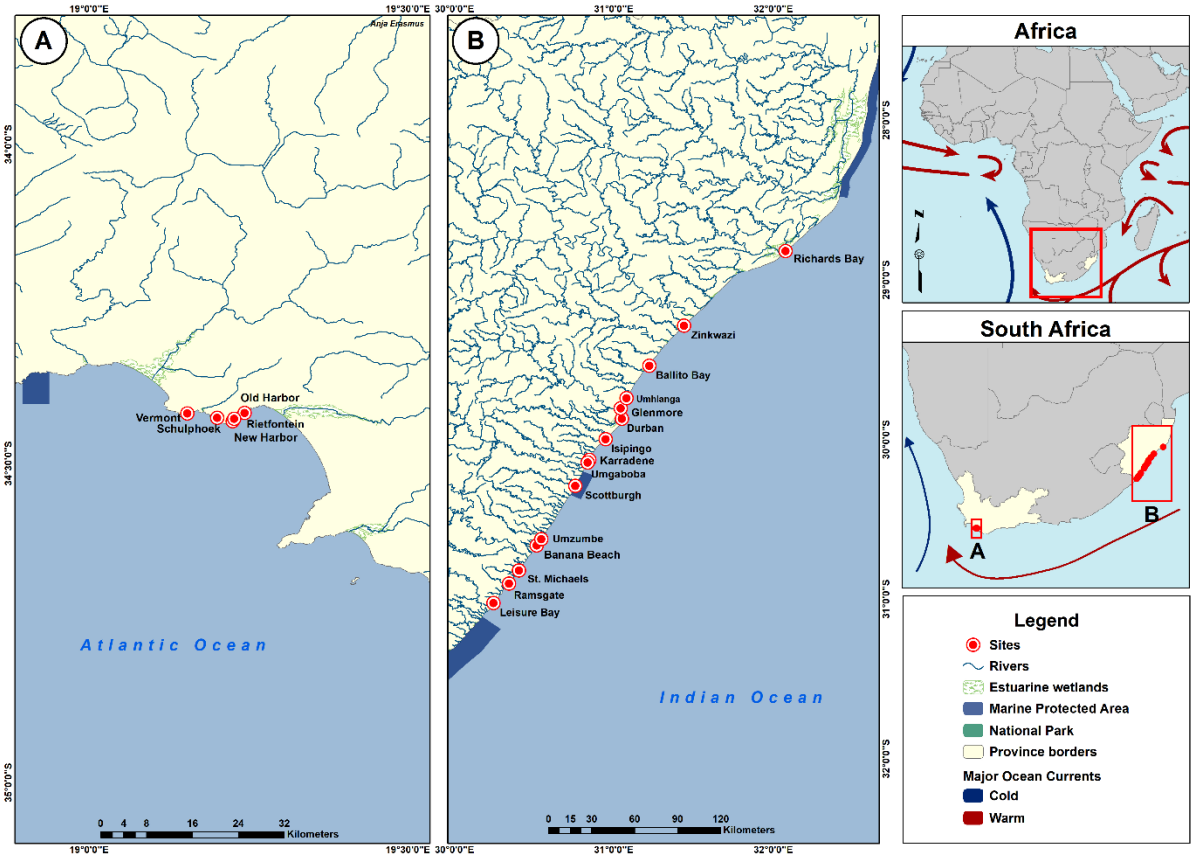

Figure 2.1: Sampling localities of elasmobranchs around the east and south coast of South Africa

As part of the South African bather protection programme, the KwaZulu-Natal Sharks Board retrieved the sharks from shark nets between 2019 and 2020. The samples acquired from SASC were caught by longlines in 2018. All shark samples were collected under the relevant permits issued by the Chief Director of Fisheries Research & Development (Department of Fisheries, Environment and Forestry). All samples were stored frozen (-20 °C) and sent to the North-West University in 2020 for organochlorine pesticide analyses.

2.2.2 Contaminant identification

Muscle tissue samples were analysed for the potential occurrence of 22 specific organochlorine pesticides. These OCPs can be grouped into Chlorobenzenes (hexachlorobenzene), Hexachlorocyclohexanes (α-HCH, β-HCH, γ-HCH, δ-HCH), Chlordanes (heptachlor, cis-heptachlor, trans-heptachlor, cis-chlordane, trans-chlordane, trans-nonachlor, cis-nanochlor, oxy-chlordane), Dieldrin's (dieldrin, aldrin, endrin), o,p'-dichlorodiphenyltrichloroethane (DDT), p,p'-dichlorodiphenyltrichloroethane (DDT), and associated metabolites (o,p'-dichlorodiphenyldichloroethylene [DDE], p,p'-dichlorodiphenyldichloroethylene [DDE], o,p'-dichlorodiphenyldichloroethane [DDD], p,p'-dichlorodiphenyldichloroethane [DDD]). All glassware and materials (aluminium) needed for

laboratory analysis were cleaned using a hexane and acetone rinsing cycle. The rinsing cycle involved three cycles of rinsing the needed glassware and aluminium material with hexane and acetone to ensure the cleanliness of laboratory conditions and consumables. Both hexane (080-03423) and acetone (010-08683) used for material cleanup and sample analysis was received from Fujifilm Wako Pure Chemical Corporation.

2.2.3 Sample extraction, clean-up and preparation

The extraction and clean-up of samples have been adapted from previous research by Yohannes *et al.* (2013) and Gerber *et al.* (2016). Approximately 10 g wet weight muscle tissue of each sample was freeze-dried and homogenised using mortar and pestle to a fine powder. Between samples, the mortar and pestle were cleaned with ethanol to avoid cross-contamination. Approximately 0.5 to 1 g of homogenised dry sample was accurately weighed to four decimals and mixed with excess anhydrous sodium sulphate from Thermo Scientific Chemicals (A19890.0I) for desiccation. The sample was transferred to an extraction thimble in a Soxtherm apparatus (S306AK Automatic Extractor, Gerhardt, Germany). Subsequently, the sample was spiked with 100 µL of the internal standard PCB77 from Dr. Ehrenstorfer (DRE-L20007700IO) with a concentration of 100 µg/L. A mixture of 120 mL hexane:acetone (3:1, v/v) was added to the sample and placed within the Soxtherm and extracted for approximately 1 hour. The total time for the extraction and cooling of the samples in the Soxtherm was about 2 hours. Lipids in tissue samples were extracted using Soxtherm extraction and QuEChERS (Quick Easy Cheap Effective Rugged Safe) for the final clean-up of the sample.

After extraction and cooling was completed, the sample was transferred to a round bottom flask. The sample was then evaporated to 2 mL using a rotary vacuum evaporator. The sample was transferred into a 15 mL polypropylene Falcon tube and rinsed with a small volume of hexane. Clean-up of the sample was completed using the QuEChERS method with 1 g EMR-$MgSO_4$ from Agilent (Bond Elut EMR Lipid pouch, 5982-0102), and 0.5 g activated florisil from Thermo Scientific Chemicals (B21870-30) was added to the sample in a 15 mL Falcon tube. The sample was vortexed for 1 minute to cause a chemical reaction and then centrifuged for 10 minutes at 5000 G. After the centrifugation was completed, the sample supernatant was transferred to a 10 mL graduated tube.

Each sample was evaporated to near dryness under a steady stream of N_2 gas at 50°C. Whereafter, the sample was reconstituted with 100 µL of 2,4,5,6-tetrachloro-m-xylene (TCmX) from Dr. Ehrenstorfer (DRE-L17382500CY) (for final volume calculation) with a concentration of 100 µg/L in n-decane. The reconstituted mixture was transferred into 2 mL autosampler

vials (Agilent Technologies) for further analysis on a triple-quad gas chromatograph with a mass spectrometer (Shimadzu triple-quad GC-MS-TQ8050 NX).

2.2.4 Sample analysis

Analysis of extracted and cleaned-up tissue samples was completed using a triple-quad gas chromatograph with a mass spectrometer (Shimadzu triple-quad GC-MS-TQ8050 NX). The samples were separated using a Shimadzu SH-I-5Sil MS capillary column with the following specifications: 250 µm internal diameter and 0.25 µm film thickness, and a total length of 30 m for the column. Nitrogen was used as carrier gas at a flow rate of 1.5 mL/min. The injection inlet temperature was set at 225°C with 1µL splitless injection. The oven program was adapted from the method described by Gerber *et al*. (2016), with the oven set at 50°C at the initiation of the sequence and held for 1 min thereafter being increased at 25°C/min until 125°C was reached. The temperature increase was changed to 10°C/min until 300°C was reached and held for 15 min. The mass spectrometer ion source temperature was set at 230°C, and the mass spectrometer interface temperature was set at 250°C.

2.2.5 Quality control and assurance

A Dr. Ehrenstorfer pesticide mix 1037 (LGC standards) containing 22 POPs pesticides was used for standard curve calibration using a range of seven concentrations between 1 µg/L and 200 µg/L. The concentrations of individual OCPs were quantified and calculated from peak areas based on the calibration equation for each compound. Peak calibrations were done based on the ratio between the target peak and IS peak areas. All the correlation coefficients (R^2) were greater than 0.99.

The limit of detection (LOD) is regarded as the lowest concentration value of any individual OCP that could be quantified within the study with a 95% confidence level. The limit of quantification (LOQ) is the lowest concentration of the OCP that can be determined and deemed acceptable with the associated confidence level (95%). The limit of detection and LOQ were calculated using the standard error of the gradient calculation for the calibration for each compound. The ratio of LOD was based on a 3:1 signal-to-noise ratio, and the range was between 0.09 and 0.47 ng/g for all OCPs. The limit of quantification was based on a 10:1 signal-to-noise ratio, and the range was between 0.3 and 1.57 ng/g for all OCPs. The recovery of the internal standard was calculated as:

*Recovery % = (internal standard [IS] peak area in sample / IS reference peak area) * 100 / 90*

Samples are then recovery adjusted (peak area * 100 / recovery %)

The internal standard recovery ranged between 40 and 60% for all the muscle tissue samples analysed. For the purposes of this study, no corrections were applied to account for the under recovery of analytes.

Lipid content percentage determination was achieved using the following equation:

*Lipid content of sample (%) = (mass after – mass before) / 0.1 / original sample mass * 100*

The lipid content percentages of the samples ranged between 0.01 and 0.62%. The latter percentage was observed in one of the muscle tissue samples from *C. carcharias*.

2.2.6 Statistical analyses

Data were tested for normality and homogeneity of variance using the D'Agostino and Pearson omnibus normality test and the Shapiro-Wilk normality test, respectively. To determine significant differences in OCP concentrations between elasmobranch species, a one-way analysis of variance with Tukey's multiple comparison test was applied, with the level of significance set at $p < 0.05$. All analyses were carried out in GraphPad Prism 10. Spatial patterns associated with OCP contaminants and elasmobranch species were evaluated using a Principal Component Analysis (PCA) conducted with the aid of Canoco v5 software. The data for the PCA were log transformed (y = log(x+1)). Subsequently, the log-transformed data used for PCA were also used for a Pearson's rank correlation test to investigate potential relationships between log-transformed concentrations of OCPs and the trophic position and sex of the elasmobranch species.

2.2.7 Human health risk assessment

Non-carcinogenic risk

To evaluate the potential for long-term non-cancerous health effects resulting from oral exposure, the average daily dose (ADD), presented as milligrams per kilogram of body weight per day, was calculated for each OCP analysed:

$$ADD = \frac{\left(average\ OCP\ concentration\ in\ elasmo.muscle\ (WW)\ x\ (food\ ingestion\ rate)\right)}{(adult\ body\ mass)\ x\ (no.of\ days\ between\ elasmo.meals)}$$

Where the average OCP concentration in the elasmobranch muscle is calculated in mg/kg wet weight, the food ingestion rate is 48.57 g, the average adult body weight is 70 kg, and the number of days between elasmobranch meals is three days (Heath *et al.* 2004).

Non-carcinogenic risk assessment for the toxic effects of pollutants uses reference doses (RfDs) as set thresholds that, if surpassed, can cause possible adverse health effects. To estimate the human health risk, a hazard quotient (HQ) was calculated for each OCP:

$$HQ = \frac{ADD}{RfD}$$

Where the value of HQ is higher than or below one, it suggests possible adverse health effects. HQ < 1 implies an unlikelihood of adverse health effects, and HQ > 1 implies a high likelihood of adverse health effects. RfD levels (µg/kg) used are as follows: HCB (0.0008); CHLs (0.0005); DDTs (0.0005) (Taylor & Wilson, 2002; ATSDR, 2018, 2019).

Carcinogenic risk

Cancer risk (CR) for the carcinogenic OCP contaminants (HCB, CHLs, DDE, DDD, DDT) were calculated as stated by the Integrated Risk Information System from the United States Environmental Protection Agency (USEPA-IRIS, 2019). The estimated daily intake (EDI) for OCPs from elasmobranch consumption:

$$EDI = \frac{(C\ x\ FIR)}{BM}$$

Where C is the mean concentration of OCPs (mg/kg wet weight), FIR is the daily food ingestion rate (48.57 g) (Hussein *et al.* 2022), and BM is the average body weight at 70 kg.

Thereafter, CR was calculated:

$$CR = EDI\ x\ CSF$$

Where the cancer slope factor (CSF) (mg/kg/day) of OCPs were identified as follows: HCB (1.6); CHLs (0.35); DDE (0.34); DDD (0.24); DDT (0.34) (USEPA-IRIS, 2019). According to public screening criteria conducted by USEPA (2005) for the risk levels of carcinogenic, the risk level is set at 10^{-6}. Any CR value below this risk level is considered an acceptable risk. Between 10^{-6} and 10^{-4} creates cause for concern, and values above 10^{-4} are considered inadmissible.

Maximum safe consumption limit

Maximum amount of elasmobranch muscle tissue that can be consumed safely and without any potential adverse human health risks per day:

$$Y = RfD\ x \frac{BM}{C}$$

Where Y is the amount of elasmobranch muscle tissue that can be safely consumed, RfD is the reference dose for non-carcinogenic risk, BM is the average body weight of the consumer, and C is the average concentration of OCPs within the elasmobranch muscle tissue.

2.2.8 Ethical considerations

This project on OCP accumulation in elasmobranch species found along the South African coast forms part of a larger study. This study concerns the conservation of ancient relationships: Integrative approach using elasmobranchs and their parasites to assess ecosystem health. This larger study has received ethical clearance (NWU-00065-19-A5) from the North-West University (NWU) Animal Care, Health and Safety, Research Ethics Committee (AnimCare) and this project was conducted with the following ethics number: NWU-01308-22-A9.

2.3 Results

2.3.1 Organochlorine pesticide levels in muscle of selected elasmobranch species

Twenty-two different OCPs were analysed in twenty-two shark species. Seven compounds were recorded in the tissue samples, with the majority of the accumulated OCPs made up of the DDxs (the sum of DDT, DDE and DDD). A list of the 22 OCPs tested for are provided in Appendix A. The mean and standard deviation of seven OCPs in the muscle tissue of shark species arranged from highest to lowest trophic position are presented in Figure 2.2. Significantly ($p<0.05$) higher total OCP concentrations were recorded in *C. carcharias* > *R. javanica* > *M. mustelus* > *C. obscurus* > *N. cepedianus* (Table 2.1). Notable was that the highest total OCP concentrations were not associated with the elasmobranchs at the highest trophic levels with many of the ray and skate species exhibited higher levels than shark species at higher trophic levels (Figure 2.2). The highest OCPs recorded were p,p-DDE concentrations, which was the most prevalent contaminant, followed by p,p-DDD > HCB > Trans-chlordane > p,p-DDT > Trans-nonachlor > Cis-chlordane. The sum of DDT, DDE and DDD (referred to as DDxs) (Figure 2.2) are the most prevalent OCP present within the different elasmobranch species followed by the chlordanes (Figure 2.2). Skates and ray species (Figure 2.3) found at the lower trophic positions displayed higher percentage contributions of HCB and chlordanes compared to the shark species in the upper trophic position (Figure 2.3), however ∑DDTs were still the most prevalent of all the OCPs. The two ray species, *M. goodoontenkee* and *R. jayakari* had significantly higher OCP levels than most of the shark species (Table 2.1). The average size of sharks sampled from the east coast was found to be 162.5 cm and 48.6 kg, while the average size of the sharks sampled from the south coast was 90 cm and 17.8 kg (Table S1). However, the data from the south coast elasmobranch species may be biased due to *N. cepedianus* collected on the south coast, as it was the largest and heaviest of all the sharks sampled. When the data of *N. cepedianus* is removed from representatives from the

south coast, the average size of the elasmobranchs falls to 61 cm and 1.65 kg. This shows that the sharks sampled from the east coast are markedly longer and heavier than the representatives from the south coast. The ray species (*M. kuhlii, M. eregoodootenkee, A. bovinus,* and *R. jayakari*) sampled from the east coast were on average 121 cm long and had an average weight of 17.35 kg. Only a single skate species (*R. straeleni*) was sampled from the south coast and was 59 cm long and had a weight of 3 kg (Table S1).

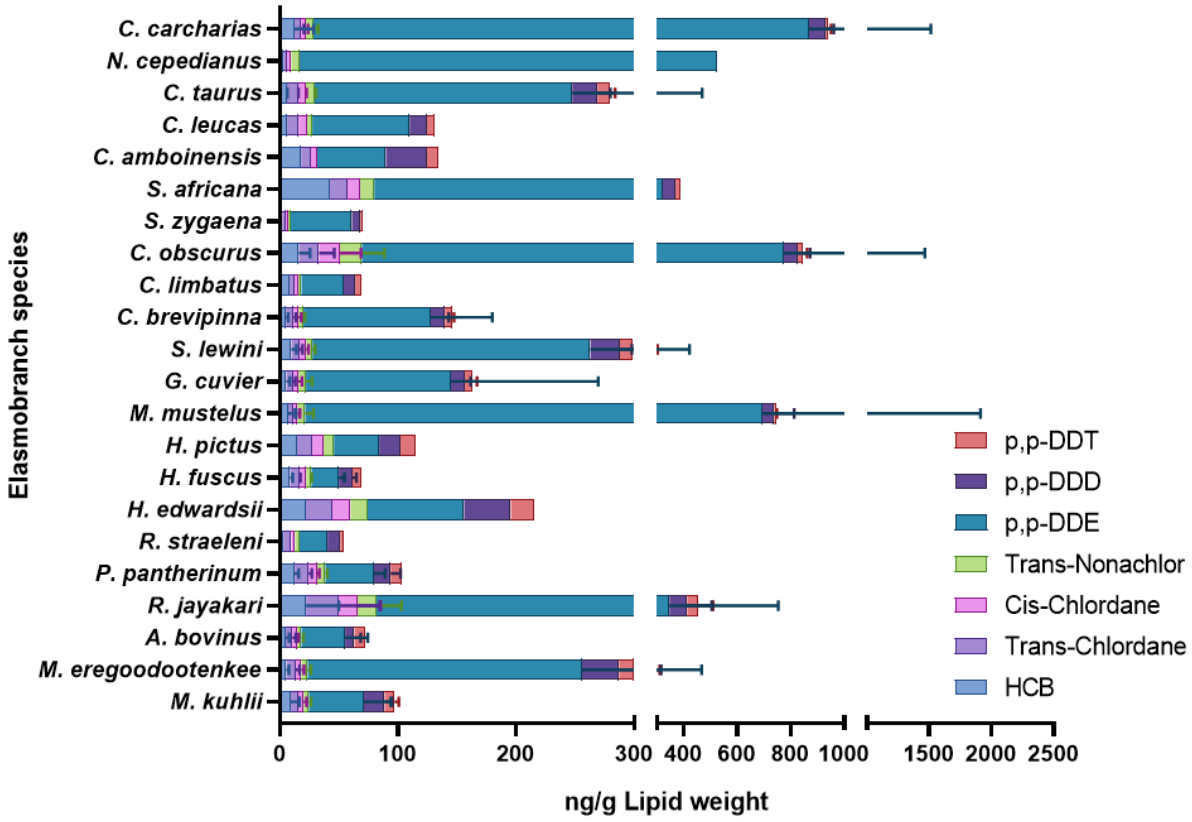

Figure 2.2: Organochlorine pesticides concentrations (ng/g lipid weight) in muscle tissue of different elasmobranch species from the east and south coast of South Africa.

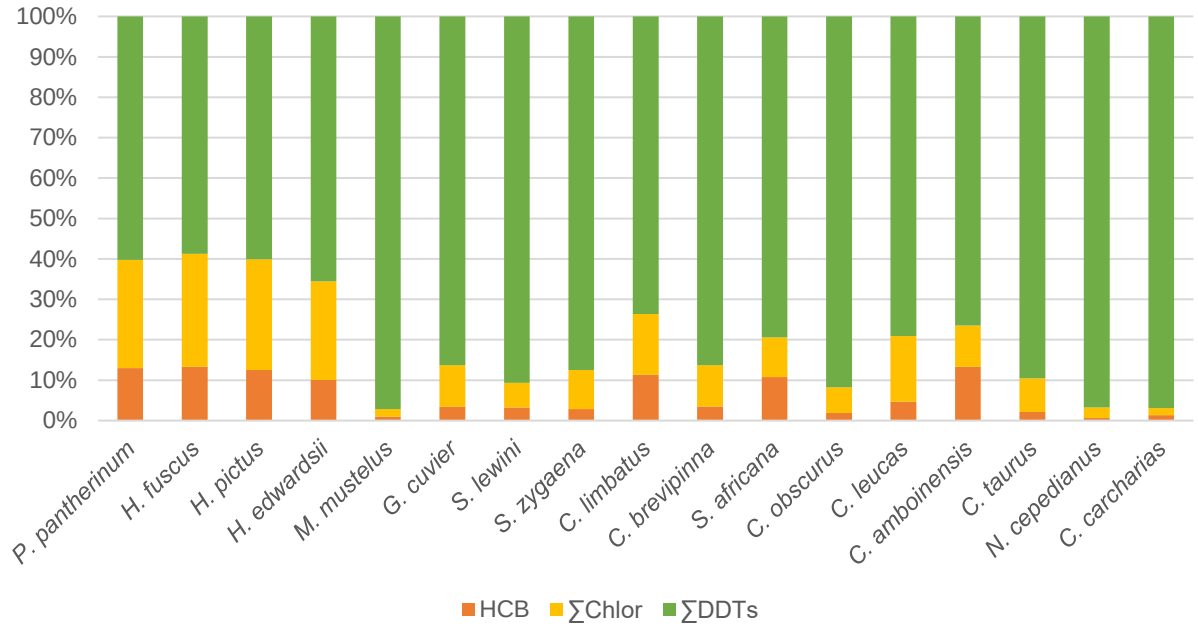

Figure 2.3: Percentage contributions of different OCPs in sampled shark species.

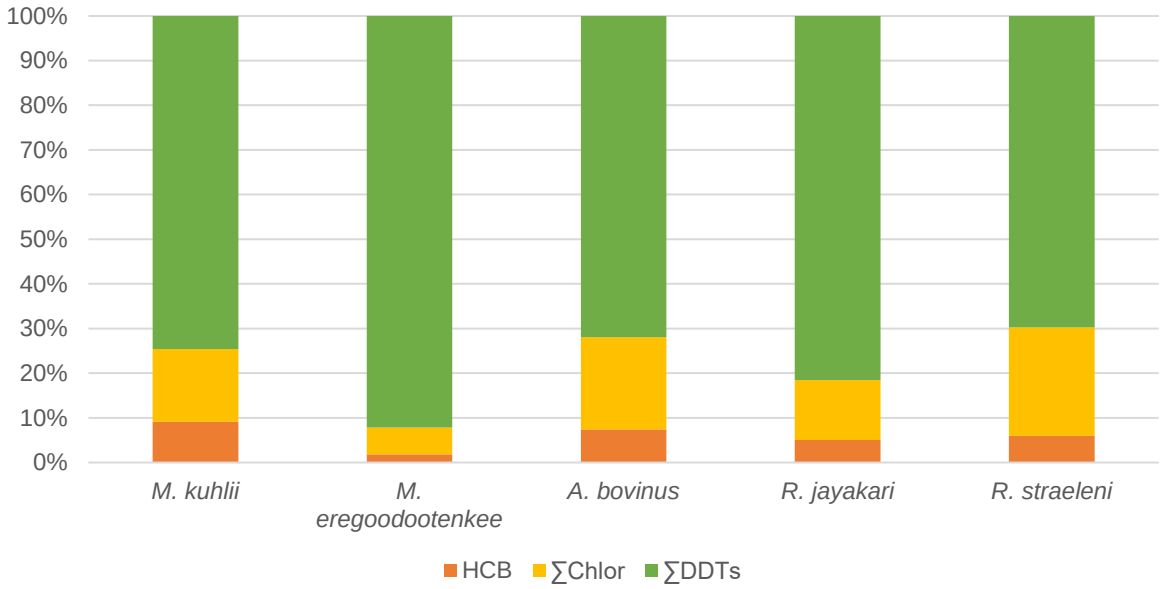

Figure. 2.4: Percentage contributions of different OCPs in sampled ray and skate species.

Table 2.1. Significant differences in total OCP concentrations (ng/g lipid weight) between different elasmobranch species. Significant differences are indicated as * $p < 0.05$; ** $p < 0.002$; *** $p < 0.0002$; **** $p < 0.0001$.

	*	**	***	****
Squatina africana	*C. leucas, C. amboinensis*			*N. cepedianus*
Carcharhinus obscurus		*M. kuhlii,*	*A. bovinus*	*S. zygaena,*
Mobula kuhlii		*R. jayakari, C. obscurus*		
Sphyrna lewini	*S. zygaena*			
Carcharhinus limbatus			*S. africana*	*C. obscurus*
Carcharhinus amboinensis		*R. jayakari*		
Aetomylaeus bovinus	*H. edwardsii*	*S. africana*	*C. obscurus*	*R. jayakari*
Mobula eregoodootenkee	*S. zygaena*			
Galeocerdo cuvier		*C. obscurus*		
Carcharhinus brevipinna	*S. africana*	*C. obscurus*		
Rhinoptera jayakari	*P. pantherinum, C. leucas*	*C. brevipinna, G. cuvier, C. amboinensis*	*H. fuscus*	*S. zygaena, R. straeleni, C. limbatus, N. cepedianus*
Carcharhinus leucas				
Carcharhinus taurus				
Sphyrna zygaena	*C. taurus*		*C. carcharias*	*S. africana, N. cepedianus*
Poroderma pantherinum				
Haploblepharus pictus	*S. zygaena*			
Haploblepharus fuscus	*S. africana*	*C. obscurus*		
Notorynchus cepedianus		*C. carcharias*		
Haploblepharus edwardsii		*C. limbatus*	*N. cepedianus*	*S. zygaena*
Mustelus mustelus	*S. zygaena*			
Raja straeleni	*C. carcharias*		*H. edwardsii*	*C. obscurus, S. africana*
Carcharodon carcharhias				

2.3.2 Dichlorodiphenyltrichloroethane and isomers

Carcharodon carcharias (white shark) had the highest mean concentration of the sum of all DDT and isomers (DDxs), followed by *M. mustelus* and *C. obscurus*, however *M. mustelus* showed the highest variation in concentrations (Figure 2.5). The levels of DDxs in *R*. jayakari and *C. obscurus* were also significantly higher ($p<0.05$) when compared to the other elasmobranch species (Table 2.3). *Carcharodon carcharias* and *M. mustelus* displayed the highest percentage contributions of DDE in muscle tissue (Figure 2.6). *Carcharhinus amboinensis* (java shark) had the highest percentage contributions of DDD followed by the cat- and shysharks (*P. pantherinum*, *H. fuscus*, *H. pictus*, *H. edwardsii*) that also had comparable percentages of DDD in the muscle tissue (Figure 2.6). The catshark and shyshark species also displayed the highest percentage contributions of DDT among all the elasmobranch species (Figure 2.6). The ray and skate species also had comparable percentage DDE contributions to the shark species (Figure 2.7).

The percentage composition for each of the DDxs isomers within elasmobranch species are as follows: 78.7% (DDE), 15.2% (DDD), and 7.5% (DDT) for shark species and 70.4% (DDE), 19.5% (DDD), 10.1% (DDT) for the ray and skate species. The ratios of DDD/DDE to ∑DDTs displayed a positive value over 0.6 for all elasmobranchs (Table 2.2). This indicates a historical input of DDT into the marine environment.

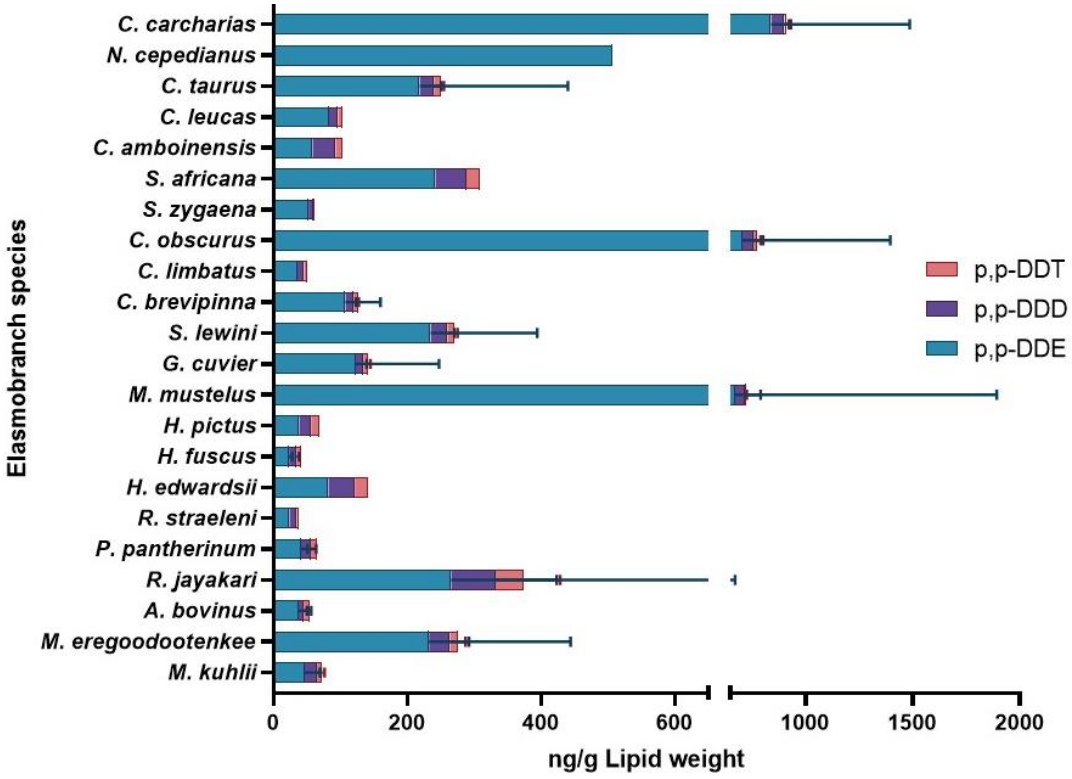

Figure 2.5: The DDx concentrations with different isomer concentrations of DDT, DDD, and DDE (ng/g lipid weight) in muscle tissue of different elasmobranch species from the east and south coast of South Africa.

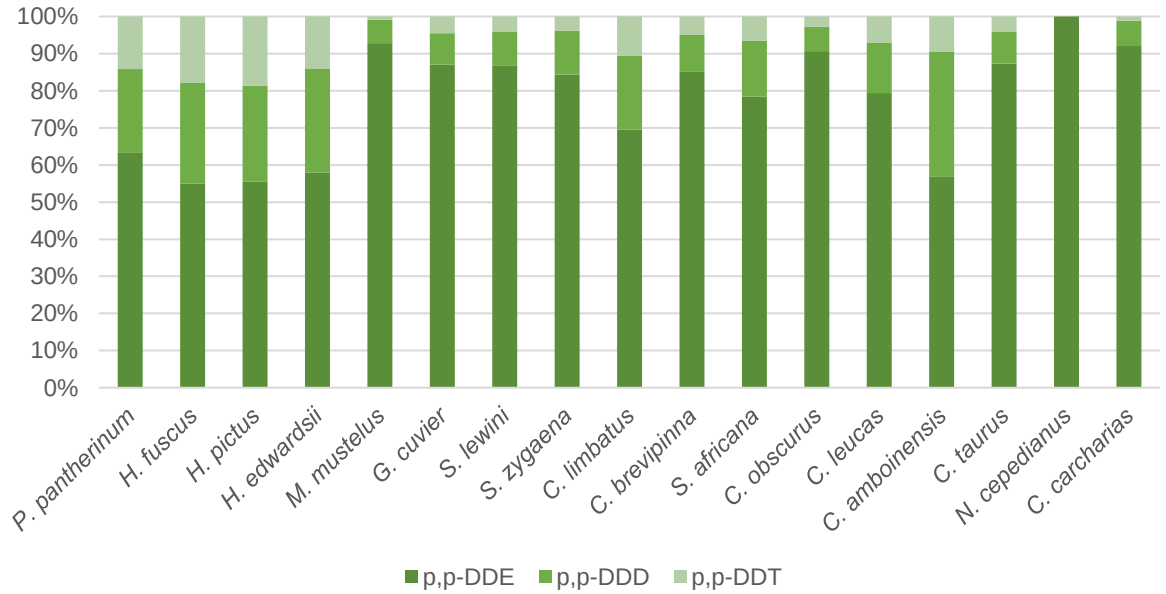

Figure 2.6: Percentage contributions of different OCP DDxs isomers in sampled shark species.

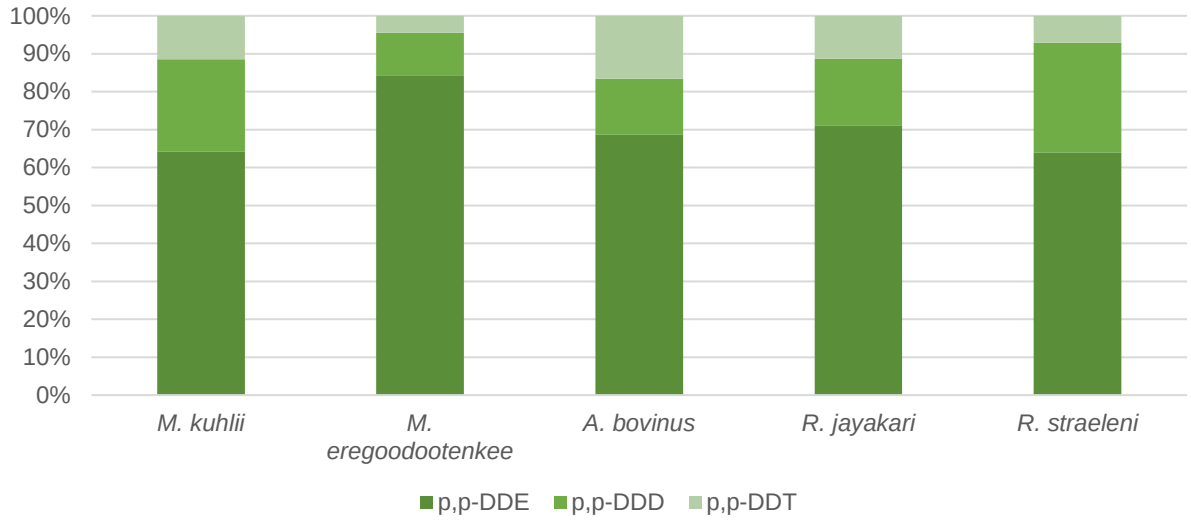

Figure 2.7: Percentage contributions of different OCP DDxs isomers in sampled ray and skate species.

Table 2.2. DDT ratios (Doong *et al*., 2002; Zhou *et al*., 2006) describing the ratio of DDT to DDD and DDE.

	Ratios of (DDE + DDD)/∑DDT
Mobula kuhlii (Shortfin devil ray)	1.4
Mobula eregoodootenkee (Longhorn devil ray)	1.1
Aetomylaeus bovinus (Bull ray)	1.2
Rhinoptera jayakari (Oman cownose ray)	1.3
Poroderma pantherinum (Leopard catshark)	1.4
Raja straeleni (Spotted skate)	1.5
Haploblepharus edwardsii (Puffadder shyshark)	1.5
Haploblepharus fuscus (Brown shyshark)	1.5
Haploblepharus pictus (Dark shyshark)	1.5
Mustelus mustelus (Smoothhound shark)	1.1
Galeocerdo cuvier (Tiger shark)	1.1
Sphyrna lewini (Scalloped hammerhead shark)	1.1
Carcharhinus brevipinna (Spinner shark)	1.1
Carcharhinus limbatus (Blacktip shark)	1.3
Carcharhinus obscurus (Dusky shark)	1.1
Sphyrna zygaena (Smooth hammerhead shark)	1.1
Squatina africana (African angelshark)	1.2
Carcharhinus amboinensis (Java shark)	1.6
Carcharhinus leucas (Bull shark)	1.2
Carcharias taurus (Ragged tooth shark)	1.1
Notorynchus cepedianus (Broadnose sevengill shark)	1
Carcharodon carcharias (Great white shark)	1.1

Table 2.3. Matrix of significant differences of DDx and its different isomers between the elasmobranchs collected from the east and south coast of South Africa. Significance was regarded as $p < 0.05$. DDE (A), DDD (B), DDT (C)

	1	2	3	4	5	6	7	8	9	10	11	12	13	14	15	16	17	18	19	20	21	22
1	X			A,B,C											A,B,C							
2		X														A,B,C						
3			X	A,B,C			A,B,C								A,B,C		A,B,C					
4				X	A,B,C	A,B,C		A,B,C			A,B,C		A,B,C	A,B,C		A,B,C		A,B,C	A,B,C		A,B,C	
5					X																	
6						X	A,B,C								A,B,C		A,B,C					A,B,C
7							X							A,B,C		A,B,C					A,B,C	
8								X							A,B,C		A,B,C					
9									X							A,B,C						
10										X						A,B,C						
11											X				A,B,C							
12												X				A,B,C						
13													X		A,B,C		A,B,C					
14														X	A,B,C		A,B,C					
15															X	A,B,C		A,B,C	A,B,C		A,B,C	
16																X	A,B,C			A,B,C		A,B,C
17																	X				A,B,C	
18																		X				
19																			X			
20																				X		
21																					X	A,B,C
22																						X

Numbers representing the different elasmobranch species: 1=*M. kuhlii,* 2=*M. eregoodootenkee,* 3=*A. bovinusi,* 4=*R. jayakari,* 5=*P. pantherinum,* 6=*R, straeleni,* 7= H. edwardsii, 8=*H. fuscus,* 9=*H. pictus,* 10=*M. mustelus,* 11=*G. cuvier,* 12=*S. lewini,* 13= *C. brevipinna,* 14=*C. limbatus,* 15=*C. obscurus,* 16=*S. zygaena,* 17=*S. africana,* 18=*C. amboinensis,* 19=*C. leucas,* 20=*C. taurus,* 21=*N. cepedianus,* 22=*C. carcharhias*

2.3.3 Hexachlorobenzene and chlordane

Hexachlorobenzene, trans-chlordane, and cis-chlordane were present in all the muscle tissues of all analysed elasmobranch (Figure 2.8). Trans-nonachlor was present in all the muscle tissue except for *C. amboinensis* (Figure 2.8). *Rhinoptera jayakari* (oman cownose ray) showed the highest concentration of HCB and chlordanes followed by *S. africana* and *H. edwardsii* (Figure 2.8). *Squatina africana* (African angelshark) had the highest concentration of HCB and *R. jayakari* the highest concentration of ∑CHLs (Figure 2.8). *Rhinoptera jayakari* (oman cownose ray), *C. obscurus*, and *S. zygaena* once again displayed significant higher ($p<0.05$) concentrations in their muscle tissue compared to the other elasmobranch species (Table 2.4). The percentage composition for each of the chlordane isomers and HCB within elasmobranch species are as follow: 32% (HCB), 26.8% (trans-chlordane), 20% (cis-chlordane), and 21.1% (T-non) for shark species and 26.6% (HCB), 33.1% (T-chlor), 20.3% (C-chlor), and 20.1% (T-non) for the ray and skate species (Figures 2.9 and 2.10).

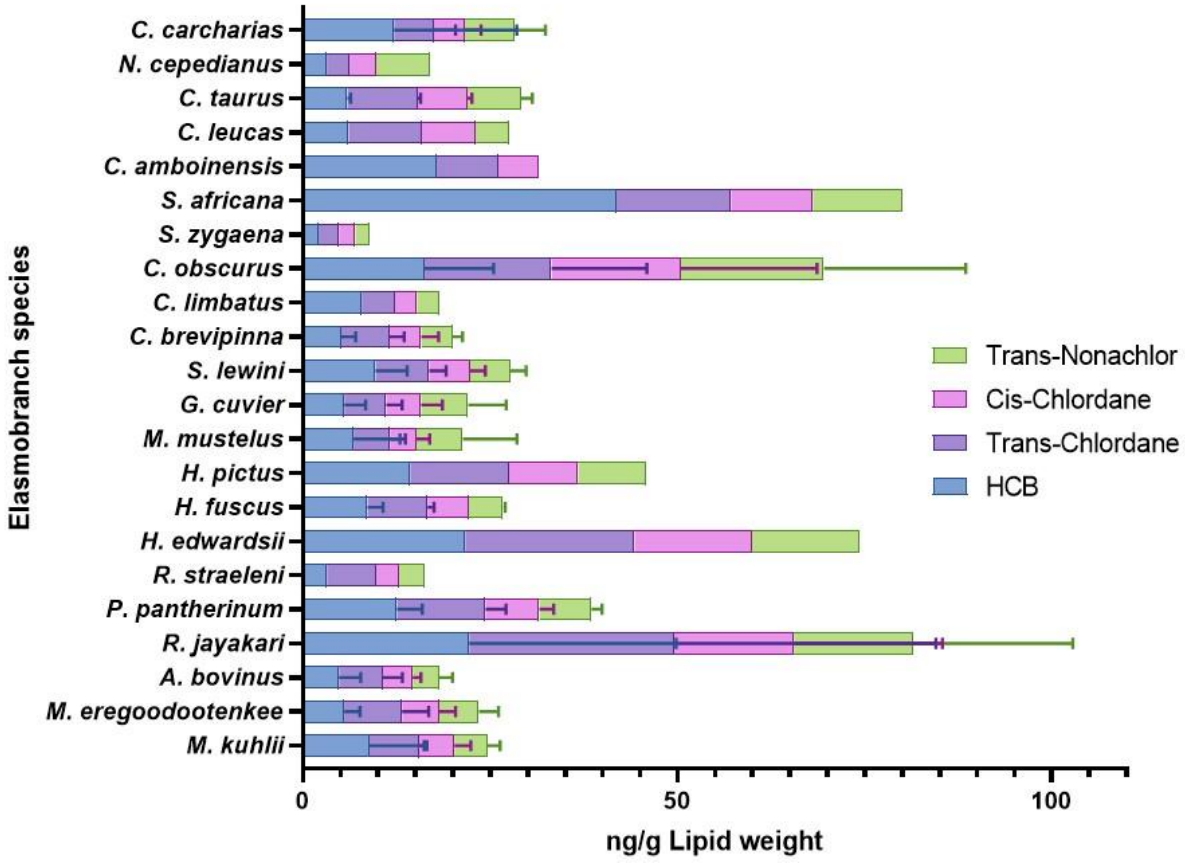

Figure 2.8: Nonachlor, Chlordanes, and HCB concentrations (ng/g LW) found within muscle tissue of different elasmobranch species collected from the east and south coast of South Africa.

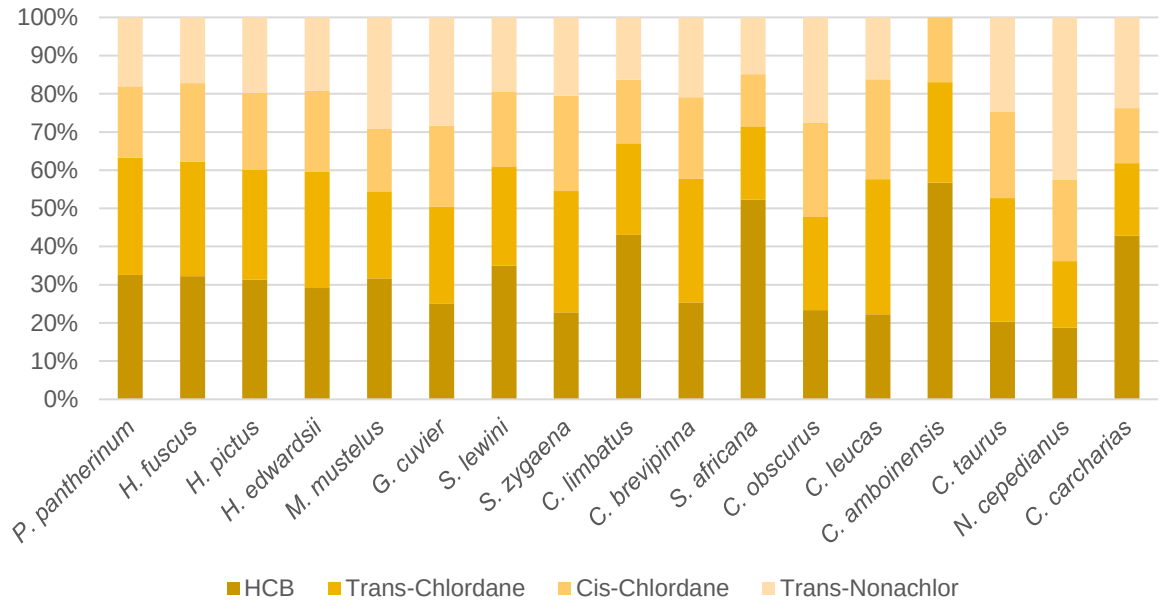

Figure 2.9: Percentage contributions of different OCP HCB and CHL isomers in sampled shark species.

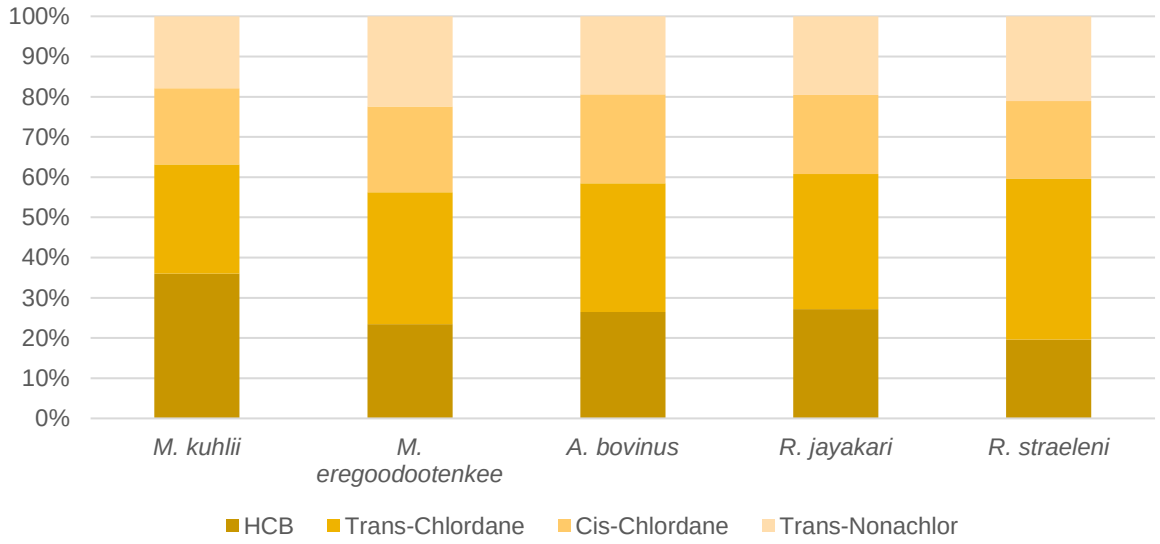

Figure 2.10: Percentage contribution of different OCP HCB and CHL isomers in sampled ray and skate species.

Table 2.4. Matrix of significant differences of Hexachlorobenzene (A) and Chlordanes (trans-chlordane (B), cis-chlordane (C), trans-nonachlor (D)) and its different isomers between the elasmobranchs collected from the east and south coast of South Africa. Significance was regarded as $p < 0.05$.

	1	2	3	4	5	6	7	8	9	10	11	12	13	14	15	16	17	18	19	20	21	22
1	X			A,B,C,D											A,B,C,D							
2		X														A,B,C,D						
3			X	A,B,C,D			A,B,C,D								A,B,C,D		A,B,D					
4				X	A,B,C,D	A,B,C,D		A,B,C,D			A,B,C,D		A,B,C,D	A,B,C,D		A,B,C,D		A,B,C,D	A,B,D		A,B,D	
5					X																	
6						X	A,B,C,D								A,B,C,D		A,B,C,D					A,B,C,D
7							X							A,B,C,D		A,B,C,D					A,B,C,D	
8								X							A,B,C,D		A,B,C,D					
9									X							A,B,C,D						
10										X						A,B,C,D						
11											X				A,B,C,D							
12												X				A,B,C,D						
13													X		A,B,C,D		A,B,C,D					
14														X	A,B,C,D		A,B,C,D					
15															X	A,B,C,D		A,B,C,D	A,B,C,D		A,B,C,D	
16																X	A,B,C,D			A,B,C,D		A,B,C,D
17																	X				B,C,D	
18																		X				
19																			X			
20																				X		
21																					X	A,B,C,D
22																						X

Numbers representing the different elasmobranch species: 1=*M. kuhlii,* 2=*M. eregoodootenkee,* 3=*A. bovinusi,* 4=*R. jayakari,* 5=*P. pantherinum,* 6=*R, straeleni,* 7= H. edwardsii, 8=*H. fuscus,* 9=*H. pictus,* 10=*M. mustelus*, 11=*G. cuvier,* 12=*S. lewini,* 13= *C. brevipinna,* 14=*C. limbatus,* 15=*C. obscurus*, 16=*S. zygaena,* 17=*S. africana,* 18=*C. amboinensis,* 19=*C. leucas,* 20=*C. taurus,* 21=*N. cepedianus*, 22=*C. carcharhias*

2.3.4 Influence of sex and trophic position on OCP levels in elasmobranchs

The increased OCPs with increasing trophic position within the female elasmobranchs were seen to be statistically significant ($p<0.05$), however the males did not display the same statistical significance. The percentage OCP composition in *M. mustelus* males (Figure 2.11) was dominated by DDxs (98%), while the females accumulated 69% DDxs, 22% chlordanes, and 8% HCB (Figure 2.13). However, when looking at the concentrations of OCPs bioaccumulated in the males and females of *M. mustelus*, the males bioaccumulated significantly higher ($p<0.05$) concentrations of OCPs than the females (Appendix A).

There were no significant differences between the different OCP ratios as well as OCP composition in male and female ray and skate species (Figure 2.12 and 2.14). When comparing the concentrations of OCP found within male and female muscle tissue, male representatives showed higher concentrations but not significantly of all OCP compared to females. Males displayed two to three and a half times more OCPs, primarily DDxs, in muscle tissue (Appendix A).

The ΣOCP concentrations and trophic position of elasmobranchs sampled from the south and east coast of South Africa (Figure 2.15A) displayed a positive but non-significant relationship ($r^2 = 0.141$, $p = 0.086$). Although the rays and skate (*M. kuhlii, M. eregoodootenkee, A. bovinus, R. jayakari,* and *R. straeleni*) sampled from the south coast of South Africa occupied the lowest trophic position they did not necessarily have the lowest OCP levels. When analysing the relationships between ∑OCP and trophic position of males (Figure 2.15B) and females (Figure 2.15C) separately it was evident that only the female elasmobranchs displayed a significant relationship ($r^2 = 0.5462$, $p = 0.0025$).

The results of ∑DDxs (Figure 2.16) (A) showed a significant correlation ($p<0.05$) with the trophic positions of the elasmobranchs. The males had no significant correlation with ∑DDxs (Figure 2.16C), however that of the females were significant (Figure 2.16E). The chlordanes did not display any significant correlation between the males and females (Figure 2.16B, D, F).

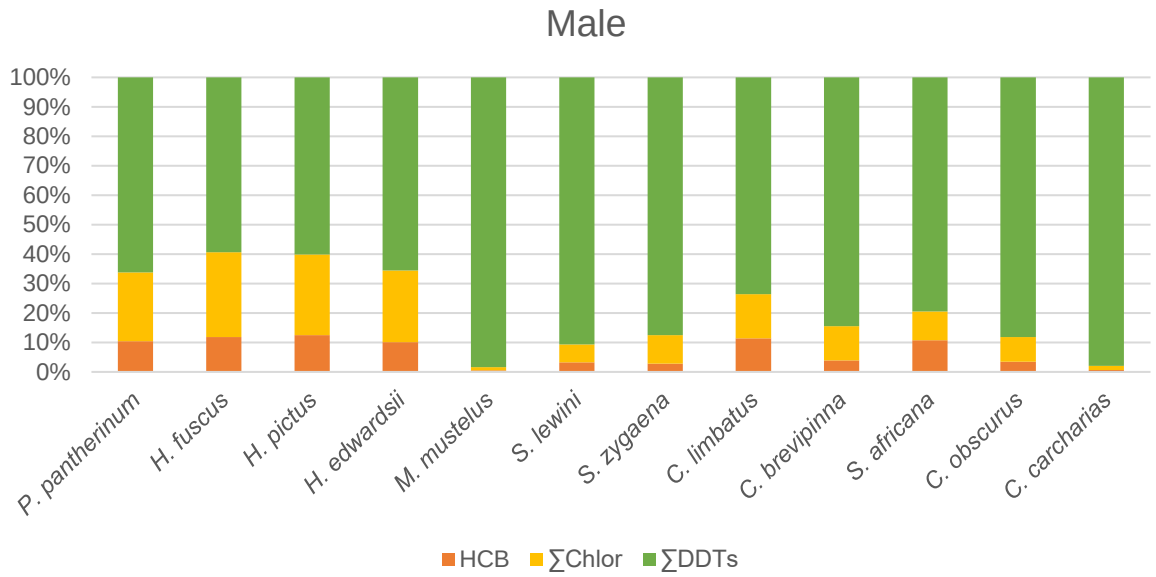

Figure 2.11: Percentage contributions of OCP concentrations analysed in sampled male shark species.

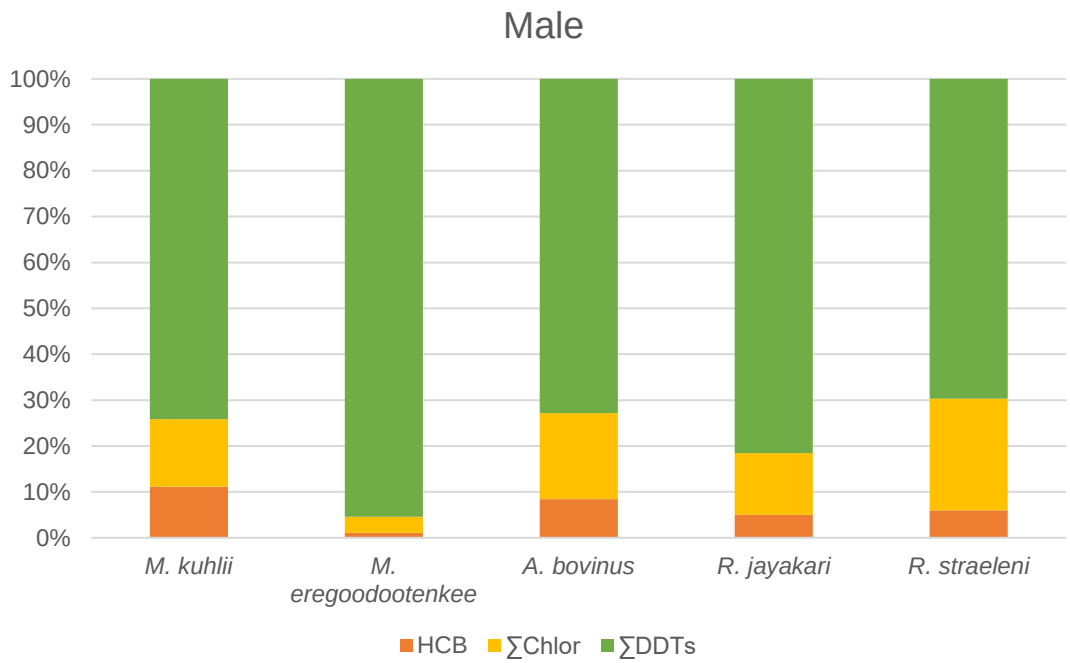

Figure 2.12: Percentage contributions of OCP concentrations analysed in sampled male ray and skate species.

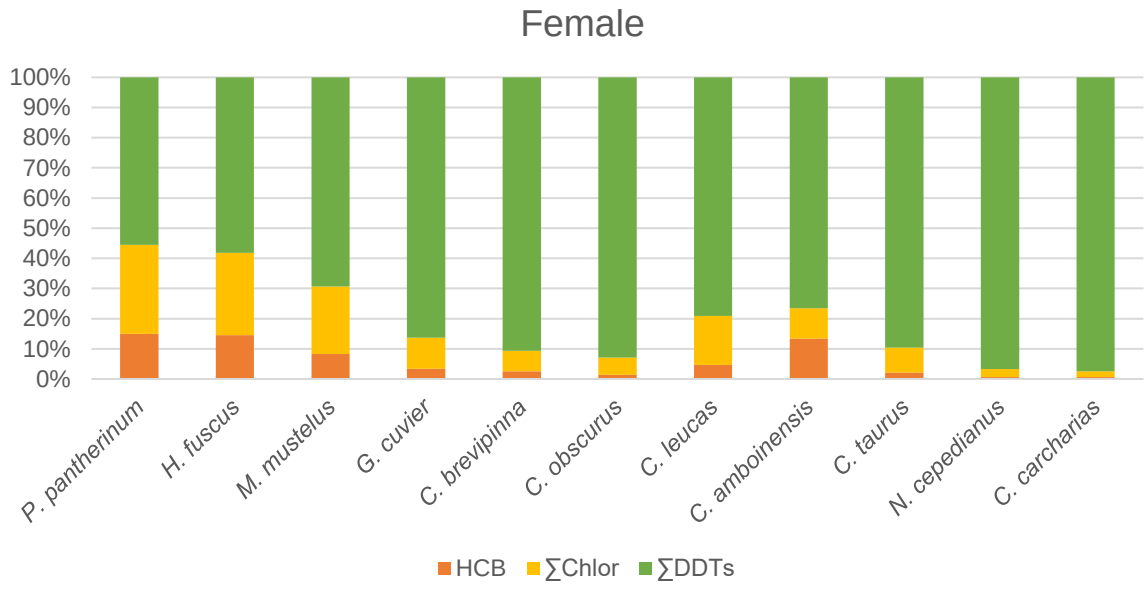

Figure 2.13: Percentage contributions of OCP concentrations analysed in sampled female shark species.

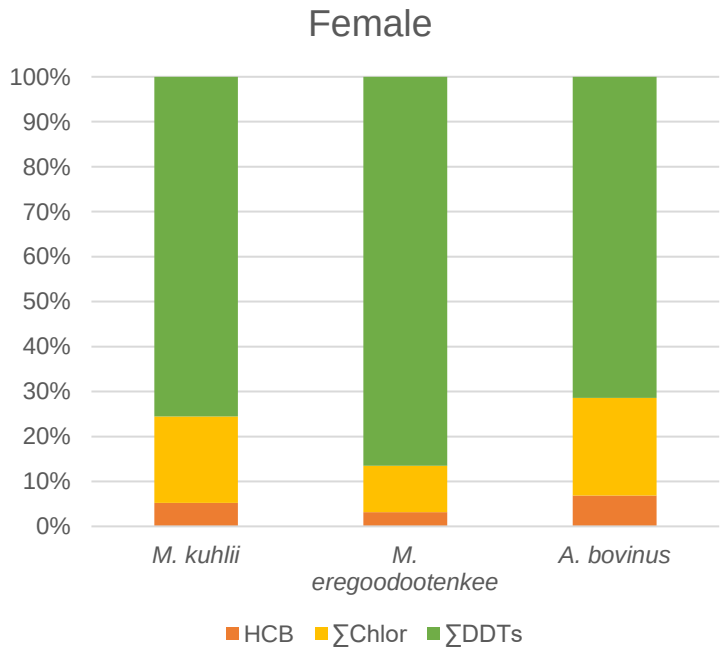

Figure 2.14: Percentage contributions of OCP concentrations analysed in sampled female ray species.

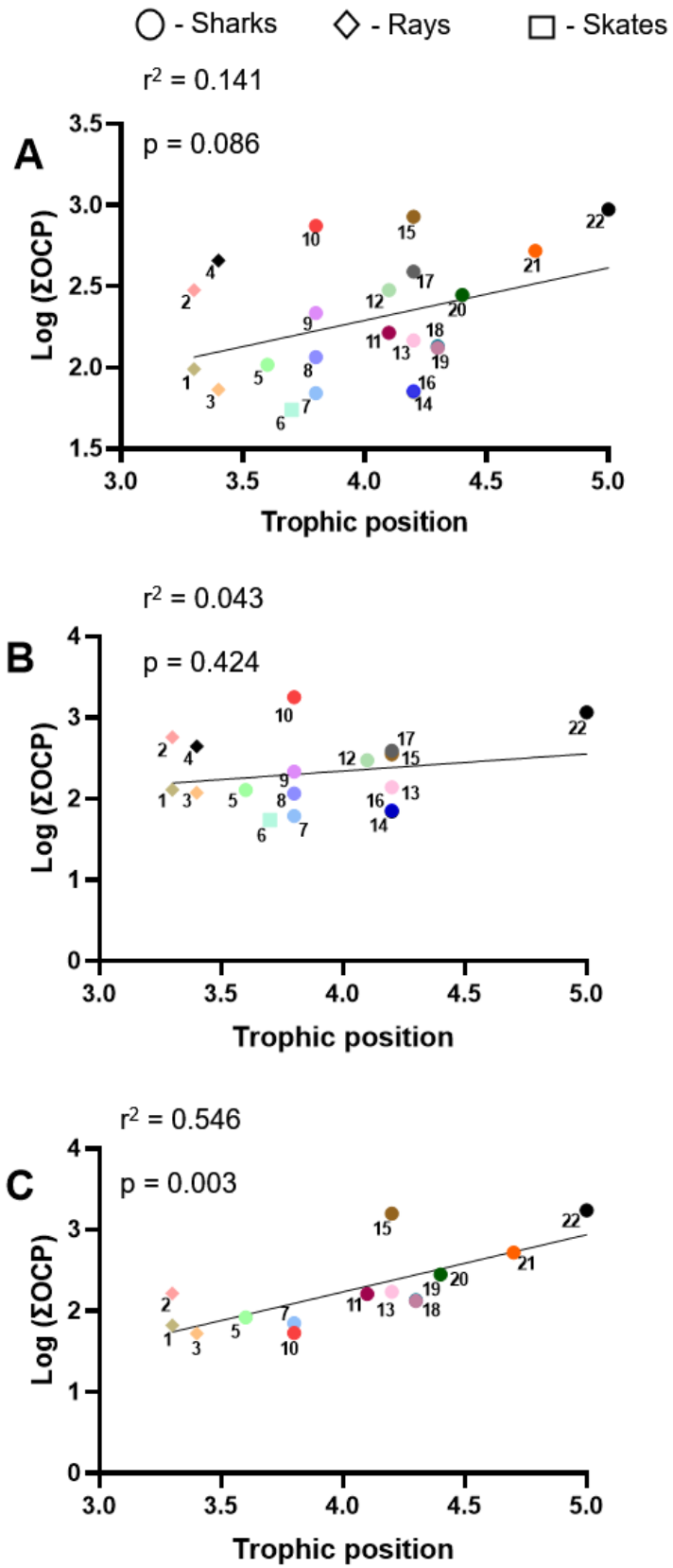

Figure 2.15: Correlation of the log of the total organochlorine pesticide (∑OCP) concentrations against the trophic position (TP) of male and female elasmobranch species collected from the east- and south coast of South Africa (r^2 = 0.141, p = 0.086) (A), Male elasmobranchs (r^2 = 0.043, p = 0.424) (B), Female elasmobranchs (r^2 = 0.546, p = 0.003) (C). Number with corresponding species are presented in the footnote of Table 2.4.

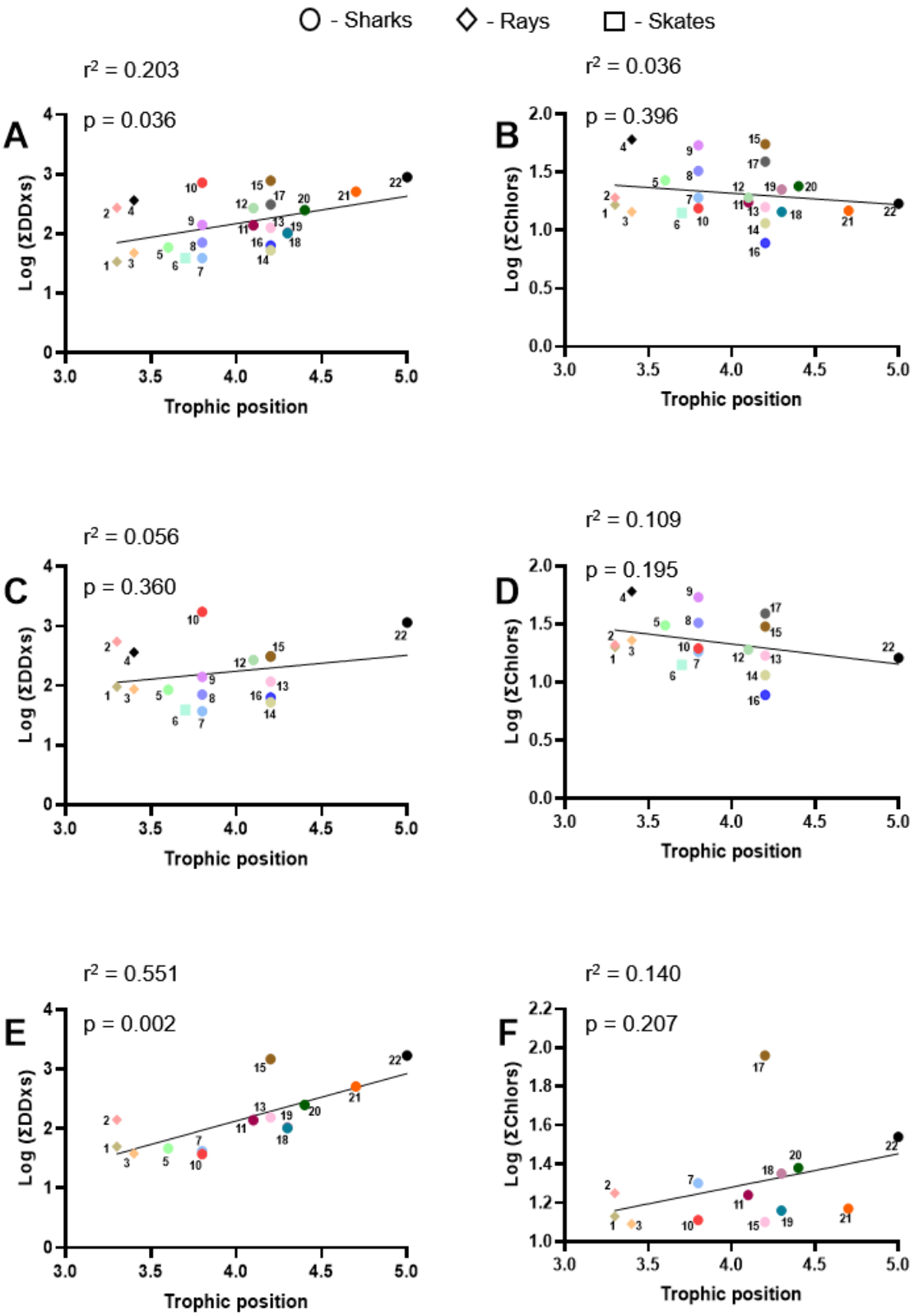

Figure 2.16: Correlation of the log of the sum of DDxs and Chlors concentrations against the trophic position (TP) of male and female elasmobranch species collected from the east- and south coast of South Africa (r^2 = 0.203, p = 0.036) (A), (r^2 = 0.036, p = 0.396) (B); Male elasmobranchs (r^2 = 0.056, p = 0.360) (C), (r^2 = 0.109, p = 0.195) (D); Female elasmobranchs (r^2 – 0.551, p – 0.002) (E), (r^2 = 0.140, p = 0.207) (F). Number with corresponding species are presented in the footnote of Table 2.4.

2.3.5 Influence of sampling region on the OCP levels

For the purpose of the regional analyses, the elasmobranch species were grouped as sharks, skates and rays from the east and south coasts of South Africa. The PCA biplot (Figure 2.17) described 82.24% of the variation on the two axes. The first axis described 66.5% of the variation, and the second described 15.75% of the variation in the OCP levels in the elasmobranchs studied.

Distinct differences were found with elasmobranchs with high p,p-DDE and trans-nonachlor grouping together and elasmobranchs with predominantly cis-chlordane, p,p-DDD, HCB, trans-chlordane, and p,p-DDT grouping together. The increasing concentrations are reflected on the second axis from left to right in the biplot. It was notable that mainly shark species displayed increased concentrations of p,p-DDE compared to the different ray and skate species. However, it was clear that there was no differentiation in OCP profiles in sharks from the east and south coasts.

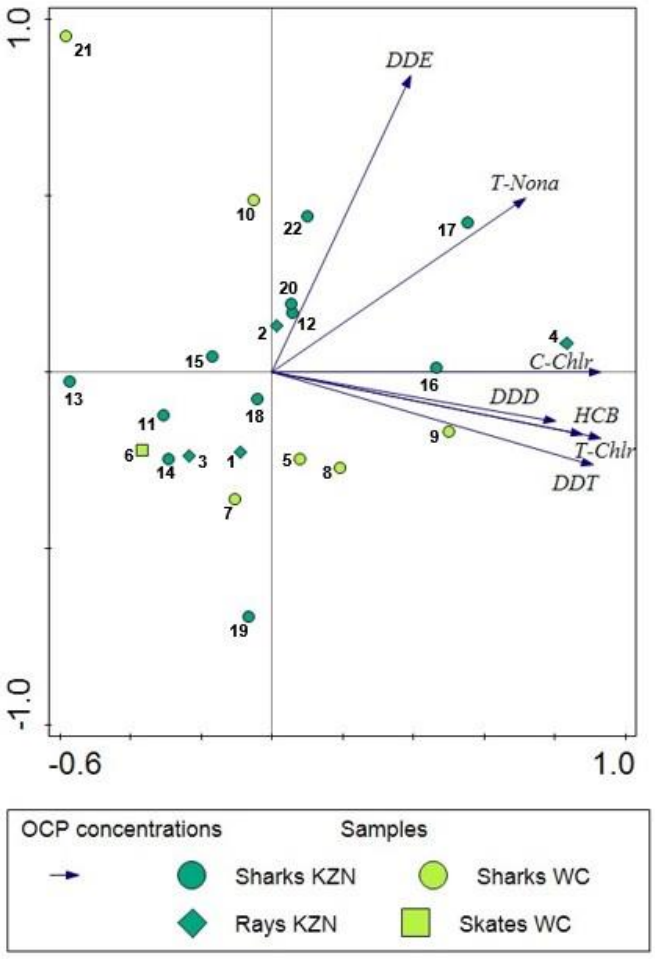

Figure 2.17: Principal component analysis (PCA) biplot graph using the mean organochlorine pesticide concentrations from the muscle samples of the elasmobranch species. Fist two axes explained 82.24% of the variation in OCP levels in elasmobranchs from the east and south coasts of South Africa.

2.3.6 Human health risks associated with the consumption of OCP contaminated elasmobranchs

The assessment of non-carcinogenic and carcinogenic human health risks involved calculating the hazard quotient and cancer risk, respectively. The estimated daily intake levels (EDI) of HCB, chlordanes, and DDxs exceeded the acceptable daily intake (ADI) for almost all the elasmobranchs (Kim *et al.,* 2013) (Table 2.5). The hazard risk quotients for HCB, ∑CHLs, and DDxs were <1, except for the DDxs HQ values for *M. mustelus* (1.6±2.4), *N. cepedianus* (2.7), and *C. carcharias* (3±2.8) (Table 2.6). This suggests a high likelihood of non-carcinogenic, adverse human health effects associated with regular consumption of these elasmobranchs contaminated with DDxs. Furthermore, all elasmobranch species exhibited an unacceptable carcinogenic risk, with cancer risk values exceeding 10^{-4}, for HCB, ∑CHLs, and DDxs (Table 2.7). The maximum safe consumption limit for the the elasmobranchs was calculated on DDE and the maximum safe consumption limit between the species ranged from 6 g to 537 g of muscle tissue per day (Table 2.8).

Table 2.5. Estimated daily intake (EDI mg/kg/day) of organochlorine pesticides calculated for South African citizens who consume elasmobranch muscle tissue and comparison to acceptable daily intake (ADIs mg/kg/day) (WHO, 1961; FAO/WHO, 1987; WHO, 1997).

	HCB	**∑CHLs**	**DDxs**
ADIs	**0.042***	**0.035***	**0.7***
Mobula kuhlii (Shortfin devil ray)	0.02±0.06	0.04±0.02	0.2±0.04
Mobula eregoodootenkee (Longhorn devil ray)	0.02±0.01	0.05±0.002	0.7±0.6
Aetomylaeus bovinus (Bull ray)	0.02±0.003	0.05±0.008	0.2±0.1
Rhinoptera jayakari (Oman cownose ray)	0.02±0.001	0.05±0.005	0.2±0.1
Poroderma pantherinum (Leopard catshark)	0.02±0.003	0.04±0.006	0.1±0.04
Raja straeleni (Spotted skate)	0.01	0.06	0.2
Haploblepharus edwardsii (Puffadder shyshark)	0.02±0.006	0.05±0.004	0.1±0.01
Haploblepharus fuscus (Brown shyshark)	0.02	0.04	0.08
Haploblepharus pictus (Dark shyshark)	0.02	0.04	0.1
Mustelus mustelus (Smoothhound shark)	0.02±0.01	0.05±0.02	2.0+4.0
Galeocerdo cuvier (Tiger shark)	0.02±0.004	0.05±0.01	0.4±0.3
Sphyrna lewini (Scalloped hammerhead shark)	0.02±0.005	0.04±0.009	0.6±0.2
Carcharhinus brevipinna (Spinner shark)	0.01	0.05	0.4
Carcharhinus limbatus (Blacktip shark)	0.03	0.04	0.2
Carcharhinus obscurus (Dusky shark)	0.02±0.0007	0.04±0.004	0.4±0.1
Sphyrna zygaena (Smooth hammerhead shark)	0.04	0.04	0.3
Squatina africana (African angel shark)	0.02±0.007	0.06±0.01	0.8±0.4
Carcharhinus amboinensis (Java shark)	0.01	0.05	0.2
Carcharhinus leucas (Bull shark)	0.04	0.03	0.2
Carcharias taurus (Ragged tooth shark)	0.01±0.0009	0.05±0.005	0.5±0.5
Notorynchus cepedianus (Broadnose sevengill shark)	0.02	0.1	4.0
Carcharodon carcharias (Great white shark)	0.06+0.09	0.07±0.02	5.0±4.0

EDI adjusted according to the 70 kg body weight of adults. EDI for HCB set at 0.6 µg/kg-day bw*, ∑CHLs set at 0.5 µg/kg-day bw*, 10 µg/kg-day bw*(Kim *et al.,* 2013).

Table 2.6. The mean and standard deviation of hazard quotients (HQ) for the elasmobranch species calculated on the mean concentration in the muscle tissue. Hazard quotient values >1 are shaded in the table below.

	HCB	**∑CHLs**	**DDxs**
Hazard quotients for non-carcinogenic risk (HQ)			
Mobula kuhlii (Shortfin devil ray)	0.008±0.002	0.028±0.011	0.12±0.026
Mobula eregoodootenkee (Longhorn devil ray)	0.007±0.0005	0.034±0.002	0.48±0.417
Aetomylaeus bovinus (Bull ray)	0.007±0.001	0.031±0.005	0.11±0.07
Rhinoptera jayakari (Oman cownose ray)	0.007±0.001	0.03±0.003	0.13±0.067
Poroderma pantherinum (Leopard catshark)	0.008±0.001	0.028±0.004	0.064±0.024
Raja straeleni (Spotted skate)	0.006	0.037	0.11
Haploblepharus edwardsii (Puffadder shyshark)	0.009±0.002	0.031±0.003	0.064±0.024
Haploblepharus fuscus (Brown shyshark)	0.007	0.025	0.054
Haploblepharus pictus (Dark shyshark)	0.007	0.029	0.077
Mustelus mustelus (Smoothhound shark)	0.01±0.006	0.035±0.012	1.6±2.4
Galeocerdo cuvier (Tiger shark)	0.007±0.002	0.035±0.012	0.28±0.17
Sphyrna lewini (Scalloped hammerhead shark)	0.009±0.002	0.027±0.006	0.38±0.17
Carcharhinus brevipinna (Spinner shark)	0.006	0.032	0.29
Carcharhinus limbatus (Blacktip shark)	0.011	0.023	0.12
Carcharhinus obscurus (Dusky shark)	0.006±0.0002	0.03±0.003	0.25±0.098
Sphyrna zygaena (Smooth hammerhead shark)	0.017	0.025	0.2
Squatina africana (African angel shark)	0.008±0.002	0.037±0.008	0.42±0.24
Carcharhinus amboinensis (Java shark)	0.006	0.033	0.16
Carcharhinus leucas (Bull shark)	0.016	0.02	0.15
Carcharias taurus (Ragged tooth shark)	0.005±0.0004	0.031±0.003	0.34±0.32
Notorynchus cepedianus (Broadnose sevengill shark)	0.01	0.072	2.7
Carcharodon carcharias (Great white shark)	0.027±0.039	0.047±0.017	3.0±2.8

RfD levels (µg/kg) used are as follows: HCB (0.0008); CHLs (0.0005); DDTs (0.0005) (ATSDR, 2018, 2019; USEPA-IRIS, 2019).

Table 2.7. The cancer risk (CR) for the elasmobranch species calculated on the mean concentration in the muscle tissue.

	HCB	**∑CHLs**	**DDxs**
Cancer risk (CR) (x10^{-4})			
Mobula kuhlii (Shortfin devil ray)	3.0±0.94	1.4±0.56	5.6±1.2
Mobula eregoodootenkee (Longhorn devil ray)	2.5±0.22	1.8±0.085	23.8±20.5
Aetomylaeus bovinus (Bull ray)	2.5±0.43	1.6±0.27	5.4±3.4
Rhinoptera jayakari (Oman cownose ray)	2.8±0.2	1.6+1.7	6.1±3.3
Poroderma pantherinum (Leopard catshark)	3.3±0.5	1.5±0.21	3.0±1.1
Raja straeleni (Spotted skate)	2.2	2.0	5.0
Haploblepharus edwardsii (Puffadder shyshark)	3.5±0.92	1.6±0.13	3.0±0.25
Haploblepharus fuscus (Brown shyshark)	2.7	1.3	2.6
Haploblepharus pictus (Dark shyshark)	2.8	1.5	3.6
Mustelus mustelus (Smoothhound shark)	3.7±2.3	1.8±0.64	79.9+118.0
Galeocerdo cuvier (Tiger shark)	2.9±0.71	1.8±0.61	13.9±9.0
Sphyrna lewini (Scalloped hammerhead shark)	3.4±0.84	1.4±0.31	18.9±8.4
Carcharhinus brevipinna (Spinner shark)	2.3	1.7	14.3
Carcharhinus limbatus (Blacktip shark)	4.2	1.2	5.5
Carcharhinus obscurus (Dusky shark)	2.4±0.11	1.6±0.15	12.5±4.9
Sphyrna zygaena (Smooth hammerhead shark)	6.6	1.3	9.9
Squatina africana (African angel shark)	3.1±1.1	1.9±0.39	25.8±12.2
Carcharhinus amboinensis (Java shark)	2.3	1.7	7.9
Carcharhinus leucas (Bull shark)	6.2	1.0	6.8
Carcharias taurus (Ragged tooth shark)	1.9±0.14	1.6±0.17	16.7±16.0
Notorynchus cepedianus (Broadnose sevengill shark)	4.0	3.8	135.2
Carcharodon carcharias (Great white shark)	10.3+15.0	2.4±0.87	151.8±138.6

Cancer slope factor (CSF) (mg/kg/day) of OCPs were identified as follows: HCB (1.6); CHLs (0.35); DDE (0.34); DDD (0.24); DDT (0.34) (USEPA-IRIS, 2019)

Table 2.8. Safe consumption limit for each species of elasmobranch when observing the highest concentration of one of the OCPs.

	p,p'-DDE
Maximum safe consumption limit per day (g)	
Mobula kuhlii (Shortfin devil ray)	218.2±38.8
Mobula eregoodootenkee (Longhorn devil Ray)	64.3±45.9
Aetomylaeus bovinus (Bull ray)	225.0±96.4
Rhinoptera jayakari (Oman cownose ray)	229.0±130.3
Poroderma pantherinum (Leopard catshark)	374.1±86.2
Raja straeleni (Spotted skate)	237.6
Haploblepharus edwardsii (Puffadder shyshark)	428.8±100.0
Haploblepharus fuscus (Brown shyshark)	537.0
Haploblepharus pictus (Dark shyshark)	363.7
Mustelus mustelus (Smoothhound shark)	158.4±142.0
Galeocerdo cuvier (Tiger shark)	93.2±51.1
Sphyrna lewini (Scalloped hammerhead shark)	61.7±32.4
Carcharhinus brevipinna (Spinner shark)	66.3
Carcharhinus limbatus (Blacktip shark)	203.1
Carcharhinus obscurus (Dusky shark)	86.0±35.5
Sphyrna zygaena (Smooth hammerhead shark)	102.1
Squatina africana (African angel shark)	41.7±19.4
Carcharhinus amboinensis (Java shark)	126.4
Carcharhinus leucas (Bull shark)	192.1
Carcharias taurus (Ragged tooth shark)	113.4+115.0
Notorynchus cepedianus (Broadnose sevengill shark)	6.1
Carcharodon carcharias (Great white shark)	78.2+137.6

2.4 Discussion

Recent studies (Porter *et al.*, 2017; Erasmus *et al*., 2020) indicated that OCPs enter the South African marine environment through rivers and estuaries and then accumulate in nearshore (intertidal) and offshore (coral reef) ecosystems. This accumulation of OCPs prompts concerns about the potential presence of these contaminants in other marine species as the processes of bioaccumulation (where pollutants are taken by organisms from their abiotic environment and their food) (Gray, 2002) raises the plausible assumption that if OCPs are found in intertidal and coral reef ecosystems, they may also be present in elasmobranchs. Although there are studies that deal with OCPs in mussels, fish, etc. (Milun *et al.,* 2020; Barnhoorn *et al.,* 2015), there is limited research carried out on elasmobranchs along the South African coastline and their exposure to OCPs. The results of this study clearly showed that OCPs accumulate in elasmobranch muscle tissues. Factors that determine OCP bioaccumulation patterns are related to intrinsic characteristics such as sex and the trophic level (as reflected in feeding habits). Larger scale extrinsic factors such as geographical location (e.g., east coast and south coast) were not seen as a major driver of OCP accumulation.

2.4.1 Organochlorine pesticide accumulation

The shark species with the highest levels of OCPs accumulation was *C. carcharias*, *N. cepedianus*, *C. obscurus*, and *M. mustelus*. *Rhinoptera jayakari* (oman cownose ray) and *M. eregoodootenkee* also had elevated concentrations compared to the other elasmobranch species occupying the same trophic position. Both *C. obscurus*, *S. zygaena,* and *R. jayakari* differed significantly ($p < 0.05$) from the other elasmobranch species. Elevated levels of OCPs were found in the muscle tissue of *Carcharhinus obscurus* (dusky shark) and *R. jayakari*, with over 90% being DDxs in the case of *C. obscurus*. *Sphyrna zygaena* (smooth hammerhead shark) had decreased OCP levels compared to other elasmobranchs occupying the same trophic position.

All OCPs concentrations in tissue samples of the respective shark species were higher when compared to previous studies, such as that by Beaudry *et al.* (2015) and Schlenk *et al.* (2005) around the coast of South Africa. When the results of Beaudry *et al.* (2015) are compared to the study by Schlenk *et al.* (2005), a notable increase in OCP levels could be identified, and when the results from Beaudry *et al.* (2015) are compared to the present study, a slight increase in HCB can be seen paired with a decrease in chlordanes and DDxs, except for the levels of DDxs identified by Boldrocchi *et al.* (2019) in *S. lewini* that was significantly higher than found in the current study. This is an indication that there has been a reduction in the

introduction of DDxs and chlordanes in the marine waters of southern Africa when compared to northern Africa. The elasmobranchs with the highest concentrations of OCPs, the sharks occupying the higher trophic positions (*C. carcharias, N. cepedianus, C.* obscurus), are those with a global distribution and distinct migratory behaviour. According to Rogers *et al*. (2013) and Cagnazzi *et al*. (2019) nomadic species, such as white sharks, hammer heads and dusky sharks, will be exposed to OCPs from a variety of sources during their migration. However, more local exposure factors resulted in shark species (*M. mustelus*) and ray species (*R. jayaka*ri and *M. eregoodootenkee*) occupying lower trophic positions to also display elevated OCP levels. This is probably related to feeding behaviour where contaminated plankton and even sediments may be the sources of OCPs (Khang *et al.,* 2022; and Cagnazzi *et al*., 2019)).

The DDxs were the highest percentage contribution of OCPs in the muscle tissue of elasmobranchs with the DDT congener ratios (DDD/DDE to DDT) indicating the implied historical use of DDT (Doong et al., 2002; Zhou et al., 2006). The percentage composition of DDE was 78.7% and 70.4% in sharks and rays, respectively. This indicates that the average DDT ratios are 1.225 and 1.3 for the sharks and rays respectively. Tsydenova *et al.* (2004) proposed that a value above 0.6 indicates no recent inputs into the environment. These ratios indicate that the DDxs composition is dominated by DDE and as such supports the breakdown of DDT within the environment and the muscle tissue of elasmobranchs into DDE through the process of dehydrochlorination (Zhang *et al.* 1999).

Schlenk *et al.* (2005) found significantly lower levels of DDxs, and Beaudry *et al.* (2015) found higher levels of DDxs in the elasmobranchs they studied. Research findings of Cagnazzi *et al.* (2019) revealed that the concentrations of DDxs within the samples of *C. carcharias* and *C. obscurus* along the southeastern coast of Australia were even higher than the concentrations found in the present research study. Concentration values of DDxs in *C. obscurus* in the current study were lower than the values recorded by Beaudry *et al.* (2015) for the same species. This discrepancy could be due to the *C. obscurus* of the Beaudry *et al.* (2015) study being larger adults individuals, whereas the *C. obscurus* from this study was considered juveniles. Findings by Erasmus *et al.* (2022) that revealed that the accumulation of contaminants in elasmobranchs was correlated with an increase in size and subsequent changes in foraging behaviour.

Rhinoptera jayakari (oman cownose ray) displayed the highest concentrations of OCPs of all elasmobranchs that occupied the same trophic position and were notably larger. *Rhinoptera jayakari* (oman cownose ray) is regarded a benthopelagic species feeding on molluscs and invertebrates, which could explain the increased levels of DDxs found, as well as the average length recorded at 134 cm, well above the maximum set at 90 cm. Cagnazzi *et al.* (2019)

found elevated levels of DDxs within *M. kuhlii* and *R. neglecta* (closely related to *R. jayakari*), except for one of the *R. jayakari* from this current study displayed DDxs levels higher than that reported by Cagnazzi *et al.* (2019) with a concentration of 545 ng/g compared to 262 ng/g, this male individual from the current study was, however, double the size than the one from Cagnazzi *et al.* (2019).

Mustelus mustelus (smoothhound shark) exhibited the presence of DDxs, although they were not sampled on the eastern coast, where DDT is actively sprayed. The potential leaching of contaminants from adjacent freshwater systems into the marine environment (Gerber *et al.,* 2016; Buah-Kwofie *et al.,* 2018; Volschenk *et al.,* 2019; Olisah *et al.,* 2020, 2021) was a possibility the reason for relatively high levels of DDE in representatives of the east coast of the current study. Elevated levels of DDE in *M. mustelus* tissue samples may be due to the combined effects of leaching and the Agulhas current that transports contaminants south along the coast of South Africa. These results could potentially also be explained by the fact that *M. mustelus* is predominately a demersal feeder (crustaceans, cephalopods, and fish) on continental shelves and uppermost slopes with minimal migratory patterns.

Comparing the OCP levels with Australia, Cagnazzi *et al.* (2019) found lower levels of HCB within *C. obscurus*. However, *C. carcharias* displayed higher levels of HCB. Chlordane levels in *M. mustelus* were also lower. However, many of the elasmobranchs showed notably increased levels of DDx *(C. carcharias, C. leucas*, *C. limbatus*, and *M. kuhlii*). Schlenk *et al.* (2005) and Cagnazzi *et al.* (2019) reported the presence of HCB within the muscle tissue of elasmobranchs from South Africa and Australia, respectively. Schlenk *et al.* (2005) identified HCB in three *C. carcharias* individuals with concentrations ranging from 1.3 ng/g lw to 4 ng/g lw. Cagnazzi *et al.* (2019) identified HCB in six different shark species (*C. carcharias, C. obscurus, C. taurus,C. leucas, S. mokarran* and *C. limbatus*) and two different species of rays (*M. kuhlii, R. neglecta*), with all individuals having higher concentrations compared to that reported by Schlenk *et al.* (2005). *Carcharodon carcharias* from the Cagnazzi *et al.* (2019) study had a threefold the concentration of HCB when compared to the highest concentration found within the current study, i.e. 155 ng/g HCB in *C. carcharias* tissue. This individual was also the largest of all the *C. carcharias* (345 cm) sampled. The current study had results of HCB concentrations in *C. carcharias comparable* to Schlenk *et al.* (2005), with only two individuals in the current study showing higher concentrations of HCB with 11 ng/g lw and 49 ng/g lw, respectively.

Hammerhead sharks (*S. lewini* and *S. zygaena*) in the current study had higher levels of HCB compared to the individuals analysed around the coast of Korea and the Gulf of California, Mexico, by Lee *et al.* (2015) and Briones *et al.* (2022), respectively. The *S. lewini* from Mexico

(Briones *et al.,* 2022) were juveniles compared to adults in the current studies, leading to the assumption of different feeding habits and the migratory patterns of the adult *S. lewini* that influence the accumulation of OCPs. The *S. zygaena* analysed in both the current study and Lee *et al.* (2015) were juveniles. However, levels of HCB and ∑Chlors were higher in the current study, suggesting remnants of chlordanes still present within the marine environment around the coast of South Africa. When compared to the results from Beaudry *et al.* (2015), the levels of chlordanes were lower in especially *C. carcharias* and *C. obscurus* analysed by Schlenk *et al.* (2005) almost 20 years ago.

2.4.2 Intrinsic factors (Sex and trophic position/feeding behaviour)

The trophic position played a significant role in the accumulation of contaminants, with the elasmobranchs that accumulated the most OCP occupied the higher trophic positions. Additionally, Erasmus *et al.* (2022) found that the size of elasmobranchs plays a significant role in accumulation of mercury, and this was also observed for OCPs in the present study. A significant increase in OCP concentrations in relation to the elasmobranchs trophic positions was only found for female ($p = 0.0025$). This could be due to the difference in lipid content found between male and female elasmobranchs (0.14% and 0.16%, respectively) due to differences in maturation, especially in female rays that showed elevated percentages of lipid content in this study. Wourms (1977) indicated the differences in gonad development within different elasmobranchs, however, no baseline on the different timeframes associated with the development thereof has been developed. Furthermore, research by Last *et al.* (2016), Ebert *et al.* (2021) and Froese & Pauly (2022) showed that the maturation of elasmobranchs will differ between males and females. This suggests some possible feeding differences between males and females due to ontogenetic diet shifts occurring within elasmobranch species. *Carcharodon carcharias, C. obscurus,* and *C. limbatus* have displayed cases of ontogenetic diet shifts occurring (Kim *et al.,* 2012; Ebert *et al.,* 2021; Matulik *et al.,* 2017).

Among sharks and different species of rays and skates, the concentration of OCP within females was higher than its male counterparts, except for *M. mustelus*, *M. eregootenkee*, and *M. kuhlii*. The female counterparts were also, on average, longer and heavier than the male counterparts, except for *M. mustelus*, where the males were longer and much heavier than the females. However, *M. mustelus females* were still regarded as juveniles, and this may be the reason for the lower levels of OCP present.

Compared to other male elasmobranchs that occupy the same trophic position, *M. mustelus* demonstrated distinct differences, such as higher concentrations of OCPs compared to their female counterparts. Male individuals were longer and heavier than most sampled females and showed markedly increased concentrations of DDE and DDD. This increase in organic

compounds associated with the increase in size of elasmobranchs was also identified by Cagnazzi *et al.* (2019) and Gilbert *et al.* (2015) off the coast of Australia. In particular, one of the female individuals had a comparable length and weight to those of the male counterparts, yet the males still showed significantly higher concentrations of DDE and DDD.

Similar increase OCP concentrations were seen in females of *C. obscurus*, which differed from the other female elasmobranchs occupying the same trophic position, when compared to the male counterparts. All male *C. obscurus* individuals were juveniles, while female *C. obscurus* was both the longest and the heaviest of all individuals, which could lead to an increased likelihood that the individual was older than the rest and thus having more opportunity to bioaccumulate these pesticides. Young *C. obscurus* are also known to forage closer to shore as they prefer shallower waters. Further research by Cagnazzi *et al.* (2019) on *C. obscurus* found HCB concentrations around 6 ng/g. This is lower than the concentrations observed in the *C. obscurus* individuals of the current study (16 ng/g). The *C. obscurus* observed in the study by Cagnazzi *et al.* (2019) was an immature female with a length of 220 cm and thus larger compared to the immature female from the current study (131 cm) with an HCB concentration of 27 ng/g. This could be attributed to the ontogenetic diet change that occurs within *C. obscurus* species, with the smaller female in the current study feeding on smaller demersal prey (Ebert *et al.,* 2021) and a lower lipid content (0.03%) compared to other *C.* obscurus specimens in this study. *Carcharhinus obscurus* (dusky shark) also prefers shallower water and rarely ventures into the deep ocean.

Results for *S, zygaena* were the opposite of what was found for *C. obscurus* and had the lowest levels of OCPs within its muscle tissue. The sampled *S. zygaena* compared to *S. africana,* which occupied a trophic position, size, and sampling location similar to S. zygaena, had significantly higher OCP levels. Boldrocchi *et al.* (2019) found DDT values many times higher in *S. lewini* around the coast of Djibouti than the values found in the *S. lewini* in the current study. The DDT values reported by Boldrocchi *et al.* (2019) indicated that DDT is still being used in Djibouti and possibly in much larger quantities than in South Africa. Cagnazzi *et al.* (2019) also showed DDxs at much higher levels within *C. leucas* compared to the current study. *Carcharhinus leucas* from both studies are considered adult females, with *C. leucas* from Cagnazzi *et al.* (2019) marginally larger. *Carcharhinus leucas* (bull shark) indivuduals are known to venture into freshwater environments and possibly be exposed to elevated levels of DDxs present within the freshwater systems of Australia.

The low concentrations of OCPs found within *R. straeleni* are unexpected, and *the R. straeleni* sampled weighed more than the internationally reported maximum weight of 1.9 kg (Froese & Pauly, 2022), even while still being a juvenile. This might potentially point to the wrong

identification of this individual. *Raja straeleni* (spotted skate) occupies the highest trophic position of all species of rays and skates, and it would be expected to show the highest concentrations of OCPs. *Raja straeleni* (spotted skate) is known to feed further offshore than the other ray species and at greater depths, and this, paired with its regular migratory tendencies, could explain the lower concentrations of OCPs present.

2.4.3 Extrinsic factors (Geographical location influencing bioaccumulation)

The east coast of South Africa has abundant freshwater systems connected to the Indian Ocean, including rivers, wetlands, and. These water bodies are surrounded by agricultural activities, making pollution inevitable. Research studies by Olisah *et al.* (2020 & 2021) in the Eastern Cape and KwaZulu-Natal regions identified OCPs in rivers and estuaries, while further investigations by Volschenk *et al.* (2019), Gerber *et al.* (2016), and Buah-Kwofie *et al.* (2018) revealed contamination and bioaccumulation of OCPs in freshwater systems adjacent to the Indian Ocean in KwaZulu-Natal. This highlights the extensive impact of agricultural activities on the east coast and the potential of OCPs reaching the marine environment from these aquatic environments. However, the assumption that increased OCP input along the east coast of South Africa was reflected in the tissues of elasmobranchs was not evident. All the elasmobranch species displayed all OCP compound groups (HCB, Chlordanes, and DDxs) in their muscle tissues. Except for the few elasmobranch species that displayed elevated OCP concentrations present along the east coast (*C. carcharias*, *C. obscurus*, *R. jayakari*, and *M. eregoodootenkee*) and south coast (*M. mustelus* and *N. cepedianus*) the OCP levels were comparable between localities.

Studies conducted on elasmobranch OCP levels in coastal environments of South Africa (Schlenk *et al.,* 2005; *Beaudry et al.,* 2015), Australia (Cagnazzi *et al.,* 2019), Korea (Lee *et al.,* 2015), and Mexico (Briones *et al.,* 2022) revealed that compared to the current study Australia displayed elevated levels of OCPs and Korea and Mexico displayed slightly lower levels of OCPs. Notably, elevated levels of DDxs in white sharks (C. carcharias) from South Africa and Australia could be attributed to rapid migration up the east coast of Africa and transoceanic movement patterns, thus exposing them to various sources of contaminants (Bonfil *et al*., 2005).

In contrast the high OCP level measured in philopatric species such as the scalloped hammerhead (*S. lewini*) and bull shark (*C. leucas*) were indicative of more regional exposure pattern. These species have more restricted movements in and around nearshore and shallower regions. The high concentrations of DDxs in *S. lewini* found in the current study, and the study by Boldrocchi *et al.* (2019), may be attributable to the species' frequent residence and feeding in refuge areas along the coast (Briones *et al.,* 2022). The findings of the present

study on *C. leucas* indicate similar patterns of elevated levels of DDxs in individuals from South Africa and Australia (Cagnazzi *et al.,* 2019), in contrast to individuals from Réunion Island (situated near the eastern coast of Madagascar) (Chynel *et al.,* 2021) and Brazil (Afonso *et al.,* 2016). This could be attributed to the abundance of refuge areas, as highlighted by Olisah *et al.* (2020 and 2021), who emphasised the presence of numerous rivers and estuaries along the east coast of South Africa. Additionally, the tendency of *C. leucas* to inhabit freshwater and hypersaline bays and rivers may contribute to these increased levels of OCP.

2.4.4 Human health risk

The accumulation of OCPs within elasmobranch species can pose serious health complications for people who regularly consume these elasmobranchs. No information is available on the consumption of these elasmobranchs around the coast of South Africa, and an estimated human health risk assessment was adapted from Erasmus *et al. (*2022) and Heath *et al.* (2004). The human health risk was based on adults of 70 kg. The human health risk assessment did not consider individuals who might exhibit greater susceptibility and sensitivity to chronic exposure to trace elements. These individuals include pregnant women, lactating mothers, infants, and children (Javed & Usmani, 2019).

The estimated daily intake of OCPs for the South African population was calculated and compared with the recommended acceptable daily intake regulatory guidelines (Kim *et al.,* 2013). Many elasmobranch species displayed estimated daily intake values that exceeded the acceptable daily intake set for an average 70 kg individual consuming 48.57 g of elasmobranch tissue within South Africa. The calculated HQ and CR values additionally show that concentrations of these contaminants in some of these elasmobranch species were a cause of potential concern for human health. The HQ values for HCB and CHLs for all the elasmobranch species displayed values less than one, and as such, the potential for adverse health effects was minimal. However, the HQ values calculated for DDT showed three elasmobranch species (*M. mustelus*, *N. cepedianus*, *C. carcharias*) with a value greater than one, implying an increased likelihood of long-term adverse health effects occurring with the consumption of tissue from these species. Further possible species of interest from around the world that are known to be consumed include *S. lewini* by Briones *et al.* (2022) and Boldrocchi *et al.* (2019), *S. zygaena, M. manazo* (starspotted smoothhound shark), and *S. acanthias* (spiny dogfish) by Lee *et al.* (2015), *M. henlei* (brown smoothhound shark) by Pantoja-Echevarría *et al.* (2021).

The cancer risk for all compounds in all 22 elasmobranch species in this current study was greater than 1×10^{-4} (USEPA, 2005), and as such the target risk is unacceptable and should be of concern to people consuming these elasmobranchs. The most notable species that

showed high DDxs CR values were *M. mustelus*, *N. cepedianus*, and *C. carcharias*, a repeat of the three species seen to be of concern with the HQ values obtained. The CR values obtained for the DDTs levels in the three elasmobranch species are 79.9 x 10^{-4} for *M. mustelus*, 135 x 10^{-4} for *N. cepedianus*, and 152 x 10^{-4} for *C. carcharias*, which translates to cancer rates of eight, 14 and 15 men in 10 000 men for each respective species consumed. These cancer rates, compared to the cancer rate data made available by the National Cancer Registry of South Africa (Cancer Association of South Africa - CANSA, 2015), show rates lower than the estimated ratio of one to eight in men and one to nine in women. The data made available by CANSA are, however, based on calculations for adults, and no consideration is made for children and infants, which can be considered high-risk groups (Erasmus *et al.,* 2022).

The maximum safe consumption limit to prevent carcinogenic health risks for elasmobranch muscle tissue from 6 g (*N.* cepedianus) to 537 g (*H.* pictus) per day for DDE, which was the OCP compound with the highest concentrations measured in this study. The maximum safe consumption limit will hypothetically differ when all of the contaminants present within muscle tissue are included, as these are only based on DDE calculations. However, chronic exposure to these contaminants could cause adverse health effects with continued consumption.

Of the three species that pose a risk to human health due to consumption, the Smooth hound shark (*M. mustelus*), and the Broadnose sevengill shark (*N cepedianus*) are harvested for shark meat. Two shark species considered in this study, *M. mustelus* and the dusky shark, (*C. obscurus*) form part of the primary demersal shark trade in southern Africa (Da Silva and Bürgener, 2007). Other species such as the Blacktip shark (*C. limbatus*), Smooth hammerhead shark (S. zygaena) and Broadnose sevengill shark are utlised to a more limited degree in the shark trade.

When exploring the consumption of various elasmobranchs globally, several studies have delved into specific species. Briones *et al.* (2022) and Boldrocchi *et al.* (2019) focused on *S. lewini*, while Lee *et al.* (2015) examined *S. zygaena, M. manazo,* and *S. acanthias* and Pantoja-Echevarría *et al.* (2021) provided information on *M. henlei*.

In their international studies, Briones *et al.* (2022) and Lee *et al.* (2015) conducted lifetime cancer risk assessments. Both studies reported acceptable risk levels in *S. lewini* (Briones *et al.,* 2022), *S. zygaena* (Lee *et al.,* 2015), and *M. henlei* (Pantoja-Echevarría *et al.* 2021). However, Lee *et al.* (2015) raised concerns about potential carcinogenic effects associated with the consumption of *M. manazo* and *S. acanthias*. Furthermore, Boldrocchi *et al.* (2019) confirmed significant carcinogenic effects from long-term consumption of *S. lewini* around the coast of Djibouti.

2.5 Conclusion

This comprehensive study on organochlorine pesticide contamination in elasmobranchs along the South African coastline sheds light on the intricate dynamics of bioaccumulation. The research revealed a significant accumulation of OCPs in muscle tissues, influenced by sex, trophic position, feeding behaviour, and geographical location. Although certain species, including *C. carcharias* and *N. cepedianus*, showed elevated OCP levels, the study emphasised the broader impact of anthropogenic activities on the east coast, introducing contaminants into freshwater systems. Human health risk assessment raised concerns about possible adverse effects, with estimated daily intake values exceeding acceptable limits and cancer risk assessments indicating concerns about levels, particularly in certain species. Overall, this investigation underscores the need for ongoing monitoring efforts to mitigate the impact of OCP contamination on elasmobranchs and human health.

Chapter 3: Mercury and selenium concentrations in elasmobranch tissue from the east and west coasts of South Africa

3.1 Introduction

While China dominates the global mercury (Hg) emissions landscape, South Africa is one of the top ten global contributors (Pacyna *et al.,* 2010; Walters *et al.,* 2011). Coal combustion is considered a major contributing factor to anthropogenic Hg emissions (Driscoll *et al.,* 2013). Other anthropogenic sources include waste incinerators, mining activities and chlor-alkali production (Alvim-Ferraz and Afonso, 2003). However, the main suspected sources of Hg in South Africa are coal-fired power plants, artisanal gold mining, and cement production (Leaner *et al.,* 2009). Beyond the influence of biological and ecological factors, it is imperative to acknowledge the potential impact of both local and long-distance Hg inputs on the observed variations in Hg levels across different regions. The presence of Hg in precipitation data underscores the idea that Hg levels within South Africa are subject to influences not only from global sources but also from regional origins (Gichuki and Mason, 2013).

A big concern about the sources of anthropogenic Hg in South Africa is that these sources are located close to or around freshwater and marine systems, and the impact thereof is still relatively unknown (Williams *et al.,* 2010). A study completed by Walters *et al.* (2011) investigated anthropogenic Hg sources around the Water Management Areas (WMAs) in South Africa. Results from this study showed that agricultural/urban effluent was the most prominent anthropogenic Hg source, followed by cement production and coal-fired power stations, with only one of the WMAs having no associated anthropogenic Hg sources nearby. However, according to Leaner et al. (2009), the largest contributors to atmospheric Hg emissions were coal-fired power plants and artisanal gold mining. Five of the WMAs are associated with coal-fired power plants or artisanal gold mining, and as such these areas can display increased concentrations of Hg contamination present within the aquatic environment (Walters *et al.,* 2011).

Within sediment in the aquatic environment, Hg is also known to accumulate over time (Walters *et al.,* 2011). The interface between sediment and water is where Hg methylation and demethylation occur (Fontanella *et al.,* 2009). Mercury concentrations are consistently seen to be higher in sediment, and as such sediment can be seen as a sink for Hg and a source of contamination for overlying water and biota (Ramalhosa *et al.,* 2006).

However, knowledge of Hg concentrations in sharks and other species that inhabit coastal marine habitats in South Africa is notably limited. There exists only a handful of studies dating

back three decades ago. The first of these focused on shortfin mako sharks (*Isurus oxyrinchus*) (Cloete and Watling, 1981) and the more recent investigations such as Bosch *et al.* (2013, 2016) on smoothhound sharks (*M. mustelus*), McKinney *et al.* (2016) into eight species of sharks discussed in this study, and the most recent by Erasmus *et al.* (2022). Furthermore, there is a lack of information on Hg concentrations in other marine fish within the region.

If Hg levels in the tissues of South African sharks are at concentrations of human health concern, it may impact the most on consumers from the countries that import shark products from South Africa. In particular, captured South African sharks are shipped to Australia for their fish and chips trade, albeit within permitted Hg limits. Additionally, shark fins are exported to the Asian market (da Silva and Bürgener, 2007). It is worth mentioning that although some species in the present study are protected, others play a significant role in the demersal shark trade in South Africa, including copper sharks (*C. brachyurus*) and dusky sharks *(C. obscurus*) sharks.

Selenium (Se), an essential trace element, supports thyroid function and strengthens antioxidant defences. It is introduced into the marine environment primarily through the weathering of rocks and can accumulate in marine organisms. An overabundance of selenium intake by humans can result in selenosis, characterised by symptoms such as hair and nail loss, skin lesions, and neurological sequelae (Chawla *et al.,* 2020; Hatfield *et al.,* 2014; Jablonska and Vinceti, 2015; Joseph, 2012; Vinceti *et al.,* 2018).

Despite the potential mitigating effects of Se on Hg, the interplay between them remains an area that warrants comprehensive investigation. Barone *et al.* (2021) and Quinn *et al.* (2011) substantiated the biomagnification of Hg through the food web into apex predators. Notably, studies conducted by Ralston *et al.* (2016) and Rayman (2000) have suggested potential health benefits associated with the consumption of fish with a surplus of selenium (HBV_{Se}).

The heightened susceptibility of sharks to contaminant accumulation throughout their lifespan are due to their characteristic traits of longevity, low metabolic rate, high trophic position, and large lipid-enriched livers (Gelsleichter and Walker, 2010; Mull *et al.,* 2012). The predominant pathway for introducing pollutants in sharks is through their diet, followed by subsequent absorption into the bloodstream and distribution throughout various organs (Merly *et al.,* 2019). Their prey preferences largely influence trace metal concentrations among shark species or populations (McMeans *et al.,* 2007; Lee *et al.,* 2015). Consequently, documented evidence of enhanced trace metal toxicity in sharks poses a significant threat to the marine environment with potential implications for human health (Sun *et al.,* 2020).

This research presented in this chapter aims to test the formulated hypotheses related to contaminant concentrations (Hg and Se) in elasmobranchs. To achieve this, the specific research aims are threefold. Firstly, the investigation seeks to determine whether species differences in contaminant concentrations can be linked to intrinsic traits, including sex, size, migratory patterns, foraging range, and diet (trophic position). Secondly, the study aims to explore the influence of extrinsic factors on contaminant concentrations. This involves assessing whether the geographical location of occurrence, along the east and west coasts of South Africa, contributes to variations in Hg and Se levels among species. Lastly, the research aims to assess the human health risk associated with the consumption of elasmobranch muscle tissue and the potential antagonistic interactions Se has with Hg to counteract its toxic properties.

3.2 Materials and Methods

3.2.1 Sampling

Elasmobranch samples were collected by the KwaZulu-Natal Sharks Board and the South African Sharks Conservancy (SASC) on the east coast of KwaZulu-Natal and the south coast of the Western Cape Province, respectively. This study makes use of the muscle tissue of the elasmobranchs for contaminant analysis. Although liver tissue would be preferred for contaminant analysis, the extraction and cleanup procedures used proved ineffective to remove all of the lipids from the liver samples without the loss of the majority of OCPs present. As such it was deemed that the muscle tissue samples would be sufficient in analysing for the presence of the Hg and Se.

A total of 59 muscle tissue samples were collected from 22 elasmobranch species, representing 17 sharks and five skates and rays. From these 59 muscle tissue samples, 25 were female, 29 male, and 5 unidentified (Table S1). Furthermore, 28 muscle tissue samples were from adult elasmobranchs, 21 from juveniles, and 10 unidentified (Table S1). The different muscle tissue samples and number per species were: *Mobula kuhlii* (Shortfin devi. ray; n = 2), *Mobula eregoodootenkee* (Longhorned devil ray; n = 3), *Aetomylaeus bovinus* (Bull ray; n = 5), *Rhinoptera jayakari* (Oman cownose ray; n = 3), *Poroderma pantherinum* (Leopard catshark; n = 3), *Raja straeleni* (Spotted skate; n = 1), *Haploblepharus fuscus* (Brown shyshark; n = 2), *Haploblepharus pictus* (Dark shyshark; n = 1), *Haploblepharus edwardsii* (Puffadder shyshark; n = 1), *Mustelus mustelus* (Smoothhound shark; n = 4), *Galeocerdo cuvier* (Tiger shark; n = 3), *Sphyrna lewini* (Scalloped hammerhead shark; n = 6), *Sphyrna zygaena* (Smooth hammerhead shark; n = 1), *Carcharhinus limbatus* (Blacktip shark; n = 1), *Carcharhinus brevipinna* (Spinner shark; n = 4), *Squatina africana* (African angelshark; n = 1), *Carcharhinus obscurus* (Dusky shark; n = 5), *Carcharhinus leucas* (Bull shark; n = 1), *Carcharhinus amboinensis* (Java shark; n = 1), *Carcharhias taurus* (Ragged tooth shark; n = 1), *Notorynchus cepedianus* (Broadnose sevengill shark; n = 1), *Carcharhinus carcharias* (Great white shark; n = 7).

As part of the South African bather protection programme, the KwaZulu-Natal Sharks Board retrieved the sharks from shark nets between 2019 and 2020. The samples acquired from SASC were caught by longlines in 2018. All shark samples were collected under the relevant permits issued by the Chief Director of Fisheries Research & Development (Department of Fisheries, Environment and Forestry). All samples were stored frozen (-20 °C) and sent to the North-West University in 2020 for further analyses.

3.2.2 Laboratory methods

3.2.2.1 Mercury

The mercury analyses methods were adapted from Erasmus *et al.* (2022). Muscle samples were initially freeze-dried for 72 hrs using a FreeZone 6 (Labconco) freeze drier. The dried samples were then homogenised, and 0.2 g of the homogenised material was subjected to acid digestion. The digestion process involved using 7.5 mL of HNO_3 (subboiled 65%) from Merck (MFCD00011349) and 2.5 mL of HCl (37%, supra pure quality) from Merck(MFCD00011324) and digested in a microwave digestion system (Ethos Easy Milestone) as described in Erasmus *et al.* (2022). Following digestion, the sample was transferred to a 50 mL volumetric flask and made up to volume using ultrapure water (MiliQ). Samples were stored in pre-cleaned polypropylene Falcon tubes prior to analysis.

A Flow Injection Mercury System (FIMS 400, PerkinElmer) was used to measure total mercury concentrations (Hg) in muscle samples and expressed as milligrams per kilogram of dry weight (mg/kg d.w.) The FIMS system used a carrier gas flow (argon) at an 80 mL/min rate, with 3% HCl serving as the carrier liquid and 52 mM sodium borohydride ($NaBH_4$) as a reducing agent. Calibration of the FIMS system was performed using a series of seven dilutions of a Hg standard solution (1000 µg/mL Hg standard in 10% HNO_3, PerkinElmer), resulting in a regression with a correlation factor of ≥0.999.

DORM-4 (fish protein certified reference material, National Research Council, Canada) was used as the reference material (CRM) and subsequently used to assess quality assurance and Hg and Se recovery. In addition, quality standards were analysed after every 20 samples. The recovery rate of the CRM samples was 95%. To monitor potential contamination, three blank samples per digestion run were prepared in the same manner as the samples and CRMs. In total, 18 blank samples were analysed, yielding a mean background concentration of 0.13 µg/L Hg.

Triplicates of each sample type (blanks, CRM, and muscle tissue) were analysed, and the average concentration was used for later calculations. The percentage relative standard deviation (%RSD) was consistently below 10%. The detection limit was determined as three times the standard deviation, using measurements from a blank sample (0.2 g), yielding a value of 1.7 ng/g. The quantification limit was 5.2 ng/g and calculated as nine times the standard deviation of the mean.

3.2.2.2 Selenium

Selenium (Se) analysis was also adapted from Erasmus *et al.* (2020). Muscle tissue samples were freeze-dried and approximately 0.2 g (dry weight) muscle sample was digested in a solution comprising 3 mL HNO_3 (65%, supra pure quality) from Merck (MFCD00011349) and 1 mL HCl (37%, supra pure quality) from Merck (MFCD00011324), following an adapted method of Djingova *et al.* (2003). The digestion was completed in a Mars 6 microwave digestion system (CEM Corporation, Kamp-Lintfort), utilising 20 mL TFM® vessels (MarsXpress, CEM). Following digestion, the resulting solution was transferred to a 5 mL volumetric flask, filled to the mark with MiliQ® water, and subsequently transferred to pre-cleaned polypropylene containers for storage at room temperature until analysis.

For the measurement of Se concentrations in the tissue samples, a quadrupole inductively coupled plasma-mass spectroscopy (ICP-MS) (PerkinElmer, Elan 6000) was employed. The detection limit was established as three times the standard deviation of the blank measurements, yielding a value of 0.003 µg/g for Se. The recovery rate for Se in the CRM DORM-4 was 91%.

3.2.3 Statistical analysis

The data were tested for normality using the D'Agostino and Pearson omnibus normality test. To determine significant differences in Hg and Se concentrations between elasmobranch species, a one-way analysis of variance with Tukey's multiple comparison test was applied, with the level of significance set at $p < 0.05$. All analyses were performed in GraphPad Prism 10. Spatial patterns associated with Hg and Se and elasmobranch species were evaluated using a Principal Component Analysis (PCA) conducted with the use of Canoco v5 software. The data for the PCA underwent log transformation ($y = \log(x+1)$). Subsequently, the log-transformed data used for PCA were also employed for a Pearson's rank correlation test to investigate potential relationships between log-transformed concentrations of elements and the trophic position and sex of elasmobranch species.

3.2.4 Human health risk assessment

Non-carcinogenic risk

To evaluate the potential for long-term non-cancerous health effects resulting from oral exposure, the average daily dose (ADD), presented as milligrams per kilogram of body weight per day, was calculated for Hg and Se analysed:

$$ADD = \frac{\left(average\ Hg\ or\ Se\ concentration\ in\ elasmo.muscle\ (WW)\ x\ (food\ ingestion\ rate)\right)}{(adult\ body\ mass)\ x\ (no.of\ days\ between\ elasmo.meals)}$$

Where the average Hg or Se concentration in the elasmobranch muscle is calculated in mg/kg wet weight, the food ingestion rate is 48.57 g, the average adult body weight is 70 kg, and the number of days between elasmobranch meals is three days (Heath *et al.,* 2004).

Non-carcinogenic risk assessment for the toxic effects of pollutants uses reference doses (RfDs) as set thresholds that, if surpassed, can cause possible adverse health effects. To estimate the human health risk, a hazard quotient (HQ) was calculated for Hg and Se:

$$HQ = \frac{ADD}{RfD}$$

Where the value of HQ above or below one suggests possible adverse health effects, HQ < 1 implies an unlikelihood of adverse health effects, and HQ > 1 implies a high likelihood of adverse health effects. RfD levels (µg/kg) used are as follows: Hg (0.1) (Alman *et al.,* 2022), Se (5) (Risher, 2003).

Maximum safe consumption limit

The maximum weight of elasmobranch muscle tissue that can be consumed safely and without any potential adverse human health risks per day:

$$Y = RfD\ x \frac{BM}{C}$$

Where Y is the amount of elasmobranch muscle tissue that can be safely consumed, RfD is the reference dose for non-carcinogenic risk, BM is the average consumer body weight, and C is the average concentration of Hg and Se in the elasmobranch muscle tissue.

Selenium Health Benefit Values (HBV_{Se})

The equation used in this study to showcase the benefits of dietary selenium and mercury risks is the following equation (Ralston and Raymond, 2016). The equation makes use of the molar concentrations of Hg (200.59) and Se (78.96) to calculate the selenium health benefit value:

$$HBVSe = \frac{Se - Hg}{Se} x\ (Se + Hg)$$

This equation has been adapted from the previous equation formulated by Ralston:

$$SeHBV = Se\left(\frac{Se}{Hg}\right) - Hg(\frac{Hg}{Se})$$

Because the previous understanding of mercury's molecular toxicity was centered on its binding to thiols, the assessments were based on pseudo-first-order reaction kinetics.

However, with the realisation that mercury irreversibly inhibits selenoenzymes, particularly at cell concentrations approaching or exceeding equimolar stoichiometries (around 1 – 2 µM), it is now imperative to employ bimolecular reaction rate equations for a more accurate evaluation of mercury exposure risks.

To facilitate these assessments for regulatory bodies and consumers, equations have been developed to delineate the benefits and risks associated with methylmercury-containing foods. Initially, the Se-HBV equation served as a reliable risk index for mercury exposures, but it lacked consistency in reflecting the positive effects of dietary selenium intake.

Therefore, the equation was modified to showcase the benefits of dietary selenium and mercury risks explicitly. This updated version is now referred to as HBV_{Se}, as mentioned previously. Like its predecessor, both selenium and mercury are measured exclusively in molar concentration units. A negative HBV_{Se} for seafood implies the risk of adverse effects on child neurodevelopment upon consumption. Conversely, a positive value suggests expectations of beneficial outcomes. The magnitude of this positive or negative value signifies the relative benefits or risks associated with the consumption of the seafood in question. However, Zhang *et al.* (2014) also highlighted the limitation of the criterion wherein a potential large positive value is associated with a "great health benefit", potentially causing Se poisoning.

3.2.5 Ethical considerations

This project on Hg and Se accumulation in elasmobranch species found along the South African coast forms part of a larger study. This larger study concerns the conservation of ancient relationships and is entitled: Integrative approach using elasmobranchs and their parasites to assess ecosystem health. This larger study has received ethical clearance (NWU-00065-19-A5) from the AnimCare research ethics committee and the samples collected were analysed under the following ethics clearance: NWU-01308-22-A9.

3.3 Results

3.3.1 Mercury and selenium levels in muscle of selected elasmobranch species

Mercury and Se were analysed in 22 elasmobranch species. Both Hg and Se were recorded in all the tissue samples, with Hg consentrations the highest, and Se displaying higher percentage contributions in certain elasmobranchs (*M. kuhlii, M. eregoodootenkee, A. bovinus, R. jayakari, R. straeleni, H. fuscus, H. pictus, H. edwardsii, M. mustelus, C. limbatus,* and *C. carcharias*). The mean and standard error of Hg and Se in the muscle tissue of elasmobranch species arranged from lowest to highest trophic position on the y-axis of Figure 3.1. When arranged from highest to the lowest the Hg concentrations were *S. lewini* > *C. leucas* > *C. taurus* > *N. cepedianus* > *C. amboinensis* (Figure 3.1). For The highest Se concentrations, it followed the following pattern: *C. limbatus* > *C. carcharias* > *R. jayakari* > *C. leucas* > *A. bovinus* (Figure 3.1).

An increase in the concentration of Hg was seen with an increase in the trophic position of the elasmobranch species. The increased Hg concentrations within the larger shark species did not coincide with concomitant increased Se concentrations. However, even though the Se and Hg concentrations were lower in skates and rays at the lower trophic positions, the percentage contribution of Se to the total Hg and Se concentrations was comparable to shark species that occupy similar trophic positions (Figures 3.2 and 3.3).

Except for the bull shark (*C. leucas*), the Hg concentrations in the smooth hammerhead shark (*S. lewini*) were significantly ($p<0.05$) higher than any of the other elasmobranch species (Table 3.1). *Carcharhinus leucas* and *C. taurus* (ragged tooth shark) were the only other elasmobranch species that had significantly higher Hg concentrations when compared to the other elasmobranch species. Eleven of the 17 shark species had a higher percentage of Hg contribution compared to Se (*P. pantherinum, G. cuvier, S. lewini, S. zygaena, C. brevipinna, S. africana, C. obscurus, C. leucas, C. amboinensis, C. taurus, and N. cepedianus*) (Figure 3.2 and 3.3), with five species having Hg in excess of 75% of the total Hg and Se levels (*S. lewini, G. cuvier, C. leucas, C. taurus,* and *N. cepedianus*). Although not significant, sharks from the east coast of South Africa had higher concentrations and percentage contributions of Hg than thos from the west coast (Figures 3.1 and 3.2).

There were no significant differences in Se concentrations between the elasmobranch species. The rays and skate species had notably higher percentage contributions of Se compared to the shark species, with Se concentrations in *R. jayakari* and *A. bovinus* higher than many of the shark species (Figure 3.1).

The species with the highest Se concentrations were *C. limbatus, C. carcharias, R. jayakari, C. leucas,* and *A. bovinus* (Figure 3.1) with all recording a Se percentage contribution greater than 50%, except *C. leucas* (Figures 3.2 and 3.3).

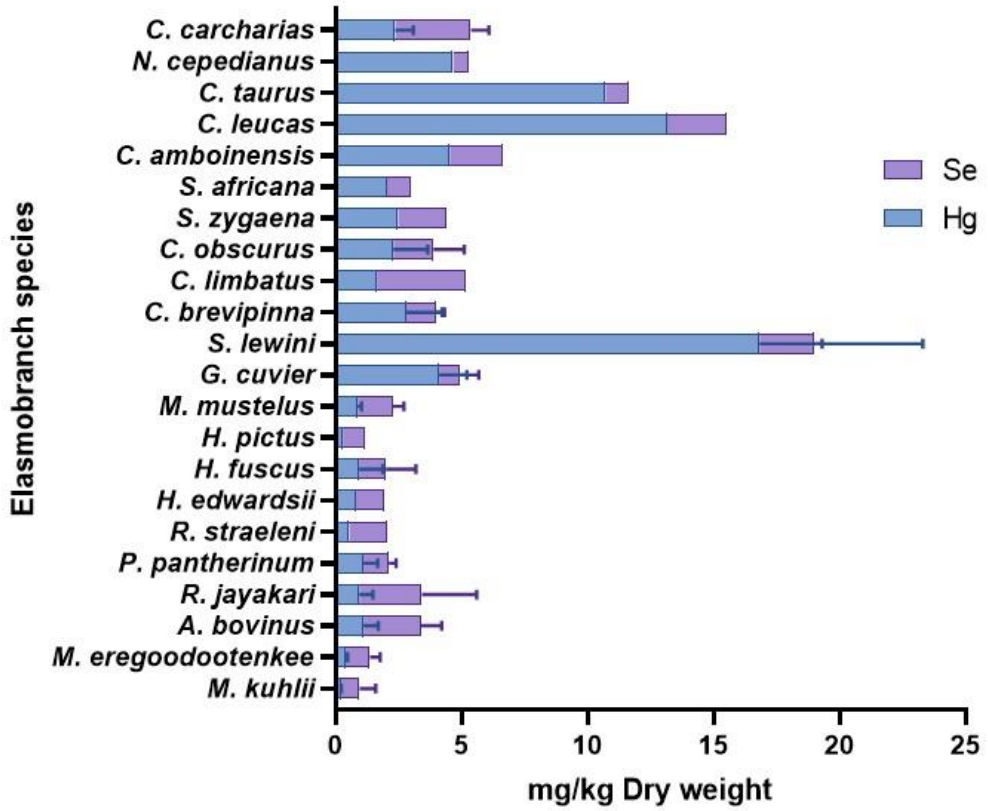

Figure 3.1: Mercury and selenium concentrations (mean ± standard error expressed in mg/kg dry weight) in muscle tissue from different elasmobranch species collected from the east and south coast of South Africa.

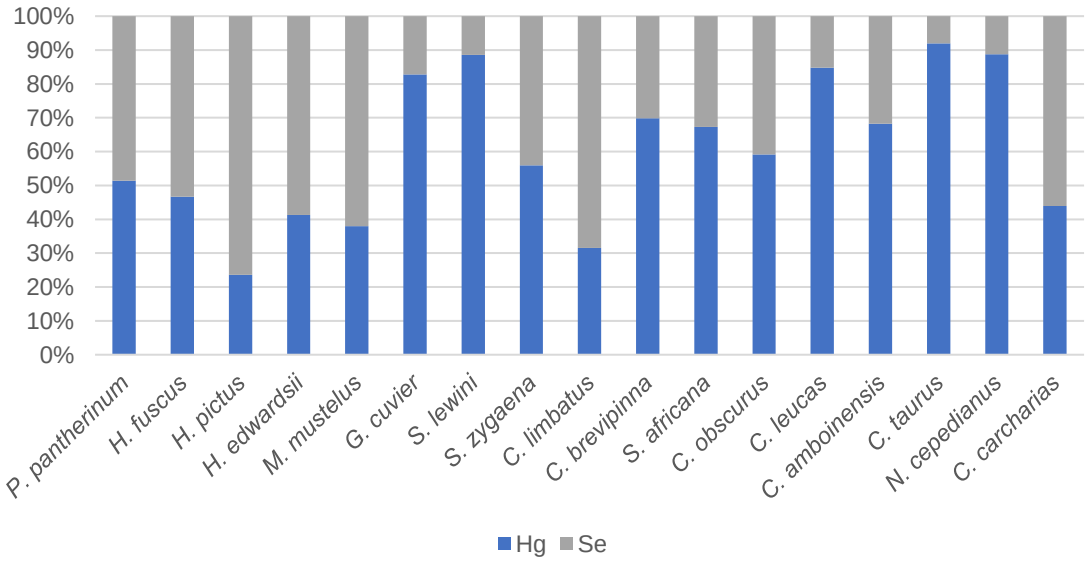

Figure 3.2: Percentage contribution of mercury and selenium concentrations analysed in sampled shark species.

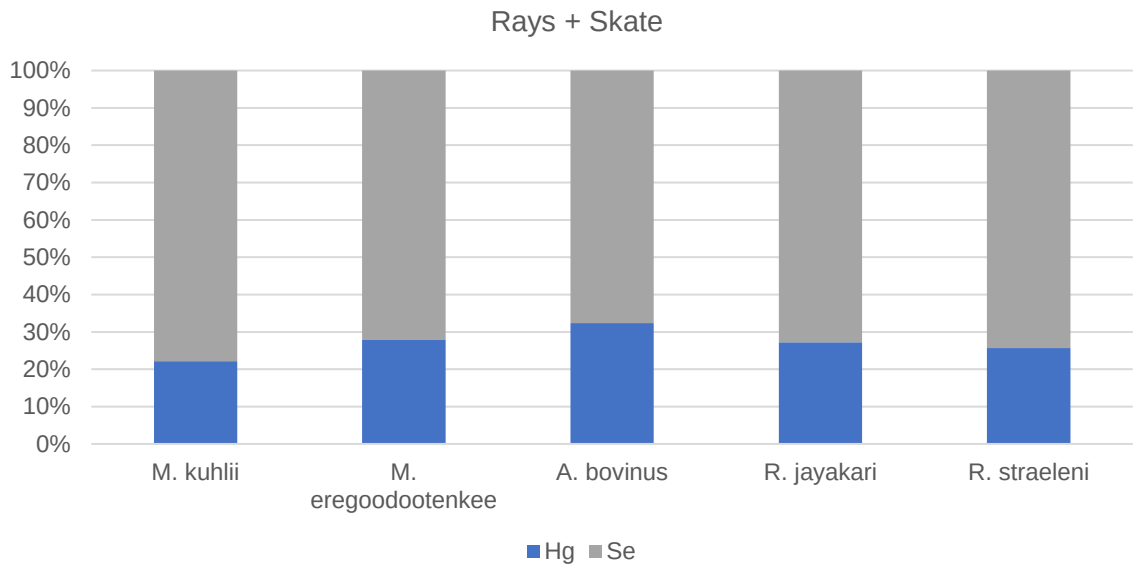

Figure 3.3: Percentage contribution of mercury and selenium concentrations analysed in sampled ray and skate species.

Table 3.1. Matrix of significant mercury (A) and differences between the elasmobranchs collected from the east and south coast of South Africa. Significance was regarded as $p < 0.05$. There were no significant differences in selenium concentrations between species.

	1	2	3	4	5	6	7	8	9	10	11	12	13	14	15	16	17	18	19	20	21	22
1	X											A										
2		X										A							A			
3			X									A							A			
4				X								A										
5					X							A										
6						X						A										
7							X					A										
8								X				A										
9									X			A										
10										X		A							A			
11											X	A										
12												X	A	A	A	A	A	A		A	A	A
13													X									
14														X								
15															X							
16																X						
17																	X					
18																		X				
19																			X			
20																				X		
21																					X	
22																						X

Numbers representing the different elasmobranch species: 1=*M. kuhlii*, 2=*M. eregoodootenkee*, 3=*A. bovinus*, 4=*R. jayakari*, 5=*P. pantherinum*, 6=*R, straeleni*, 7= H. edwardsii, 8=*H. fuscus*, 9=*H. pictus*, 10=*M. mustelus*, 11=*G. cuvier*, 12=*S. lewini*, 13= *C. brevipinna*, 14=*C. limbatus*, 15=*C. obscurus*, 16=*S. zygaena*, 17=*S. africana*, 18=*C. amboinensis*, 19=*C. leucas*, 20=*C. taurus*, 21=*N. cepedianus*, 22=*C. carcharhias*

3.3.2 Influence of sex and trophic position on mercury and selenium levels in sharks

The percentage contribution of Hg in females increased with increasing trophic position (Figure 3.6), which was not evident in males of the same species (Figure 3.4). *Haploblepharus fuscus* (dark shy shark) and *S. lewini* males had percentage Hg contributions of over 80% (Figure 3.4). However, the percentage contribution of Se in female *H. fucus* was over 80% (Figure 3.6). For both male and female rays and skates, the percentage contributions of Hg and Se to the total concentrations were very similar. Notable was that in most cases the Hg contribution was lower than Se (Figures 3.5 and 3.7).

There was a significant positive correlation between Hg and trophic position ($p < 0.05$) for all elasmobranchs (Figure 3.8A), males (Figure 3.8B) and females (Figure 3.8C). There was no significant correlation ($p > 0.05$) between Se and increased trophic positions (Figure 3.8D, E, F). Although the rays and skate (*M. kuhlii, M. eregoodtenkee, A. bovinus, R. jayakari,* and *R. straeleni*) occupy the lowest trophic positions (Figure 3.8D) they did not necessarily have the lowest levels of Se. This is especially true when compared to *C. carcharias* that was at the highest trophic position.

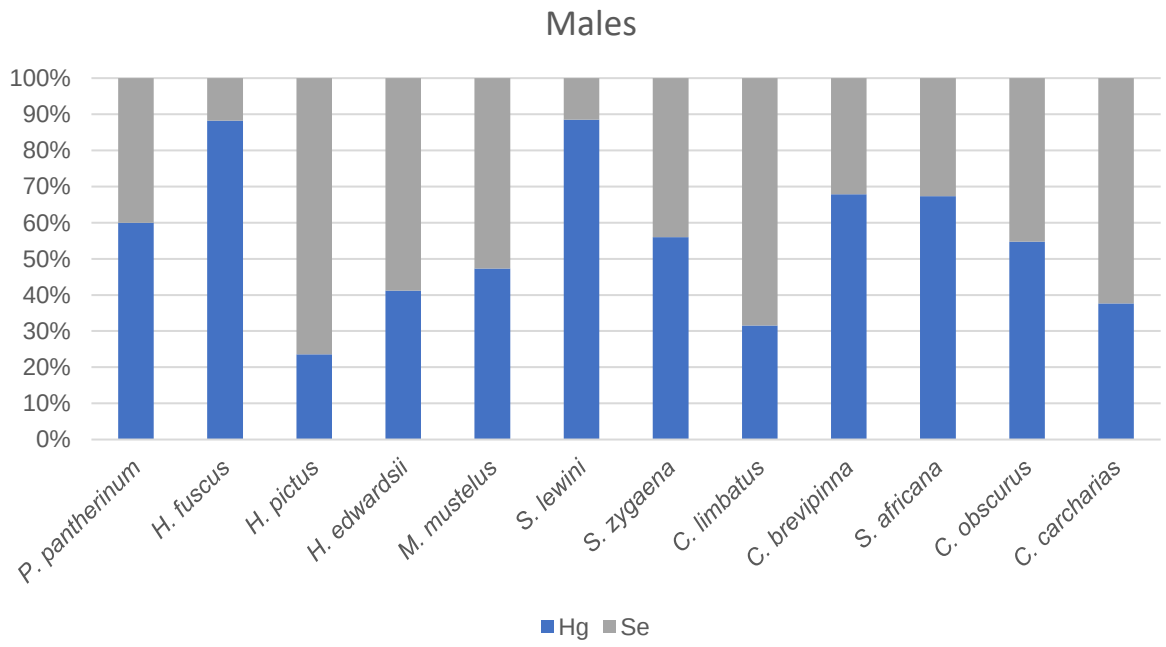

Figure 3.4: Percentage contribution of mercury and selenium concentrations analysed in sampled male shark species.

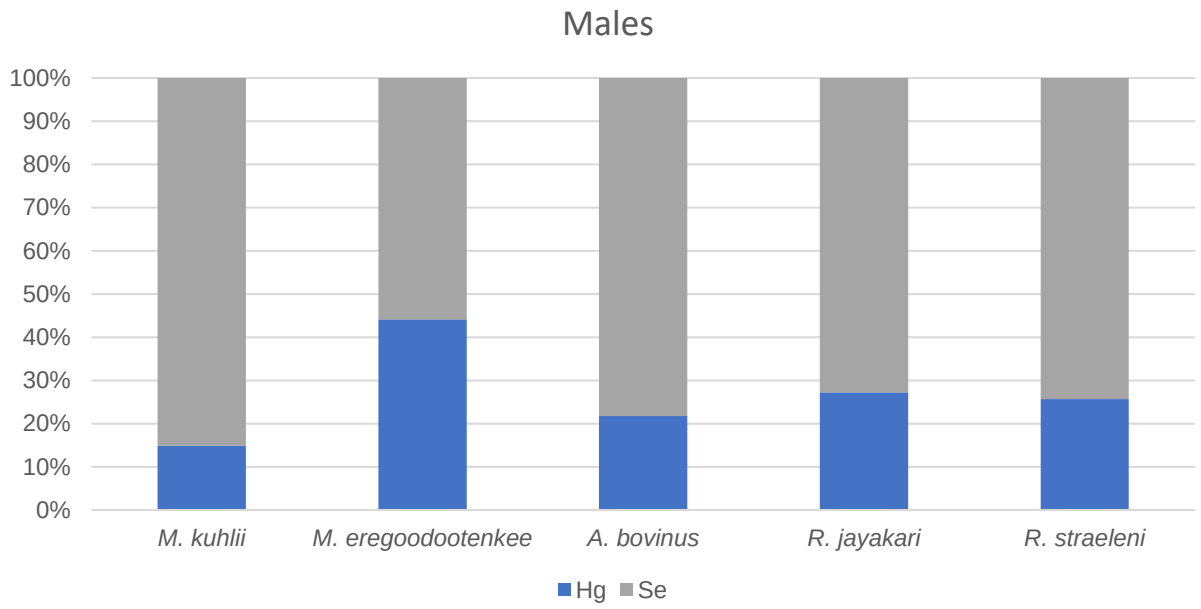

Figure 3.5: Percentage contribution of mercury and selenium concentrations analysed in sampled male ray and skate species.

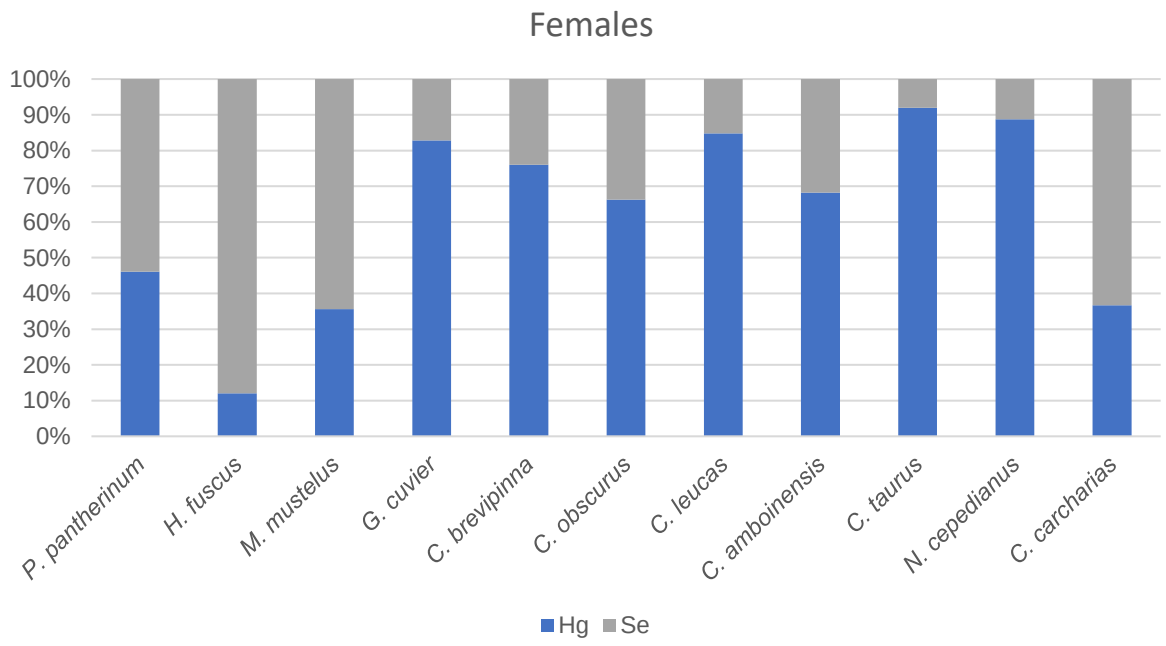

Figure 3.6: Percentage contribution of mercury and selenium concentrations analysed in sampled female shark species.

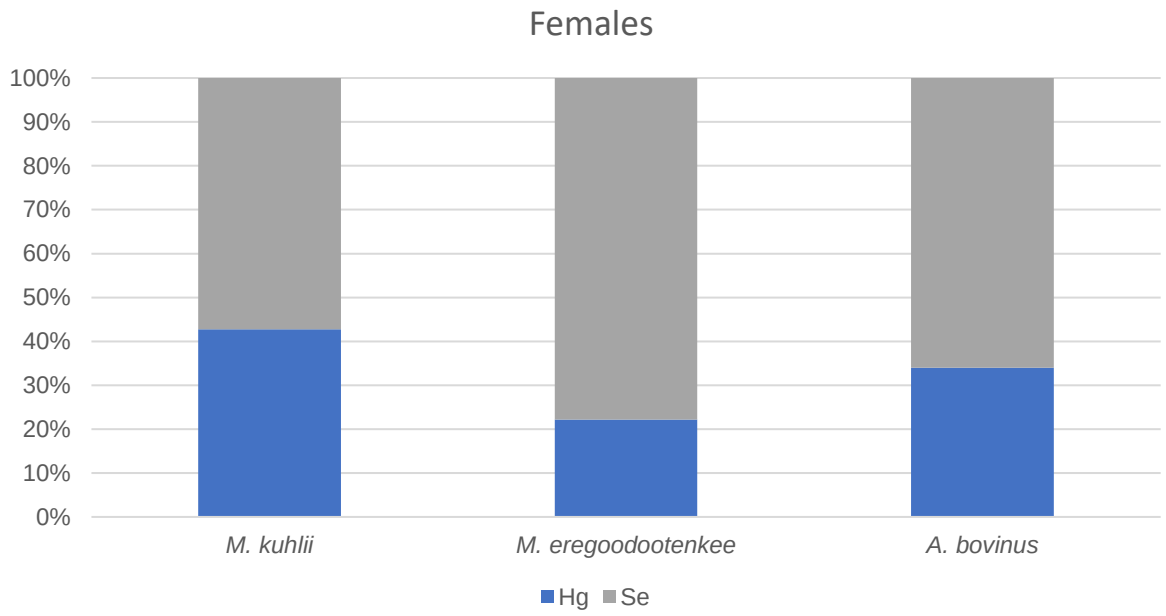

Figure 3.7: Percentage contribution of mercury and selenium concentrations analysed in sampled female ray and skate species.

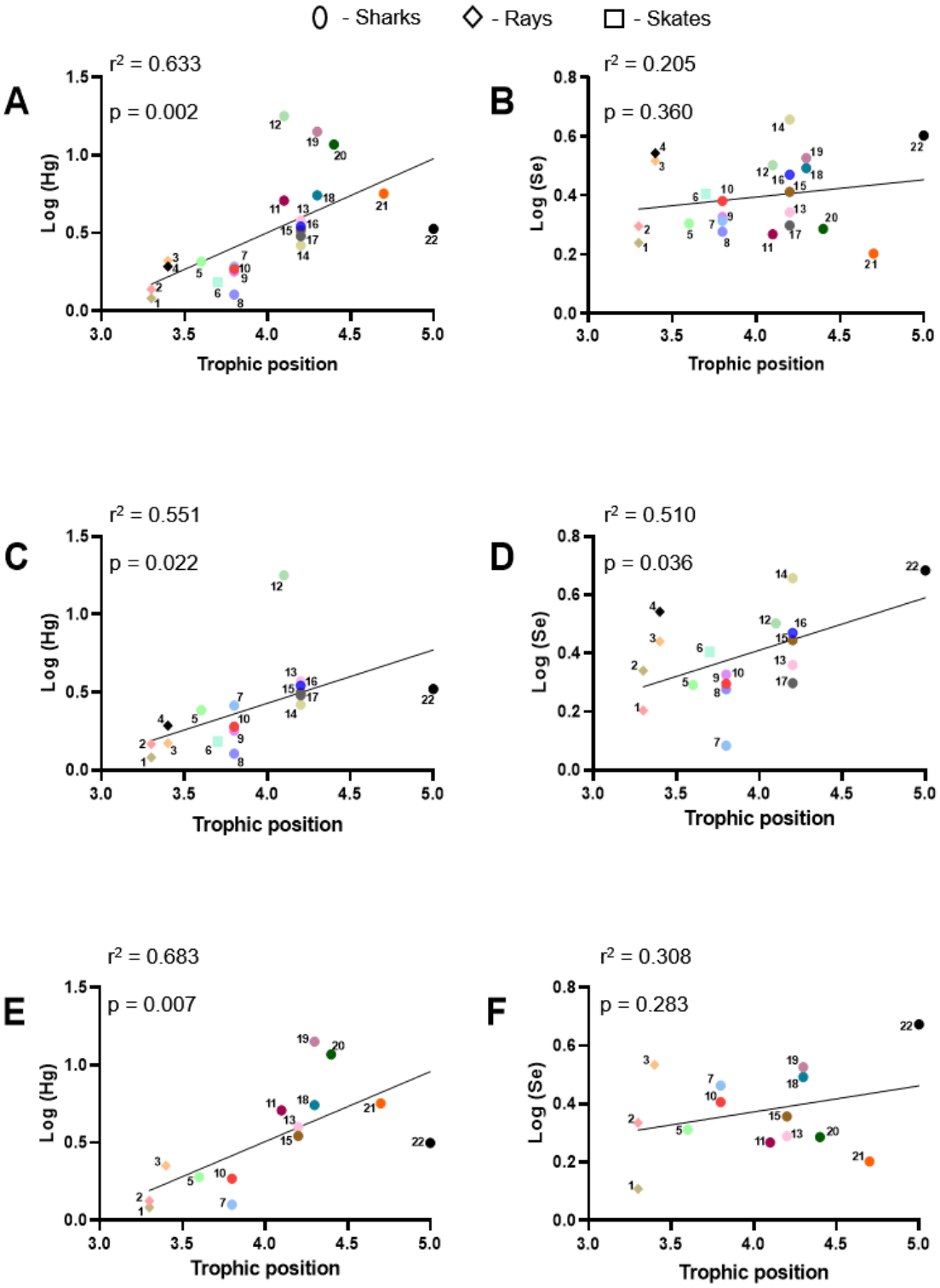

Figure 3.8: Correlation of the log of the sum of mercury and selenium concentrations against the trophic position of male and female elasmobranch collected from the east- and south coast of South Africa (r^2 = 0.633, p = 0.002) (A), (r^2 = 0.205, p = 0.360) (B); Male elasmobranchs (r^2 = 0.551, p = 0.022) (C), (r^2 = 0.510, p = 0.036) (D); Female elasmobranchs (r^2 = 0.683, p = 0.007) (E), (r^2 = 0.308, p = 0.283) (F). Number with corresponding species are presented in the footnote of Table 3.1.

3.3.3 Influence of sampling region on the mercury and selenium levels

For the regional analyses, elasmobranch species were grouped into larger taxonomic groups, i.e., sharks, skates and rays from the east and south coasts of South Africa. The PCA biplot (Figure 3.9) describes 100% of the variation on the two axes. The first axis described 60.36% of the variation, and the second axis described 39.64% of the variation in the Hg and Se levels in elasmobranchs. The first axis differentiated between elasmobranchs from the east coast (which had higher Hg and Se concentrations) from the south coast. Species occupying higher trophic positions, with higher Hg concentrations, are also differentiated from lower trophic positions on axis 1. Axis 2 differentiates between the Hg and Se concentrations in sharks, and rays and skates.

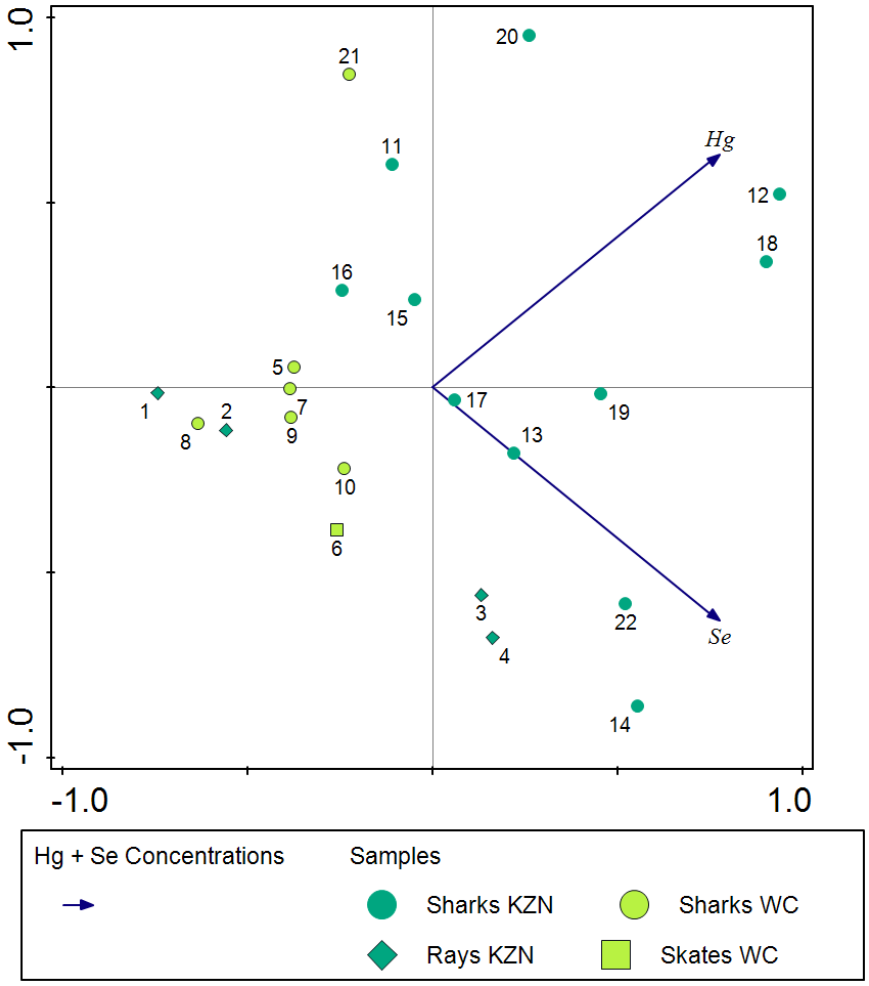

Figure 3.9: Principal component analysis (PCA) biplot graph based on the mean mercury and selenium concentrations in muscle tissue of the elasmobranch species. First two axes explained 100% of the variation in elasmobranchs from the east and south coasts of South Africa.

3.3.4 Human health risks associated with the consumption of mercury and selenium contaminated elasmobranchs

The assessment of non-carcinogenic human health risks was based on the calculation of the hazard quotient (HQ) and the selenium health benefit (HBV_{Se}). The TDIs for Hg in all of the elasmobranch species (Table 3.2) were higher than the allowable 0.02 mg/kg/day (Watanabe *et al.*, 2021) for a 70 kg adult. The HQ values (Table 3.3) for half of the elasmobranch species were >1 (*G. cuvier*, *S. lewini*, *S. zygaena*, *C. brevipinna*, *S. africana*, *C. obscurus*, *C. leucas*, *C. amboinensis*, *C. taurus*, *N. cepedianus*, *C. carcharias*). This suggests a high likelihood of non-carcinogenic and adverse human health effects associated with regular consumption of these elasmobranchs contaminated with Hg.

The TDI for Se is 0.4 mg/day and is considered the highest level of daily nutrient intake that does not pose any risk of adverse effects (Meyer *et al.,* 2006). This value was surpassed by *R. jayakari, C. limbatus,* and *C. carcharias* (Table 3.2), leading to the possibility of possible adverse effects with continued regular consumption of these elasmobranchs. None of the elasmobranchs had HQ values >1 for Se (Table 3.3) and as such this suggests that there is no likelihood of non-carcinogenic and adverse human health effects associated with the regular consumption of these species.

The maximum safe consumption limit of Hg-contaminated muscle tissue in elasmobranchs ranged between 2 g for scalloped hammerhead shark (*S. lewini*) and 140 g for shortfin devil ray (*M. kuhlii*) per day (Table 3.4). A positive HBV_{Se} value (Table 3.9) was calculated for most of the elasmobranch species. This indicated that the levels of Se present within the muscle tissue of the elasmobranch sampled could potentially counteract the toxic effects of Hg. However, *G.* cuvier, *S. lewini, C. leucas, C. taurus*, and *N. cepedianus* all had negative HBV_{Se} values, indicating that the toxic effects of Hg could be evident when consuming muscle tissue from these species.

Table 3.1. Estimated daily intake (EDI mg/kg/day) of mercury and selenium calculated for people who consume South African elasmobranch muscle tissue and comparison to tolerable daily intake (TDI mg/kg/day) for an adult individual of 70 kg body weight (Meyer *et al.*, 2006; Watanabe *et al.,* 2021).

	Mercury (Hg)	Selenium (Se)
TDI (mg/kg)	**0.02***	**0.4**
Mobula kuhlii (Shortfin devil ray)	0.03±0.0003	0.12±0.08
Mobula eregoodootenkee (Longhorn devil ray)	0.06±0.01	0.16±0.06
Aetomylaeus bovinus (Bull ray)	0.18±0.09	0.38±0.12
Rhinoptera jayakari (Oman cownose ray)	0.16±0.07	0.41±0.3
Poroderma pantherinum (Leopard catshark)	0.18±0.08	0.17±0.04
Raja straeleni (Spotted skate)	0.09	0.26
Haploblepharus edwardsii (Puffadder shyshark)	0.15±0.11	0.18±0.14
Haploblepharus fuscus (Brown shyshark)	0.05	0.15
Haploblepharus pictus (Dark shyshark)	0.13	0.19
Mustelus mustelus (Smoothhound shark)	0.14±0.02	0.23±0.06
Galeocerdo cuvier (Tiger shark)	0.68±0.15	0.14±0.1
Sphyrna lewini (Scalloped hammerhead shark)	2.8±0.99	0.36±0.05
Carcharhinus brevipinna (Spinner shark)	0.41	0.32
Carcharhinus limbatus (Blacktip shark)	0.27	0.59
Carcharhinus obscurus (Dusky shark)	0.46±0.21	0.2±0.05
Sphyrna zygaena (Smooth hammerhead shark)	0.34	0.16
Squatina africana (African angel shark)	0.35±0.07	0.3±0.18
Carcharhinus amboinensis (Java shark)	2.19	0.39
Carcharhinus leucas (Bull shark)	0.75	0.35
Carcharias taurus (Ragged tooth shark)	1.78	0.16
Notorynchus cepedianus (Broadnose sevengill shark)	0.78	0.1
Carcharodon carcharias (Great white shark)	0.39±0.11	0.5±0.11

TDI adjusted according to the 70 kg body weight of adults. Watanabe *et al.* (2021) TDI for methyl mercury set at 0.292 µg/kg bw.

Table 3.2. The mean and standard error of hazard quotients (HQ) for the elasmobranch species based on the mean concentrations of mercury and selenium in the muscle tissue. Hazard quotient values >1 are shaded in the table below.

Hazard quotients for non-carcinogenic risk (HQ)	Mercury (Hg)	Selenium (Se)
Mobula kuhlii (Shortfin devil ray)	0.12±0.001	0.008±0.005
Mobula eregoodootenkee (Longhorn devil ray)	0.21±0.038	0.011±0.004
Aetomylaeus bovinus (Bull ray)	0.61±0.29	0.025±0.008
Rhinoptera jayakari (Oman cownose ray)	0.52±0.25	0.028±0.02
Poroderma pantherinum (Leopard catshark)	0.6±0.27	0.01±0.003
Raja straeleni (Spotted skate)	0.29	0.02
Haploblepharus edwardsii (Puffadder shyshark)	0.52±0.37	0.012±0.01
Haploblepharus fuscus (Brown shyshark)	0.15	0.01
Haploblepharus pictus (Dark shyshark)	0.44	0.01
Mustelus mustelus (Smoothhound shark)	0.48±0.08	0.02±0.004
Galeocerdo cuvier (Tiger shark)	2.28±0.5	0.01
Sphyrna lewini (Scalloped hammerhead shark)	9.34±3.29	0.02±0.003
Carcharhinus brevipinna (Spinner shark)	1.38	0.02
Carcharhinus limbatus (Blacktip shark)	0.91	0.04
Carcharhinus obscurus (Dusky shark)	1.55±0.5	0.013±0.003
Sphyrna zygaena (Smooth hammerhead shark)	1.13	0.01
Squatina africana (African angel shark)	1.18±0.24	0.02±0.01
Carcharhinus amboinensis (Java shark)	7.3	0.03
Carcharhinus leucas (Bull shark)	2.51	0.02
Carcharias taurus (Ragged tooth shark)	5.94	0.01
Notorynchus cepedianus (Broadnose sevengill shark)	2.59	0.007
Carcharodon carcharias (Great white shark)	1.31±0.37	0.033±0.007

RfD levels set at 5 µg/kg for Se (Risher, 2003) and 0.1 µg/kg for Hg (Alman *et al.*, 2022).

Table 3.3. Maximum safe consumption limits (g) of elasmobranch meat based on mercury and selenium levels.

Maximum safe consumption limit per day (g)	Mercury (Hg)	Selenium (Se)
Mobula kuhlii (Shortfin devil ray)	140±1.4	3195±1968
Mobula eregoodootenkee (Longhorn devil ray)	79±12.6	1685±573
Aetomylaeus bovinus (Bull ray)	333±15.4	706±223
Rhinoptera jayakari (Oman cownose ray)	48.1±35	932±522
Poroderma pantherinum (Leopard catshark)	38±24.6	1510±339
Raja straeleni (Spotted skate)	55	948
Haploblepharus edwardsii (Puffadder shyshark)	64.9±46.6	3830±3064
Haploblepharus fuscus (Brown shyshark)	106	1635
Haploblepharus pictus (Dark shyshark)	37	1298
Mustelus mustelus (Smoothhound shark)	34.8±6	1110±275
Galeocerdo cuvier (Tiger shark)	7.4±1.5	2728±1616
Sphyrna lewini (Scalloped hammerhead shark)	2±0.92	681±93.4
Carcharhinus brevipinna (Spinner shark)	11.8	747.9
Carcharhinus limbatus (Blacktip shark)	17.9	412.2
Carcharhinus obscurus (Dusky shark)	12.5±4.8	1279.6±291.9
Sphyrna zygaena (Smooth hammerhead shark)	14.4	1481.0
Squatina africana (African angel shark)	14.3±3.0	1103.0±534.8
Carcharhinus amboinensis (Java shark)	2.2	618.4
Carcharhinus leucas (Bull shark)	6.5	692.1
Carcharias taurus (Ragged tooth shark)	2.7	1560.4
Notorynchus cepedianus (Broadnose sevengill shark)	6.3	2456.0
Carcharodon carcharias (Great white shark)	13.5±4.1	509.7±116.2

Table 3.4. Selenium health benefit values (HBV_{Se}) for the elasmobranch species from the east and south coast of South Africa.

	HBV_{Se}
Mobula kuhlii (Shortfin devil ray)	2.19±1.41
Mobula eregoodootenkee (Longhorn devil ray)	2.88±1.06
Aetomylaeus bovinus (Bull ray)	6.65±2.26
Rhinoptera jayakari (Oman cownose ray)	7.15±5.70
Poroderma pantherinum (Leopard catshark)	2.50±0.64
Raja straeleni (Spotted skate)	4.60
Haploblepharus edwardsii (Puffadder shyshark)	0.39-5.39
Haploblepharus fuscus (Brown shyshark)	2.67
Haploblepharus pictus (Dark shyshark)	3.16
Mustelus mustelus (Smoothhound shark)	4.0±1.23
Galeocerdo cuvier (Tiger shark)	-16.9+19.3
Sphyrna lewini (Scalloped hammerhead shark)	-62.4±43.8
Carcharhinus brevipinna (Spinner shark)	4.45
Carcharhinus limbatus (Blacktip shark)	10.41
Carcharhinus obscurus (Dusky shark)	0.24+2.14
Sphyrna zygaena (Smooth hammerhead shark)	1.03
Squatina africana (African angel shark)	3.87+4.08
Carcharhinus amboinensis (Java shark)	-27.31
Carcharhinus leucas (Bull shark)	1.85
Carcharias taurus (Ragged tooth shark)	-54.9
Notorynchus cepedianus (Broadnose sevengill shark)	-15.5
Carcharodon carcharias (Great white shark)	8.16±2.29

3.4 Discussion

Human activities are the primary contributors to the release of Hg emissions into the environment, consequently impacting aquatic ecosystems globally. The escalation of these emissions is leading to elevated levels of Hg in the world's oceans (Driscoll *et al.,* 2013; Lamborg *et al.,* 2014). South Africa has emerged as a major player in global Hg emissions, particularly attributed to its coal-fired power stations, mainly in the Mpumalanga Highveld region, which contribute a significant 84% to the country's electricity production (Belelie *et al.,* 2019; EMBER, 2022). Once released, Hg contaminates local areas and disperses extensively through long-distance atmospheric transport, with a predominant pattern directing the pollution from the Mpumalanga Highveld towards the east coast of southern Africa (Mason *et al.,* 1998; Freiman and Piketh, 2003). These power stations also serve as crucial sources of selenium in the environment (Lemly, 2002). Selenium is also inadvertently introduced into the environment through various sources such as phosphate fertilisers, sewage sludge, manure, and Se-containing pesticides and fungicides (Fordyce, 2013).

Mercury and selenium accumulation

All the elasmobranchs had measurable concentrations of both Hg and Se in their muscle tissue. To date, only five studies have been published on Hg contamination in sharks from South Africa. A single study on shortfin mako sharks (*Isurus oxyrinchus*) collected off the east coast (Cloete and Watling*,* 1981), two studies concentrated on smooth-hound sharks (*M. mustelus*) from the west coast in 2013 and 2016 respectively (Bosch *et al.,* 2013, 2016), a study on 17 species collected along the east coast based on data collected from 2005 to 2010 (McKinney *et al.,* 2016) and most recently, research by Erasmus *et al.* (2022) who studied the Hg contamination in 22 species collected from various sites off coast of South Africa.

The Hg concentrations found in the in elasmobranchs of this study were higher than reported in the previous research on South African elasmobranchs (Bosch *et al.,* 2013 & 2016; Zaera & Johnson, 2011; McKinney *et al.,* 2016). The highest Hg concentrations were found in *S. lewini, C. taurus,* and *C. leucas*. Compared to the previous study by McKinney *et al.* (2016) on juveniles, these three species displayed higher levels of Hg, were all larger and can be regarded as adults. *Carcharhinus leucas* had Hg concentrations three times higher than the *C. leucas* sampled by McKinney *et al.* (2016), however the *C. leucas* specimens sampled by McKinney *et al.* (2016) ranged between juveniles and adults with the single *C. leucas* from this study being regarded as an adult female (Froese and Pauly, 2022). *Sphyrna lewini* had elevated levels of Hg compared to the *S. lewini* from McKinney *et al.* (2016), and the same trend could also be seen with *C. leucas* from Mckinney *et al.* (2016) with many of the

individuals of *S. lewini* regarded as juveniles, whereas *S. lewini* from this current study were all regarded as adults (Froese and Pauly, 2022).

The Hg levels *Carcharias taurus* were slight lower when compared to the levels in *C. taurus* reported by McKinney *et al.* (2016) Interestingly the *C. taurus* from the current study was an adult, and the *C. taurus* from McKinney *et al.* (2016) were juveniles (Froese and Pauly, 2022). A possible reason for this is the feeding ranges and differences in prey availability between juveniles and adults from different studies.

The Australian *M. kuhlii, M. eregoodtenkee,* and *C. leucas* had higher Hg levels, while *C. taurus* hadl levels (Cagnazzi *et al.,* 2019) compared to the same elasmobranch species from South Africa. Comparing Hg levels of the USA (Rumbold *et al.,* 2014; Matulik *et al.,* 2017; Suk *et al.,* 2009, and Lyons *et al.,* 2013) and Mexico (Pantoja-Echevarría *et al.,* 2021; García-Hernández *et al.* 2007; Espinoza-García, 2016; Hurtado-Banda *et al.,* 2012; Bergés-Tiznado *et al.* 2015; Ruelas-Inzunza *et al.,* 2020; Maz-Courrau *et al.,* 2012; Escobar-Sánchez *et al.,* 2010; Ruelas-Inzunza *et al.,* 2011) to the current study the majority of the elasmobranchs displayed lower levels of Hg except for *C. leucas* and *S. lewini* again with elevated levels. *Carcharhinus leucas* from García-Hernández *et al.* (2007), Ruelas-Inzunza *et al.* (2011), and Matulik *et al.* (2017) were all juveniles, with only Rumbold *et al.* (2014) reported the Hg data from adult *C. leucas*. The same trend is seen with *S. lewini* and the Hg results reported by García-Hernández *et al.* (2007), Ruelas-Inzunza *et al.* (2020), and Hurtado-Banda (2012), who reported that many of the sampled *S. lewini* were juveniles and as such the potential time and opportunities to bioaccumulate Hg were not as plentiful as the ones that were.

To date, only Bosch *et al.* (2016) provided data on the Se concentrations in elasmobranchs off South Africa. The only other data on Se in marine organisms are for mussels from various localities around the coast of South Africa (Nekhoroshkov *et al.,* 2021a, b). Although the Se concentrations did not differ significantly between the species in the current study, the levels were variable and could be attributed to geo-environmental factors and biological traits of the species (Wyatt *et al.,* 1996). The Se levels in elasmobranchs from the Mediterranean (Grgec *et al.,* 2020, Storelli *et al.,* 2013, Kousteni *et al.,* 2016, Nicolaus *et al.,* 2017, Giovos *et al.,* 2022, Storelli *et al.*, 2022), and reported an average of 0.51 mg/kg for both rays and sharks. This was higher than the average Se levels measured in this study of 0.39 mg/kg and 0.38 mg/kg in the rays and sharks, respectively. Studies on hammerhead sharks (*S. lewini*, *S. zygaena*) from the Pacific Ocean surrounding Mexico (Escobar-Sánchez *et al.* 2010; Lara *et al.,* 2022; Bergés-Tiznado *et al.* 2015; Ruelas-Inzunza *et al.* 2020) had Se concentrations comparable to those measured in the same species from the current study.

Intrinsic factors influencing mercury and selenium concentrations

Trophic position of the elasmobranchs played a significant role in Hg bioaccumulation within both male and female elasmobranchs of this study. There were some notable exceptions related to Hg concentrations and trophic positions. The white shark (*C. carcharias*), that occupies the highest trophic position of all the species studied, had one of the lowest Hg concentrations. However, it did have the second highest Se levels of all elasmobranch species. The high percentage contribution of Se in *C. carcharias* may potentially be due to *C. carcharias* feeding on the rays and skates that have high Se levels (*R. jayakari, A. bovinus, R. straeleni*) or possibly feeding on colonies of seals that have high levels of Se in their muscle tissue (Dietz *et al.,* 1998, McHuron *et al.,* 2014).

There were no significant differences in Hg levels between males and females, and therefore, as Erasmus *et al.* (2022) showed, the size of the elasmobranchs was the influencing factor determining the Hg concentrations and not the sex. Although not significant, there were interesting differences in Hg and Se uptake patterns between male and female ray species and one shark species (*H. fuscus*).

Male and female *M. kuhlii* had similar Hg concentrations in their muscle tissue; however, Se levels were much higher in males (0.29 mg/kg) compared to females (0.07 mg/kg). The reason for the lower Se in females may be due to maternal offloading (Weijs *et al.,* 2015). Opposite patterns in Hg and Se concentrations were observed in males and females of *M. eregoodtenkee,* which is a conspecific of *M. kuhlii* (Last *et al.,* 2016), were observed. The female *M. eregoodtenkee* (0.28 mg/kg) had Se levels double those found in males (0.14 mg/kg). Females were also found to be heavier than males at 21.8 kg compared to 12 kg with similar lengths of 120 cm to 106 cm. *Mobula kuhlii* (shortfin devil ray) and *M. eregoodtenkee* displayed similar sizes and contaminant load despite the differences in the percentage contributions of Se between males and females.

Extrinsic factors (Geographical location influencing bioaccumulation)

Given the level of anthropogenic sources of Hg near the eastern coast of South Africa, Hg deposition may occur in the marine environment along the country's east coast (Freiman and Piketh, 2003).

The east coast elasmobranch species (*M. kuhlii, M. eregoodtenkee, A. bovinus, R. jayakari, G. cuvier, S. lewini, C. brevipinna, C. limbatus, C. obscurus, S. zygaena, S. africana, C. amboinensis, C. leucas, C. taurus,* and *C. carcharhias*) had higher levels of Hg, except for the rays, compared to the elasmobranchs from the south coast (*P. pantherinum, R. straeleni, H. edwardsii, H. fuscus, H. pictus, M. mustelus*). Thus, the increased Hg levels in the east coast

elasmobranchs can be attributed to the increased anthropogenic input of Hg from the coal-fired power stations (Freiman and Piketh, 2003).

According to Courtman *et al*. (2012) the soils along the South African east coast have a much higher Se content than the rest of the country. These Se-containing soils leach into the numerous rivers, estuaries, and bays along the east coast of South Africa (Olisha *et al.,* 2020 and 2021) introducing Se into the marine environment. The higher Se levels were then recorded in elasmobranchs from the east coast of South Africa, and more specifically those species that were more likely to be associated with shallower waters (e.g., *R. jayakari, A. bovinus, S. zygaena, C. obscurus, C. leucas,* and *C. limbatus*). The south coast also had elasmobranchs associated with shallower waters and demersal feeders (*R. straeleni, P. pantherinum, H. edwardsii, H. fuscus, H. pictus,* and *M. mustelus*), however, the increased levels of Se were not observed in these species as in the east coast species. This contributes to the assumption that the elasmobranchs from the east coast are exposed to higher Se levels either from anthropogenic sources or natural occurrence in the soils (Courtman *et al.,* 2012; Fordyce, 2012).

The increased Se levels within the east coast elasmobranchs can also be contributed to the increased trophic positions and diet. Figure 3.1 substantiates these findings, and the levels of Hg and Se can be seen to noticeably higher in the east coast representatives. Research completed by Bergés-Tiznado *et al.* (2015) also found that Se was found a positive correlation between the Se found in the muscle and liver of the shark. This indicates that Se levels may not be contingent on factors such as size, weight or age. Instead, the levels of Se might be impacted by diet and foraging habitat. Bergés-Tiznado *et al.* (2015) also mentions that selenocysteine acts as a trap for MeHg within the muscle tissue of *S. lewini* by keeping the MeHg in circulation by binding to it. However, Bergés-Tiznado *et al.* (2015) also mentions that the species-specific differences in metabolism and excretion also influences the levels of both Se and Hg. Faganeli *et al.* (2018) found that pelagic species of rays had higher levels of Se compared to feeders found closer to shore and this can also explain the higher concentration of Se found within the more migratory species of sharks found on the east coast compared to the south coast.

Human health risk

Mercury concentrations are significantly elevated in marine fish and shellfish, with piscivorous species such as tuna notably affected. The consumption of marine fish and seafood is a primary pathway for Hg exposure in humans, particularly in communities heavily dependent on fish as a source of food, protein, and nutrients (Driscoll *et al.,* 2013).

The presence of Hg and, to a lesser extent Se, in elasmobranch species raises concerns about the potential health risks for individuals who regularly consume these marine organisms. The consumption patterns of elasmobranchs along the coast of South Africa are unknown. To address this gap, an estimated health risk assessment was adapted from studies by Erasmus *et al.* (2022), Heath *et al.* (2004), and Ralston *et al.* (2016), focusing on adults with an average weight of 70 kg. This assessment did not account for individuals who may be more vulnerable to trace elements, including pregnant women, lactating mothers, infants, and children, all of whom are known to exhibit greater susceptibility and sensitivity to these contaminants (Javed and Usmani, 2019).

The estimated daily intake values for Hg and Se for the South African population were calculated and compared to the tolerable daily intake regulatory guidelines (Otten *et al.*, 2006; Watanabe *et al.,* 2021). Calculations were based on individuals who consumed 48.57 g of elasmobranch tissue, and the estimated daily intake of Hg was higher in all species of elasmobranch compared to the tolerable daily intake values. The tolerable daily intake of Se was only exceeded by the estimated daily intake values of *R. jayakari, C. limbatus* and *C. carcharias.* The HQ calculated for Hg further indicated that the consumption of some of the elasmobranchs poses the possibility of adverse health risks. The Hg HQ values indicated that half of the elasmobranchs (*G. cuvier, S. lewini, S. zygaena, C. brevipinna, S. africana, C. obscurus, C. leucas, C. amboinensis, C. taurus, N. cepedianus, C. carcharias*) pose risks of potential adverse health effects with the long-term consumption of the muscle tissue from these species. However, as referred to in Chapter 2 the commonly harvested elasmobranchs off the coast of South Africa are *M. mustelus, C. brevipinna, C. limbatus, S, zygaena* and *N. cepedianus* to a more limited degree. Of these four species, only *M. mustelus* had a HQ value less than one, and the rest posed a potential health risk with consumption.

The maximum safe consumption limit, aimed at preventing non-carcinogenic health risks associated with elasmobranch muscle tissue, ranges from 2 g (*S. lewini*) to 140 g (*M. kuhlii*) per day for Hg, the compound with the highest concentrations observed in this study. The four commonly commercially harvested elasmobranchs around the South African coast had safe consumption limits ranging from 6.3 g (*N. cepedianus*) to 34.8 g (*M. mustelus*) per day for Hg (Da Silva & Bürgener, 2007).

In comparison to the international literature, the following studies have published data on their respective HBV_{Se} values obtained from various elasmobranch species. Teixeira *et al.* (2020) recorded a negative value (-14.56) for *Deania Calcea* in the North-East Atlantic, mirroring the findings of Ralston *et al.* (2016) in *I. oxyrinchus* (-16.4). *Mustelus henlei* (brown smoothhound shark) from the Pacific Ocean displayed an HBV_{Se} close to zero (0.08) from Medina-Morales

et al. (2020). Contrarily, other shark species in the following studies (Mirlean *et al.,* 2019; Grgec *et al.,* 2020) found positive HBV_{Se} in *I. oxyrinchus* (4.6)*, M. mustelus* (8.11)*.*

The HBV_{Se} criterion serves as a valuable tool for streamlining the assessment of Hg exposure risk, providing a reliable index for accurately predicting associated risks (Ralston *et al.,* 2016). Opting for elasmobranchs with a high positive HBV_{Se} value can lead to excess Se intake. Conversely, selecting elasmobranchs with negative values indicates a potential Se deficiency, posing the risk of adverse consequences related to Hg exposure for the consumer (Ralston *et al.,* 2016).

The calculated HBV_{Se} values revealed that all elasmobranchs on the south coast of South Africa had a positive HBV_{Se} value, except for *N. cepedianus*. Some of the east coast elasmobranchs had negative HBV_{Se} (*G. cuvier, S. lewini, C. leucas,* and *C. taurus*). The elasmobranchs (*M. mustleus, C. limbatus, C. brevipinna, S. zygaena, and N. cepedianus*) commonly harvested around South Africa all had a positive HBV_{Se} value, with only *N. cepedianus* showing a negative value. Therefore, elasmobranchs with a negative HBV_{Se} value will potentially have a Se deficiency and, as such, pose a risk of Hg exposure. Those elasmobranchs with positive HBV_{Se} values likely have sufficient Se levels thereby reducing the toxic effects associated with Hg (Kaneko and Ralston, 2007). Other comparable studies found positive HBV_{Se} values in *S. lewini* from the Pacific Ocean on the coast of Mexico (Ruelas-Inzunza *et al.,* 2020), as well as *M. mustelus* from the Mediterranean Sea (Storelli *et al.,* 2022) and Adriatic Sea (Grgec *et al.,* 2020) (Table S8), indicating that the toxic effects of Hg contamination may be reduced.

3.5 Conclusion

This study on Hg and Se concentrations in elasmobranchs along the South African coastline provides some insight into the bioaccumulation of these elements. The research revealed that the significant accumulation of Hg in muscle tissue was mainly influenced by size, trophic position, feeding behaviour, and geographical location. *Carcharodon carcharias* did not have the highest Hg levels which was attributable to the high Se levels accumulated from consuming Se-containing prey. The human health risk assessment raised concerns about adverse effects from long-term consumption of elasmobranch muscle tissue, emphasising the importance of cautious consumption. The study also showed the potential for Se to mitigate Hg toxicity.

Chapter 4: Conclusions and recommendations

4.1 Summary of the findings of the study

The South African coast has several unique biogeographical regions (Erasmus *et al.,* 2022). This distinctiveness is primarily attributed to two major ocean currents. The Agulhas current along the east coast brings warm and nutrient-poor water from the subtropical Indian Ocean, while the Benguela current along the west coast transports cold and nutrient-rich waters from the Antarctic (Griffiths *et al.,* 2010; Wepener & Degger, 2019). As a result, South Africa's coastal area is one of the most species diverse regions on the African continent, ranking third globally in terms of the highest number of species per unit area (Griffiths *et al.,* 2010; Wepener & Degger, 2019). Elasmobranch biodiversity encompasses a wide range of cartilaginous fish, including sharks, rays, and skates, with over 500 described shark species and over 600 described ray and skate species. These marine organisms play crucial roles in maintaining the balance of ocean ecosystems, yet many face conservation challenges due to factors such as overfishing and habitat degradation.

Currently, research addressing organochlorine pesticides (OCPs) in elasmobranchs off the coast of South Africa are limited to two studies (Beaudry *et al.,* 2015; Schlenk *et al.,* 2005). Mercury (Hg) and selenium (Se) studies on elasmobranchs around South Africa include Zaera and Johnsen (2011), Bosch *et al.* (2013, 2016), and McKinney *et al.* (2016). To address this knowledge gap this study was undertaken to assess the current state of OCPs and inorganic compounds (Hg and Se) in selected elasmobranch species collected from the east and south coast of South Africa.

In Chapter 2, the accumulation of OCPs in the elasmobranchs from the south and east coast was determined. The elasmobranchs from the east coast of South Africa had higher levels of OCPs compared to the species from the south coast, with the compound with the highest concentrations being p,p'-DDE. The highest levels of OCPs were measured in *C. carcharias* (white shark), *N. cepedianus* (broadnose sevengill shark)*, C. obscurus* (dusky shark) and *M. mustelus* (smoothhound shark). The concentrations of DDxs measured in this study were higher than the levels in elasmobranchs from Australia and Djibouti. Similarly, Australian elasmobranchs also had higher HCB concentrations compared to South Africa. Elasmobranchs from Mexico and Korea had lower levels compared to the current study.

Furthermore, the study highlighted the significance of trophic position in the accumulation of OCPs in elasmobranchs. Higher trophic levels were associated with increased OCP levels. The trophic positions of elasmobranchs were also stronger drivers of OCP accumulation than geographical location. Results also indicated that elasmobranch size and maturation rather

than different sexes influenced OCP levels, with females generally exhibiting higher levels compared to males. This was mainly due to the fact that females were in general larger than the males.

The health risk assessments indicated that there was a cancer risk associated with the long-term consumption of the elasmobranch species analysed. The maximum safe consumption limit for OCPs ranged from as little as 6 g in *N. cepedianus* (broadnose sevengill shark) to 537 g in *H. fucus* (brown shyshark) per day.

Chapter 3 presented data on the accumulation of Hg and Se in the same elasmobranch species that were studied in Chapter 2.

There was a statistically significant relationship between Hg concentrations and trophic levels in female elasmobranchs. However, this relationship was not present for Se concentrations in elasmobranchs.

There was an increase in Hg concentrations in elasmobranchs when compared to previous studies on South African elasmobranchs, with significant increases in *S*. *lewini* (scalloped hammerhead shark) and *C. leucas* (bull shark). These increases were attributed to the larger size and possible increased age of the sharks from the current study. These species had Hg levels similar to those of elasmobranchs from Australia and Mexico. Selenium levels were attributed to geographical location and specific species biological traits. Overall, the Se levels measured in elasmobranchs from this study were lower than levels recorded in sharks from the Mediterranean, but similar to elasmobranchs from Mexico. There were distinct differences in the Hg and Se concentrations between males and females of two ray species [*M. kuhlii* (shortfin devil ray) and *M. eregoodootenkee* (longhorn devil ray)].

The east coast elasmobranchs had higher Hg and Se concentrations compared to the south coast elasmobranchs. This was attributed to both higher trophic positions as well as increased element input into the marine environment through rivers and estuaries. The elasmobranchs with the highest Se levels were associated with shallower waters [*R. jayakari* (oman cownose ray), *A. bovinus* (bull ray), *S. zygaena* (smooth hammerhead shark), *C. obscurus* (dusky shark), *C. leucas* (bull shark), and *C. limbatus* (blacktip shark)]. Therefore, the data from this study support the first hypothesis that OCP levels in elasmobranch species along the South African coast are related to different intrinsic (sex, size, migratory, and foraging habits) and extrinsic traits (geographical position).

Health risk assessments were conducted to assess the potential risks associated with the consumption of elasmobranchs with Hg and Se in their muscle tissues. The estimated daily intake values of Hg in all elasmobranchs were higher than the tolerable daily intake. The Se

estimated daily intake values in *R. jayakari* (oman cownose ray), *C. limbatus* (blacktip shark), and *C. carcharias* (white shark) were higher than the tolerable daily intake levels. Hazard quotient values for Hg in all east coast elasmobranchs except for *C. limbatus* (blacktip shark), pose potential risks of adverse health effects associated with the prolonged consumption of their muscle tissue. To mitigate non-carcinogenic health risks associated with the consumption of elasmobranch muscle tissue, the safe consumption limits for Hg were calculated as between 2.2 g per day for *C. leucas* and 140 g per day for *M. kuhlii*. Therefore, the data support the hypothesis that contaminants (OCPs, Hg and Se) in elasmobranch tissues pose a health risk to humans who consume them.

Elasmobranchs from the south coast of South Africa generally had a positive Se health benefit (HBV_{Se}), except for *N. cepedianus* (broadnose sevengill shark). On the east coast, *G. cuvier* (tiger shark), *S. lewini* (scalloped hammerhead shark), *C. leucas* (bull shark), and *C. taurus* (ragged tooth shark) exhibit negative HBV_{Se} values, suggesting potential selenium deficiency and a risk of toxic Hg exposure when muscle tissue from these species are consumed. Conversely, those with positive HBV_{Se} values, including all the rays and skate as well as the remaining shark species from the east and south coast of South Africa would suggest a healthy amount of Se and counteracting the toxic effects of Hg exposure. Therefore, the data do not support the hypothesis that there is an antagonistic relationship between Se and Hg levels in the elasmobranch species studied, as many species from the east coast had a negative Se health benefit value.

This study, with the limited number of samples and limited species available, contributed to providing baseline concentrations of organic and inorganic compounds present in many South African elasmobranch species for which no data are available.

4.2 Recommendations for future studies

The findings of this study identified the following aspects that can be considered for future studies:

- The inclusion of more replicates for each species and the inclusion of prey sources to obtain a clearer picture of the levels of contaminants in the marine environment and food webs surrounding the coast of South Africa.
- The use of QuECHERS should be further studied and optimised to improve OCP extractions since it is fast and cheaper than solvent extractions and cleanup procedures.
- Since elasmobranch livers are known to be very lipid-rich organs, future research should aim to establish more effective measures of removing the lipids from the samples in order to confidently analyse these samples. The lip-rich liver samples may also damage the analytical equipment if all of the lipids are not removed before analysis.
- Completing the analysis of different organs within the elasmobranch species in order to assess possible compartmentalisation of the contaminants.
- Assessing contaminant bioaccumulation in other marine organisms. Future research should explore the potential cascading effects and ecological consequences of these pesticide contaminants.
- Conduct human health risk assessments on commonly consumed fish species around the coast of South Africa such as hake, kingklip, and tuna.
- Sediment analysis around the coast can be performed to determine possible OCP contamination in estuaries, bays, and harbours.
- A wider array of compounds can be analysed for future studies, such as legacy pollutants, e.g., PAHs, PCBs, and PBDEs; and current use pesticides.
- Assessing the results obtained from the research and potentially implementing these in management plans in the future in order to better protect these elasmobranch species.

Chapter 5: References

Adams, D.H. 2004. Total mercury levels in tunas from offshore waters of the Florida Atlantic coast. *Marine Pollution Bulletin,* 49(7-8):659-663.

Afful, S., Anim, A.K. & Serfor-Armah, Y. 2010. Spectrum of Organochlorine Pesticide Residues in Fish Samples from the Densu Basin. *Research Journal of Environmental and Earth Sciences,* 2(3):133-138.

Afonso, A.S., Niella, Y.V., Cavalcanti, E., Andrade, M.B., Afonso, J.S., Pinto, P.S. & Hazin, F.H.V. 2016. Spinal deformities in free-ranging bull sharks, *Carcharhinus leucas* (Müller and Henle, 1839), from the western South Atlantic Ocean. *Journal of Ichthyology,* 32(6):1217-1220.

Agency for Toxic Substances and Disease Registry (ATSDR). 2007. Toxicological profile for Heptachlor and Heptachlor epoxide. Atlanta, GA: U.S. Department of Health and Human Services, Public Health Service.

Agency for Toxic Substances and Disease Registry (ATSDR). 2018. Toxicological Profile for Chlordane. Atlanta, GA: U.S. Department of Health and Human Services, Public Health Service.

Agency for Toxic Substances and Disease Registry (ATSDR). 2019. Toxicological profile for DDT, DDE, DDD (Draft for Public Comment). Atlanta, GA: U.S. Department of Health and Human Services, Public Health Service.

Akan, J. C., Mohammed, Z., Jafiya, L. & Ogugbuaja, V. O. 2013. Organochlorine pesticide residues in fish samples from Alau Dam, Borno state, North Eastern Nigeria. *Journal of Environmental and Analytical Toxicology*, *3*(3):171-178.

Alman, B., Antezana, A., Fay, M., Derrick, H., Chiger, A., Hall, S., Lynch, M., Diskin, K. & Sonawane, B. 2022. Toxicological profile for mercury: draft for public comment: April 2022.

Alvim-Ferraz, M.C. & Afonso, S.A. 2003. Incineration of different types of medical wastes: emission factors for particulate matter and heavy metals. *Environmental Science & Technology*, 37(14):3152-3157.

AMAP/UN Environment. 2019. Technical Background Report for the Global Mercury Assessment 2018. Arctic Monitoring and Assessment Programme, Oslo, Norway/UN Environment Programme, Chemicals and Health Branch, Geneva, Switzerland, 426.

Amezcua, F., Ruelas-Inzunza, J., Coiraton, C., Spanopoulos-Zarco, P. & Páez-Osuna, F. 2022. A Global Review of Cadmium, Mercury, and Selenium in Sharks: Geographical

Patterns, Baseline Levels and Human Health Implications. *Reviews of Environmental Contamination and Toxicology,* 260(1):1-13.

Amin, K.A. & Hashem, K.S. 2012. Deltamethrin-induced oxidative stress and biochemical changes in tissues and blood of catfish (*Clarias gariepinus*): antioxidant defense and role of alpha-tocopherol. *BMC Veterinary Research,* 8:45.

Amouroux, D., Liss, P. S., Tessier, E., Hamren-Larsson, M. & Donard, O. F. 2001. Role of oceans as biogenic sources of selenium. *Earth and Planetary Science Letters*, *189*(3-4):277-283.

Amos, H.M., Jacob, D.J., Streets, D.G. & Sunderland, E.M. 2013. Legacy impacts of all-time anthropogenic emissions on the global mercury cycle. *Global Biogeochemical Cycles*, 27(2):10-421.

Aneck-Hahn, N.H., Schulenburg, G.W., Bornman, M.S., Farias, P. & de Jager, C. 2007. Impaired semen quality associated with environmental DDT exposure in young men living in a malaria area in the Limpopo Province, South Africa. *Journal of Andrology,* 28(3):423-434.

Azad, A.M., frantzen, S., Bank, M.S., Nilsen, B.M., Duinker, A., Madsen, L. & Maage, A. 2019. Effects of geography and species variation on selenium and mercury molar ratios in Northeast Atlantic marine fish communities. *Science of the Total Environment,* 652:1482-1496.

Barnhoorn, I.E.J., van Dyk, J.C., Genthe, B., Harding, W.R., Wagenaar, G.M. & Bornman, M.S. 2015. Organochlorine pesticide levels in *Clarias gariepinus* from polluted impoundments in South Africa and associated human health risks. *Chemosphere,* 120:391-397.

Barone, G., Dambrosio, A., Storelli, A., Garofalo, R., Busco, V.P. & Storelli, M.M. 2018. Estimated Dietary intake of trace metals from swordfish consumption: a human health problem. *Toxics,* 6(2):1-11.

Barone, G., Storelli, A., Meleleo, D., Dambrosio, A., Garofalo, R., Busco, A. & Storelli, M.M. 2021. Levels of mercury, methylmercury and selenium in fish: Insights into children food safety. *Toxics*, 9(2):39.

Beaudry, M.C., Hussey, N.E., McMeans, B.C., McLeod, A.M., Wintner, S.P., Cliff, G., Dudley, S.F. & Fisk, A.T. 2015. Comparative organochlorine accumulation in two ecologically similar shark species (Carcharodon carcharias and Carcharhinus obscurus) with divergent uptake based on different life history. *Environmental Toxicology and Chemistry*, 34(9):2051-2060.

Belelie, M.D., Piketh, S.J., Burger, R.P., Venter, A.D. & Naidoo, M. 2019. Characterisation of ambient total gaseous mercury concentrations over the South African Highveld. *Atmospheric Pollution Research*, 10(1):12-23.

Bergés-Tiznado, M.E., Márquez-Farías, F., Lara-Mendoza, R.E., Torres-Rojas, Y.E., Galván-Magaña, F., Bojórquez-Leyva, H. & Páez-Osuna, F. 2015. Mercury and selenium in muscle and target organs of scalloped hammerhead sharks *Sphyrna lewini* of the SE Gulf of California: dietary intake, molar ratios, loads, and human health risks. *Archives of Environmental Contamination and Toxicology*, 69:440-452.

Bjørklund, G., Dadar, M., Mutter, J. & Aaseth, J. 2017. The toxicology of mercury: Current research and emerging trends. *Environmental Research,* 159:545-554.

Blocksom, K.A., Walters, D.M., Jicha, T.M., Lazorchak, J.M., Angradi, T.R. & Bolgrien, D.W. 2010. Persistent organic pollutants in fish tissue in the mid-continental great rivers of the United States. *Science of the Total Environment,* 408(5):1180-1189.

Blum, J.D., Popp, B.N., Drazen, J.C., Anela Choy, C. & Johnson, M.W. 2013. Methylmercury production below the mixed layer in the North Pacific Ocean. *Nature Geoscience*, 6(10):879-884.

Blumberg, L., Frean, J. & Moonasar, D. 2014. Successfully controlling malaria in South Africa. *South African Medical Journal*, 104(3):224-227.

Binelli, A. & Provini, A. 2003. POPs in edible clams from different Italian and European markets and possible human health risk. *Marine Pollution Bulletin,* 46:879-886.

Boldrocchi, G., Monticelli, D., Omar, Y.M. & Bettinetti, R. 2019. Trace elements and POPs in two commercial shark species from Djibouti: Implications for human exposure. *Science of the Total Environment*, 669:637-648.

Bonfil, R., Meÿer, M., Scholl, M.C., Johnson, R., O'Brien, S., Oosthuizen, H., Swanson, S., Kotze, D. & Paterson, M. 2005. Transoceanic migration, spatial dynamics, and population linkages of white sharks. *Science,* 310:100-103.

Bouwman, H. (2003). POPs in Southern Africa. In: Fiedler, H. ed. *Persistent Organic Pollutants. The Handbook of Environmental Chemistry*. Berlin, Heidelberg: Springer, pp. 297-320.

Bouwman, H. 2004. South Africa and the Stockholm Convention on Persistent Organic Pollutants: science policy. *South African Journal of Science,* 100(7):323-328.

Bornatowski, H., Braga, R.R., Abilhoa, V. & Corrêa, M.F.M. 2014. Feeding ecology and trophic comparisons of six shark species in a coastal ecosystem off southern Brazil. *Journal of fish Biology*, 85(2):246-263.

Bosch, A.C., Sigge, G.O., Kerwath, S.E., Cawthorn, D.M. & Hoffman, L.C. 2013. The effects of gender, size and life-cycle stage on the chemical composition of smoothhound shark (*Mustelus mustelus*) meat. *Journal of the Science of Food and Agriculture*, 93(10):2384-2392.

Bosch, A.C., O'Neill, B., Sigge, G.O., Kerwath, S.E. & Hoffman, L.C. 2016. Heavy metal accumulation and toxicity in smoothhound (*Mustelus mustelus*) shark from Langebaan Lagoon, South Africa. *Food chemistry*, 190:871-878.

Branco, V., Canário, J., Vale, C., Raimundo, J. & Reis, C. 2004. Total and organic mercury concentrations in muscle tissue of the blue shark (*Prionace glauca* L.1758) from the Northeast Atlantic. *Marine Pollution Bulletin,* 49(9-10):871-874.

Buah-Kwofie, A., Humphries, M.S. & Pillay, L. 2018. Bioaccumulation and risk assessment of organochlorine pesticides in fish from a global biodiversity hotspot: iSimangaliso Wetland Park, South Africa. *Science of the Total Environment,* 621:273-281.

Buccini, J. 2003. The development of a global treaty on persistent organic pollutants (POPs). In: Fiedler, H. ed. *Persistent Organic Pollutants. The Handbook of Environmental Chemistry*. Berlin, Heidelberg: Springer, pp. 13-30.

Briones, A.A., Hernández-Guzmán, F.A., González-Armas, R., Galván-Magaña, F., Marmolejo-Rodríguez, A.J., Sánchez-González, A. & Ramírez-Ālvarez, N. 2022. Organochlorine pesticides in immature scalloped hammerheads *Sphyrna lewini* from the western coast of the Gulf of California, Mexico: Bioaccumulation patterns and human exposure. *Science of the Total Environment,* 806:151369.

Cabanéro, A.I., Madrid, Y. & Cámara, C. 2007. Mercury-selenium species ratio in representative fish samples and their bioaccessibility by an in vitro digestion method. *Biological Trace Element Research,* 119(3):195-211.

Cagnazzi, D., Consales, G., Broadhurst, M.K. & Marsili, L. 2019. Bioaccumulation of organochlorine compounds in large, threatened elasmobranchs off northern New South Wales, Australia. *Marine Pollution Bulletin*, 139:263-269.

Carwile, J.L., Butler, L.J., Janulewicz, P.A., Winter, M.R. & Aschengrau, A. 2016. Childhood fish consumption and learning and behavioral disorders. *International Journal of Environmental Research and Public Health,* 13(11):1069.

Caserta, D., Graziano, A., Monte, G.L., Bordi, G. & Moscarini, M. 2013. Heavy metals and placental fetal-maternal barrier: a mini-review on the major concerns. *European Review for Medical and Pharmacological Sciences,* 1(16):2198-2206.

Chawla, R., Filippini, T., Loomba, R., Cilloni, S., Dhillon, K.S. & Vinceti, M. 2020. Exposure to a high selenium environment in Punjab, India: Biomarkers and health conditions. *Science of the Total Environment*, 719:134541.

Chen, C., Lim, Y.C., Ju, Y., Albarico, F.P.J.B., Chen, C. & Dong, C. 2022. Comparing the applicability of ecological risk indices of metals based on PCA-APCS-MLR receptor models for ports surface sediments. *Marine Pollution Bulletin,* 185:114361.

Choy, C.A., Popp, B.N., Kaneko, J.J. & Drazen, J.C. 2009. The influence of depth on mercury levels in pelagic fishes and their prey. *Proceedings of the National Academy of Sciences of the United States of America,* 106(33):13865-13869.

Chynel, M., Munschy, C., Bely, N., Héas-Moisan, K., Pollono, C. & Jaquemet, S. 2021. Legacy and emerging organic contaminants in two sympatric shark species from Reunion Island (Southwest Indian Ocean): Levels, profiles and maternal transfer. *Science of the Total Environment,* 751:141807.

Cloete, C. E. & Watling, R. J. 1981. South African marine pollution monitoring programme, 1979-1982.

Cortés, E. 1999. Standardized diet compositions and trophic levels of sharks. *ICES Journal of Marine Science*, 56(5):707-717.

Cortés, E. 2000. Life History Patterns and Correlations in Sharks. *Reviews in Fisheries Science,* 8(4):299-344.

Cossa, D., Averty, B. & Pirrone, N. 2009. The origin of methylmercury in open Mediterranean waters. *Limnology and Oceanography*, 54(3):837-844.

Cossa, D., Heimbürger, L.E., Lannuzel, D., Rintoul, S.R., Butler, E.C., Bowie, A.R., Averty, B., Watson, R.J. & Remenyi, T. 2011. Mercury in the southern ocean. *Geochimica et Cosmochimica Acta*, 75(14):4037-4052.

Courtman, C., van Ryssen, J.B.J. & Oelofse, A. 2012. Selenium concentration of maize grain in South Africa and possible factors influencing the concentration. *South African Journal of Animal Science,* 42(5):454-458.

Da Silva, C. & Bürgener, M. 2007. South Africa's demersal shark meat harvest. *TRAFFIC Bulletin,* 21(2):55-65.

Dallaire, R., Dewailly, É., Ayotte, P., Forget-Dubois, N., Jacobson, S.W., Jacobson, J.L. & Muckle, G. 2013. Exposure to organochlorines and mercury through fish and marine mammal consumption: associations with growth and duration of gestation among Inuit newborns. *Environment International*, 54:85-91.

Dalvie, M.A. & London, L. 2006. The impact of aerial application of organophosphates on the cholinesterase levels of rural residents in the Vaalharts district, Northern Cape Province, South Africa. *Environmental Research,* 102(3):326-332.

Dalvie, M.A., Africa, A. & London, L. 2009. Change in the quantity and acute toxicity of pesticides sold in South African crop sectors, 1994-1999. *Environmental International,* 35(4):683-687.

De Gieter, M., Leermakers, M., Van Ryssen, R., Noyen, J., Goeyens, L. & Baeyens, W. 2002. Total and toxic arsenic levels in North Sea fish. *Archives of Environmental Contamination and Toxicology,* 43(4):406-417.

Dent, F. & Clarke, S. 2015. State of the global market for shark products. *FAO Fisheries and Aquaculture Technical Paper,* 590:I.

Dietz, R., Paludan-Müller, P., Agger, C.T. & Nielsen, C.O. 1998. Cadmium, mercury, zinc and selenium in ringed seals (*Phoca hispida*) from Greenland and Svalbard. *NAMMCO Scientific Publications,* 1:242-272.

Dixon, R. & Jones, B. 1994. Mercury concentrations in stomach contents and muscle of five fish species from the north east coast of England. *Marine Pollution Bulletin,* 28:741-745.

Djingova, R., Heidenreich, H., Kovacheva, P. & Markert, B. 2003. On the determination of platinum group elements in environmental materials by inductively coupled plasma mass spectrometry and microwave digestion. *Analytica Chimica Acta,* 489:245-251.

Doong, R.A., Sun, Y.C., Liao, P.L., Peng, C.K. & Wu, S.C. 2002. Distribution and fate of organochlorine pesticide residues in sediments from the selected rivers in Taiwan. *Chemosphere*, 48(2):237-246.

Driscoll, C.T., Mason, R.P., Chan, H.M., Jacob, D.J. & Pirrone, N. 2013. Mercury as a global pollutant: sources, pathways, and effects. *Environmental Science & Technology*, 47(10):4967-4983.

Dulvy, N.K., Fowler, S.L., Musick, J.A., Cavanagh, R.D., Kyne, P.M., Harrison, L.R., Carlson, J.K., Davidson, L.N.K., Fordham, S.V., Francis, M.P., Pollock, C.M., Simpfendorfer, C.A., Burgess, G.H., Carpenter, K.E., Compagno, L.J.V., Ebert, D.A., Gibson, C., Heupel, M.R., Livingstone, S.R., Sanciangco, J.C., Stevens, J.D., Valenti, S. & White, W.T. 2014. Extinction risk and conservation of the world's sharks and rays. *eLife,* 3:1-34.

Ebert, D.A. & Bizzarro, J.J. 2009. Standardized diet compositions and trophic levels of skates (Chondrichthyes: Rajiformes: Rajoidei). *Biology of skates*, 115-131.

Ebert, D.A. & van Hees, K.E. 2015. Beyond *Jaws*: rediscovering the 'lost sharks' of southern Africa. *Journal of Marine Science,* 37(2):141-156.

Ebert, D.A., Dando, M. & Fowler, S. 2021. *Sharks of the world: a complete guide*. United Kingdom, Oxfordshire: Princeton University Press.

EMBER Report. 2022. Progress towards clean power targets, 2000-2040: Africa. https://ember-climate.org/countries-and-regions/regions/africa/. Date accessed: 12 August 2023.

Endo, T., Hisamichi,Y., Haraguchi, K., Kato, Y., Ohta, C. & Koga, N. 2008. Hg, Zn and Cu levels in the muscle and liver of tiger sharks (*Galeocerdo cuvier*) from the coast of Ishigaki Island, Japan: relationship between metal concentrations and body length. *Marine Pollution Bulletin*, 56:1774-1780.

Endo, T., Kimura, O., Ogasawara, H., Ohta, C., Koga, N., Kato, Y. & Haraguchi, K. 2015. Mercury, cadmium, zinc and copper concentrations and stable isotope ratios of carbon and nitrogen in tiger sharks (*Galeocerdo cuvier*) culled off Ishigaki Island, Japan. *Ecological Indicators,* 55:86-93.

Erasmus, A., Ikenaka, Y., Nakayama, S.M.M., Ishizuka, M., Smit, N.J. & Wepener, V. 2020. Trophic transfer of pollutants within two intertidal rocky shore ecosystems in different biogeographic regions of South Africa. *Marine Pollution Bulletin,* 157:111309.

Erasmus, J.H., Smit, N.J., Gerber, R., Schaeffner, B.C., Nkabi, N. & Wepener, V. 2022. Total mercury concentrations in sharks, skates and rays along the South African coast. *Marine Pollution Bulletin,* 184:114142.

Escobar-Sánchez, O., Galván-Magaña, F. & Rosíles-Martínez, R. 2010. Mercury and selenium bioaccumulation in the smooth hammerhead shark, *Sphyrna zygaena* Linnaeus, from the Mexican Pacific Ocean. *Bulletin of Environmental Contamination and Toxicology,* 84:488-491.

Espinoza-García, S. 2016. Bioaccumulation y biomagnification de Cd, Hg, y Pb en *Mustelus henlei* (Gill 1863) de la costa surroccidental de Baja California Sur. Unpublished MSc dissertation. Centro Interdisciplinario de Ciencias Marinas La Paz, Brazil.

Faganeli, J., Falnoga, I., Horvat, M., Klun, K., Lipej, L. & Mazej, D. 2018. Selenium and mercury interactions in apex predators from the Gulf of Trieste (Northern Adriatic Sea). *Nutrients*, *10*(3):278.

Farrington, J.W. & Takada, H. 2014. Persistent organic pollutants (POPs), polycyclic aromatic hydrocarbons (PAHs), and plastics: Examples of the status, trend, and cycling of organic chemicals of environmental concern in the ocean. *Oceanography,* 27(1):196-213.

Fatoki, O. & Awofolu, O. 2004. Levels of organochlorine pesticide residues in marine-, surface-, ground- and drinking waters from the Eastern Cape Province of South Africa. *Journal of Environmental Science and Health, Part B,* 39:101-114.

Fernández-Bautista, T., Gómez- Gómez, B., Palacín-García, R., Gracia-Lor, E., Pérez-Corona, T. & Madrid, Y. 2022. Analysis of Se and Hg biomolecules distribution and Se speciation in poorly studied protein fractions of muscle tissues of highly consumed fishes by SEC-UV-ICP-MS and HPLC-ESI-MS/MS. *Talanta,* 237(122922):1-9.

Ferriss, B.E. & Essington, T.E. 2011. Regional patterns in mercury and selenium concentrations of yellowfin tuna (*Thunnus obesus*) in the Pacific Ocean. *Canadian Journal of Fisheries and Aquatic Sciences,* 68(12):2046-2056.

Fitzgerald, L. & Wikoff, D.S. 2014. Persistent organic pollutants. In: Wexler, P. ed. *Encyclopedia of Toxicology*. United Kingdom, Oxford: Academic Press. pp. 820-825.

Fordyce, F. M. 2012. Selenium deficiency and toxicity in the environment. In: Selinus, O. ed. *Essentials of medical geology: Revised edition.* Netherlands, Dordrecht: Springer. pp. 375-416.

Fontanella, M. C., Ravera, O., Beone, G. M., Riccardi, N. & Cattani, I. 2009. Mercury distribution in the main compartments of the eutrophic Lake Candia (Northern Italy). *Journal of Limnology*, *68*(2):352.

Forsyth, D.S., Casey, V., Dabeka, R.W. & McKenzie, A. 2004. Methylmercury levels in predatory fish species marketed in Canada. *Food Additives and Contaminants,* 21:849-856.

Freiman, M.T. & Piketh, S.J. 2003. Air Transport into and out of the Industrial Highveld Region of South Africa. *Journal of Applied Meteorology,* 42(7):994-1002.

Froese, R. & Pauly, D. 2022. Fishbase. https://www.fishbase.org/. Date accessed: 1 July 2023.

García-Hernández, J., Cadena-Cárdenas, L., Betancourt-Lozano, M., García-De-La-Parra, L.M., García-Rico, L. & Márquez-Farías, F. 2007. Total mercury content found in edible tissues of top predator fish from the Gulf of California, Mexico. *Environmental and Toxicological Chemistry,* 89:507-522.

Gelsleichter, J. & Walker, C. J. 2010. Pollutant exposure and effects in sharks and their relatives. In: Carrier, J.C., Musick, J.A. & Heithaus, M.R. eds. *Sharks and their relatives II.* Boca Raton: CRC Press. pp. 507-554.

Gerber, R., Wepener, V. & Smit, N.J. 2015. Application of multivariate statistics and toxicity indices to evaluate the water quality suitability for fish of three rivers in the Kruger National Park, South Africa. *African Journal of Aquatic Science,* 40(3):247-259.

Gerber, R., Smit, N.J., Van Vuren, J.H.J., Nakayama, S.M.M., Yohannes, Y.B., Ikenaka, Y., Ishizuka, M. & Wepener, V. 2016. Bioaccumulation and human health risk assessment of DDT and other organochlorine pesticides in an apex aquatic from a premier conservation area. *Science of the Total Environment,* 550:522-533.

Gerber, R., Bouwman, H., Govender, D., Ishizuka, M., Ikenaka, Y., Yohannes, Y.B., Smit, N. & Wepener, V. 2021. Levels of DDTs and other organochlorine pesticides in healthy wild Nile crocodiles (*Crocodylus niloticus*) from a flagship conservation area. *Chemosphere,* 264:128368.

Gichuki, S.W. & Mason, R.P. 2013. Mercury and metals in South African precipitation. *Atmospheric Environment,* 79:286-289.

Gilbert, J.M., Baduel, C., Li, Y., Rechelt-Brushett, A.J., Butcher, P.A., McGrath, S.P., Peddemors, V.M., Hearn, L., Mueller, J. & Cristidis, L. 2015. Bioaccumulation of PCBs in liver tissue of dusky *Carcharhinus obscurus*, sandbar *C. plumbeus* and white *Carcharodon carcharias* sharks from south-eastern Australian waters. *Marine Pollution Bulletin,* 101(2):908-913.

Gilbert, J.M., Reichelt-Brushett, A.J., Butcher, P.A., McGrath, S.P., Peddemors, V.M., Bowling, A.C. & Christidis, L. 2015. Metal and metalloid concentrations in the tissues of dusky *Carcharhinus obscurus*, sandbar *C. plumbeus* and white *Carcharodon carcharias* sharks from south-eastern Australian waters, and the implications for human consumption. *Marine Pollution Bulletin,* 92:186-194.

Giovos, I., Brundo, M.V., Doumpas, N., Kazlari, Z., Loukovitis, D., Moutopoulos, D.K., Spyridopoulou, R.N.A., Papadopoulou, A., Papapetrou, M., Tiralongo, F., Ferrante, M. & Copat, C. 2022. Trace elements in edible tissues of elasmobranchs from the North Aegean Sea (Eastern Mediterranean) and potential risks for consumption. *Marine Pollution Bulletin,* 184:114129.

Gray, J.S. 2002. Biomagnification in marine systems: the perspective of an ecologist. *Marine Pollution Bulletin,* 45(1-12):46-52.

Grgec, A.S., Kljaković-Gašpić, Z., Orct, T., Tićina, V., Sekovanic, A., Jurasović, J. & Piasek, M. 2020. Mercury and selenium in fish from the eastern part of the Adriatic Sea: A risk-benefit assessment in vulnerable population groups. *Chemosphere,* 261:127742.

Grieb, T.M., Bowie, G.L., Driscoll, C.T., Gloss, S.P., Schofield, C.L. & Porcella, D.B. 1990. Factors affecting mercury accumulation in fish in the upper Michigan peninsula. *Environmental Toxicology and Chemistry*, 9(7):919-930.

Griffiths, C., Robinson, T.B., Lange, L. & Mead, A. 2010. Marine biodiversity in South Africa: an evaluation of current states of knowledge. *PLoS ONE,* 5:e12008.

Hallenbeck, W.H. & Cunningham-Burns, K.M. 2012. *Pesticides and human health.* New York: Springer Science & Business Media.

Han, L. & Sapozhnikova, Y. 2020. Semi-automated high-throughput method for residual analysis of 302 pesticides and environmental contaminants in catfish by fast low-pressure GC-MS/MS and UHPLC-MS/MS. *Food Chemistry,* 319:126592.

Harada, M. 1978. Congenital Minamata disease: Intrauterine methylmercury poisoning. *Teratology,* 18(2):285-288.

Harper, C., Wohlers, D. W., Keith, S., Citra, M., Klotzbach, J. & Sierco, S. 2022. Toxicological profile for aldrin and dieldrin. Georgia, Atlanta: Agency for Toxic Substances and Disease Registry.

Hatfield, D. L., Tsuji, P. A., Carlson, B. A. & Gladyshev, V. N. 2014. Selenium and selenocysteine: roles in cancer, health, and development. *Trends in biochemical sciences*, *39*(3):112-120.

Heath, R.G.M., du Preez, H.H., Genthe, B. & Avenant-Oldewage, A. 2004. Freshwater Fish and human health. Reference Guide. WRC Report No. TT212/04. Water Research Commission, Pretoria.

Holmes, C.D., Jacob, D.J., Corbitt, E.S., Mao, J., Yang, X., Talbot, R. & Slemr, F. 2010. Global atmospheric model for mercury including oxidation by bromine atoms. *Atmospheric Chemistry and Physics,* 10(24):12037-12057.

Hsu-Kim, H., Kucharzyk, K.H., Zhang, T. & Deshusses, M.A. 2013. Mechanisms regulating mercury bioavailability for methylating microorganisms in the aquatic environment: a critical review. *Environmental Science &Technology,* 47:2441-2456.

Hurtado-Banda, R., Gomez-Alvarez, A., Márquez-Faríasa, J.F., Cordoba-Figueroa, M., Navarro-García, G. & Medina-Juáarez, L.A. 2012. Total mercury in liver and muscle tissue of

two coastal sharks from the northwest of Mexico. *Bulletin of Environmental Contamination and Toxicology,* 88:971-975.

Hussein, M.A., Hammad, O.S., Tharwat, A.E., Darwish, W.S., Sayed-Ahmed, A., Zigo, F., Farkašová, Z. & Rehan, I.F. 2022. Health risk assessment of organochlorine pesticide residues in edible tissue of seafood. *Frontiers in Veterinary Science,* 9:1042956.

Hussey, N. E., McCann, H. M., Cliff, G., Dudley, S. F., Wintner, S. P. & Fisk, A. T. 2012. Size-based analysis of diet and trophic position of the white shark (*Carcharodon carcharias*) in South African waters. *Global perspectives on the biology and life history of the white shark*, 27-49.

Jablonska, E. & Vinceti, M. 2015. Selenium and human health: witnessing a Copernican revolution? *Journal of Environmental Science and Health, Part C: Environmental Carcinogenesis and Ecotoxicology Reviews,* 33(3):328-368.

Jacobsen, I.P. & Bennet, M.B. 2013. A comparative analysis of feeding and trophic level ecology in stingrays (Rajiformes; Myliobatoidei) and electric rays (Rajiformes: Torpedinoidei). *PLoS ONE,* 8(8):e71348.

Javed, M. & Usmani, N. 2019. An overview of the adverse effects of heavy metal contamination on fish health. *Proceedings of the National Academy of Sciences India Section B – Biological Sciences,* 89(2):389-403.

Jepson, P.D., Deaville, R., Barber, J.L., Aguilar, A., Borrell, A., Murphy, S., Barry, J., Brownlow, A., Barnett, J., Berrow, S., Cunningham, A.A., Davison, N.J., ten Doeschate, M., Esteban, R., Ferreira, M., Foote, A.D., Genov, T., Giménez, J., Loveridge, J., Llavona, A., Martin, V., Maxwell, D.L., Papachlimitzou, A., Penrose, R., Perkins, M.W., Smith, B., de Stephanis, R., Tregenza, N., Verborgh, P., Fernandez, A. & Law, R.J. 2016. PCB pollution continues to impact populations of orcas and other dolphins in European waters. *Scientific Reports,* 6:1-17.

Jeremiason, J.D., Engstrom, D.R., Swain, E.B., Nater, E.A., Johnson, B.M., Almendinger, J.E., Monson, B.A. & Kolka, R.K. 2006. Sulfate addition increases methylmercury production in an experimental wetland. *Environmental Science and Technology,* 40(12):3800-3806.

Joseph, J. 2012. Selenium and cardiometabolic health: inconclusive yet intriguing evidence. *The American Journal of the Medical Sciences,* 346(3):216-220.

Kamman, N.C., Chalmers, A., Clair, T.A., Major, A., Moore, R.B., Norton, S.A. & Shanley, J.B. 2005. Factors influencing mercury in freshwater surface sediments of northeastern North America. *Ecotoxicology,* 14:101-111.

Kaneko, J.J. & Ralston, N.V.C. 2007. Selenium and mercury in pelagic fish in the central north Pacific near Hawaii. *Biological Trace Element Research,* 119(3):242-254.

Kartalović, B., Novakov, N., Mihaljev, Ž., Petrović, J., Prica, N., Babić, J. & Ćirković, M.A. 2016. Organochlorine pesticides in canned tuna and sardines on the Serbian market. *Food Additives and Contaminants: Part B Surveillance,* 9(4):299-304.

Khan, M.A.K. & Wang, F. 2010. Chemical demethylation of methylmercury by selenoamino acids. *Chemical Research in Toxicology,* 23(7):1202-1206.

Khang, Y., Zhang, R., Yu, K., Han, M., Pei, J., Chen, Z. & Wang, Y. 2022. Organochlorine pesticides (OCPs) in corals and plankton from a coastal coral reef ecosystem, south China sea. *Environmental Research,* 214:114060.

Kim, D., Ryu, H.Y., Lee, J.H., Lee, J.H., Lee, Y.J., Kim, H.K., Jang, D.D., Kim, H.S. & Yoon, H. S. 2013. Organochlorine pesticides and polychlorinated biphenyls in Korean human milk: contamination levels and infant risk assessment. *Journal of Environmental Science and Health, Part B*, *48*(4):243-250.

Kiszka, J.J., Aubail, A., Hussey, N.E., Heithaus, M.R., Caurant, F. & Bustamante, P. 2015. Plasticity of trophic interactions among sharks from the oceanic South-Western Indian Ocean revealed by stable isotope and mercury analyses. Deep Sea Research Part I: Oceanographic Research Papers, 96:49-58.

Kitamura, S., Shimizu, Y., Shiraga, Y., Yoshida, M., Sugihara, K. & Ohta, S. 2002. Reductive metabolism of p,p'-DDT and o,p'-DDT by rat liver cytochrome P450. *Drug Metabolism and Disposition*, 30:113-118.

Knip, D.M., Heupel, M.R. & Simpfendorfer, C.A. 2010. Sharks in nearshore environments: models, importance, and consequences. *Marine Ecology Progress Series,* 402:1-11.

Kousteni, V., Megalofonou, P., Dassenakis, M. & Stathopoulou, E. 2006. Total mercury concentrations in edible tissues of two elasmobranch species from Crete (Eastern Mediterranean Sea). *Cybium,* 30(4):119-123.

Kumar, M., Lakshmi, C.V. & Khanna, S. 2008. Biodegradation and bioremediation of endosulfac contaminated soil. *Bioresource Technology,* 99(8):3116-3122.

Lamborg, C.H., Hammerschmidt, C.R., Bowman, K.L., Swarr, G.J., Munson, K.M., Ohnemus, D.C., Lam, P.J., Heimbürger, L., Rijkenberg, M.J.A. & Saito, M.A. 2014. A global ocean

inventory of anthropogenic mercury based on water column measurements. *Nature,* 512(1):65-68.

Lara, A., Galván-Magaña, F., Elorriaga-Verplancken, F.R., Mermolejo-Rodríguez, A.J., González-Armas, R., Areola-Mendoza, L., Sujitha, S.B., Jonathan, M.P. & Pantoja-Echevarría, L.M. 2022. Mercury, selenium and cadmium in juvenile blue (*Prionace glauca*) and smooth hammerhead (*Sphyrna zygaena*) sharks from the northwest Mexican Pacific coast. *Marine Pollution Bulletin,* 175:11331.

Last, P., Naylor, G., Seret, B., White, W., de Carvalho, M. & Stehmann, M. 2016. *Rays of the World*. Australia: CSIRO publishing.

Lavoie, R.A., Jardine, T.D., Chumchal, M.M., Kidd, K.A. & Campbell, L.M. 2013. Biomagnification of mercury in aquatic food webs: a worldwide meta-analysis. *Environmental Science and Technology,* 47(23):13385-13394.

Leaner, J. J., Dabrowski, J. M., Mason, R. P., Resane, T., Richardson, M., Ginster, M., Gericke, G., Peterson, C.R., Masekoameng, E., Ashton, P.J. & Murray, K. 2009. Mercury emissions from point sources in South Africa. In: Mason, R. & Pirrone, N. eds. *Mercury Fate and Transport in the Global Atmosphere: Emissions, Measurements and Models.* Boston, MA: Springer US. pp. 113-130.

Lemly, A. D. & Lemly, A. D. 2002. Selenium pollution around the world. *Selenium Assessment in Aquatic Ecosystems: A Guide for Hazard Evaluation and Water Quality Criteria*, 3-17.

Le Bourg, B., Kiszka, J.J., Bustamante, P., Heithaus, M.R., Jaquemet, S. & Humber, F. 2019. Effect of body length, trophic position and habitat use on mercury concentrations of sharks from contrasted ecosystems in the southwestern Indian Ocean. *Environmental Pollution,* 169:387-395.

Le Croizier, G., Lorrain, A., Sonke, J.E., Jaquemet, S., Schaal, G., Renedo, M., Besnard, L., Cherel, Y. & Point, D. 2020. Mercury isotopes as tracers of ecology and metabolism in two sympatric shark species. *Environmental Pollution*, 265:114931.

Lee, H., Jeong, Y., Lee, S., Jeong, W., Choy, E., Kang, C., Lee, W., Kim, S. & Moon, H. 2015. Persistent organochlorines in 13 shark species from offshore and coastal waters of Korea: Species-specific accumulation and contributing factors. *Ecotoxicology and Environmental Safety,* 115:195-202.

Lee, C. & Fisher, N.S. 2016. Methylmercury uptake by diverse marine phytoplankton. *Limnology and Oceanography,* 61(5):1626-1639.

Lenz, M. & Lens, P.N.L. 2009. The essential toxin: The changing perception of selenium in environmental sciences. *Science of the Total Environment,* 407(12):3620-3633.

Lepping, R.J., Honea, R.A., Martin, L.E., Liao, K., Choi, I., Lee, P., Papa, V.B., Brooks, W.M., Shaddy, D.J., Carlson, S.E., Colombo, J. & Gustafson, K.M. 2019. Long-chain polyunsaturated fatty acid supplementation in the first year of life after brain function, structure, and metabolism at age nine years. *Developmental Psychobiology,* 61(1):5-16.

Letcher, R.J., Bustnes, J.O., Dietz, R., Jenssen, B.M., Jørgensen, E.H., Sonne, C., Verreault, J., Vijayan, M.M. & Gabrielsen, G.W. 2010. Exposure and effects assessment of persistent organohalogen contaminants in arctic wildlife and fish. *Science of the Total Environment,* 408(15):2995-3043.

Li, D. & Liu, S. 2018. *Water quality monitoring and management: Basis, Technology and Case Studies*. United Kingdom, London: Academic Press.

Lim, Y., Chen, C., Tsai, M., Wu, C., Lin, Y., Wang, M., Albarico, F.P.J.B., Chen, C. & Dong, C. 2022. Impacts of fishing vessels on the heavy metal contamination in sediments: a case study of Qianzhen Fishing Port in southern Taiwan. *Water,* 14(7):1174.

Luek, J.L., Dickhut, R.M., Cochran, M.A., Falconer, R.L. & Kylin, H. 2017. Persistent organic pollutants in the Atlantic and southern oceans and oceanic atmosphere. *Science of the Total Environment,* 583:64-71.

Lyman, W. J., Reehl, W. F. & Rosenblatt, D. H. 1990. Handbook of chemical property estimation methods. United States: American Chemical Society.

Lyons, K., Carlisle, A., Preti, A., Mull, C., Blasius, M., O'Sullivan, J., Winkler, C. & Lowe, C.G. 2013. Effects of trophic ecology and habitat use on maternal transfer of contaminants in four species of young of the year lamniform sharks. *Marine Environmental Research,* 90:27-38.

Lyons, K. & Adams, D.H. 2015. Maternal offloading of organochlorine contaminants in the yolk-sac placental scalloped hammerhead shark (*Sphyrna lewini*). *Ecotoxicology,* 24(3):553-562.

Lyons, K. & Adams, D.H. 2017. First evidence of persistent organic contaminants as potential anthropogenic stressors in the Barndoor Skate *Dipturus laevis*. *Marine Pollution Bulletin,* 116(1-2):534-537.

Mársico, E.T., Machado, M.E.S., Knoff, M. & Sáo Clemente, S.C. 2007. Total mercury in sharks along the southern Brazilian coast. *Arquivo Brasileiro de Medicina Veterinária e Zootecnia,* 59:1593-1596.

Mason, R.P., Rolfhus, K.R. & Fitzgerald, W.F. 1998. Mercury in the North Atlantic. *Marine Chemistry,* 61:37-53.

Matulik, A.G., Kerstetter, D.W., Hammerschlag, N., Divoll, T., Hammerschmidt, C.R. & Evers, D.C. 2017. Bioaccumulation and biomagnification of mercury and methylmercury in four sympatric coastal sharks in a protected subtropical lagoon. *Marine Pollution Bulletin,* 116:357-364.

Maz-Courrau, A., López-Vera, C., Galván-Magaña, F., Escobar-Sánchez, O., Rosíles-Martínez, R. & Sanjuán-Muñoz, A. 2012. Bioaccumulation and biomagnification of total mercury in four exploited shark species in the Baja California peninsula, Mexico. *Bulletin of Environmental Contamination and Toxicology,* 88:129-134.

McHuron, E.A., Harvey, J.T., Castellini, J.M., Stricker, C.A. & O'Hara, T.M. 2014. Selenium and mercury concentrations in harbor seals (*Phoca vitulina*) from central California: Health implications in an urbanized estuary. *Marine Pollution Bulletin,* 1(15):48-57.

McKinney, M.A., Dean, K., Hussey, N.E., Cliff, G., Wintner, S.P., Dudley, S.F.J., Zungu, M.P. & Fisk, A.T. 2016. Global versus local causes and health implications of high mercury concentrations in sharks from the east coast of South Africa. *Science of the Total Environment,* 541:176-183.

McMeans, B.C., Borgå, K., Bechtol, W.R., Higginbotham, D. & Fisk, A.T. 2007. Essential and non-essential element concentrations in two sleeper shark species collected in arctic waters. *Environmental Pollution,* 148:281-290.

Medina-Morales, S.A., Corro-Espinosa, D., Escobar-Sánchez, O., Delgado-Alvarez, C.G., Ruelas-Inzunza, J., Frías-Espericueta, M.G., Jara-Marini, M.E. & Páez-Osuna, F. 2020. Mercury (Hg) and selenium (Se) content in the shark *Mustelus henlei* (Triakidae) in the northern Mexican Pacific. *Environmental Science and Pollution Research*, *27*:16774-16783.

Merly, L., Lange, L., Meÿer, M., Hewitt, A.M., Koen, P., Fischer, C., Muller, J., Schilack, V., Wentzel, M. & Hammerschlag, N. 2019. Blood plasma levels of heavy metals and trace elements in white sharks (*Carcharodon carcharias*) and potential health consequences. *Marine Pollution Bulletin,* 142:85-92.

Milun, V., Grgas, D., Radman, S., Štefanac, T., Ibrahimašić, J. & Dragičević, T.L. 2020. Organochlorines accumulation in caged mussels *Mytilus galloprovincialis* – possible influence of biological parameters. *Applied Sciences,* 10(11):10-12.

Mirlean, N., Ferraz, A. H., Seus-Arrache, E. R., Andrade, C. F. F., Costa, L. P. & Johannesson, K. H. 2019. Mercury and selenium in the Brazilian subtropical marine products: Food composition and safety. *Journal of Food Composition and Analysis*, *84*:103310.

Mohammed, A. and Mahammed, T. 2017. Mercury, arsenic, cadmium and lead in two commercial shark species (*Sphyrna lewini* and *Carcharinus porosus*) in Trinidad and Tobago. *Marine Pollution Bulletin,* 119:214-218.

Morgan D.P. and Roan C.C. 1971. Absorption, storage, and metabolic conversion of ingested DDT and DDT metabolites in man. *Archives of Environmental Health,* 22(3):301-308.

Mormede, S. & Davies, I.M. 2001. Heavy metal concentrations in commercial deep-sea fish from Rockall Trough. *Continental Shelf Research,* 21(8-10):899-916.

Mull, C. G., Blasius, M. E., O'Sullivan, J. B. & Lowe, C. G. 2012. Heavy metals, trace elements, and organochlorine contaminants in muscle and liver tissue of juvenile white sharks, *Carcharodon carcharias*, from the Southern California Bight. *Global perspectives on the biology and life history of the white shark*, *59*:75.

Muir, D.C.G., Norstrom, R.J. & Simon, M. 1988. Organochlorine contaminants in arctic marine food chains: Accumulation of specific polychlorinated biphenyls and chlordane-related compounds. *Environmental Science and Technology,* 22:1071-1079.

Murillo-Cisneros, D.A., O'Hara, T.M., Castellini, J.M., Sánchez-González, A., Elorriaga-Verplancken, F.R., Marmolejo-Rodríguez, A.J., Marín-Enríquez, E. & Galván-Magaña, F. 2018. Mercury concentrations in three ray species from the Pacific coast of Baja California Sur, Mexico: Variations by tissue type, sex and length. *Marine Pollution Bulletin,* 126:77-85.

Natasha, S.M., Niazi, N.K., Khalid, S., Murtaza, B., Bibi, I. & Rashid, M.I. 2018. A critical review of selenium biogeochemical behavior in soil-plant system with an inference to human health. *Environmental Pollution,* 234:915-934.

Navia, A.F., Mejía-Falla, P.A., López-García, J., Giraldo, A. & Cruz-Escalona, V.H. 2016. How many trophic roles can elasmobranchs play in a marine tropical network. *Marine and Freshwater Research,* 68:1-12.

Nekhoroshkov, P., Bezuidenhout, J., Zinicovscaia, I., Yushin, N., Vergel, K. & Frontasyeva, M. 2021. Levels of elements in typical mussels from the Southern Coast of Africa (Namibia, South Africa, Mozambique): Safety Aspect. *Water,* 13:3238.

Nekhoroshkov, P.S., Bezuidenhout, J., Frontasyeva, M.V., Zinicovscaia, I.I., Yushin, N.S., Vergel, K.N. & Petrik, L. 2021. Trace elements risk assessment for consumption of wild mussels along South Africa coastline. *Journal of Food Composition and Analysis,* 98:103825

Nicolaus, E.E.M., Bendall, V.A., Bolam, T.P.C., Maes, T. & Ellis, J.R. 2016. Concentrations of mercury and other trace elements in porbeagle shark *Lamna nasus*. *Marine Pollution Bulletin,* 112(1-2):406-410.

Nicolaus, E.E.M., Barry, J., Bolam, T.P.C., Lorance, P., Marandel, F., McCully Phillips, S.R., Neville, S. & Ellis, J.R. 2017. Concentrations of mercury and other trace elements in two offshore skates: sandy ray *Leucoraja circularis* and shagreen ray *L. fullonica*. *Marine Pollution Bulletin,* 123(1-2):387-394.

Norstrom, R.J. 2002. Understanding Bioaccumulation of POPs in Food Webs. *Environmental Science and Pollution Research,* 9(5):300-303.

Ohi, G., Nishigaki, S., Seki, H., Tamura, Y., Maki, T., Minowa, K., Shimamura, Y., Mizoguchi, I., Inaba, Y., Takizawa, Y. & Kawanishi, Y. 1980. The protective potency of marine animal meat against the neurotoxicity of methylmercury: Its relationship with the organ distribution of mercury and selenium in the rat. *Food and Cosmetics Toxicology,* 18(2):139-145.

Olisah, C., Okoh, O. & Okoh, A. 2020. Occurrence of organochlorine pesticide residues in biological and environmental matrices in African: A two-decade review. *Heliyon,* 6(3):e03518.

Olisah, C., Adams, J.B. & Rubidge, G. 2021. The state of persistent organic pollutants in South African estuaries: A review of environmental exposure and sources. *Ecotoxicology and Environmental Safety,* 219:112316.

Olmedo, P., Hernández, A.F., Pla, A., Femia, P., Navas-Acien, A. & Gil, F. 2013. Determination of essential elements (copper, manganese, selenium and zinc) in fish and shellfish samples. Risk and nutritional assessment and mercury-selenium balance. *Food and Chemical Toxicology,* 62:299-307.

Otten, J.J., Hellwig, J.P. & Meyers, L.D. 2006. *Dietary reference intakes: the essential guide to nutrient requirements.* Washington, D.C.: National Academies Press.

Pacyna, E.G., Pacyna, J.M., Sundseth, K., Munthe, J., Kindborn, K., Wilson, S., Steenhuisen, F. & Maxson, P. 2010. Global emission of mercury to the atmosphere from anthropogenic sources in 2005 and projections to 2020. *Atmospheric Environment,* 44(20):2487-2499.

Pantoja-Echevarría, L.M., Marmolejo-Rodríguez, A.J., Galván-Magaña, F., Elorriaga-Verplancken, F.R., Tripp-Valdez, A., Tamburin, E., Lara, A., Jonathan, M.P., Sujitha, S.D. & Arreola-Mendoza, L. 2021. Mercury and selenium concentrations in different tissues of brown smooth-hound shark (*Mustelus henlei*) from the western coast of Baja California Sur, Mexico. *Marine Pollution Bulletin,* 170:112609.

Parizek, J. & Ostadalova, I. 1967. The protective effect of small amounts of selenite in sublimate intoxication. *Experientia,* 23:142-143.

Peterson, S.A., Ralston, N.V.C., Peck, D.V., Sickle, J.V., Robertson, J.D., Spate, V.L. & Morris, J.S. 2009. How might selenium moderate the toxic effects of mercury in stream fish of the western U.S.? *Environmental Science and Technology,* 43:3919-3925.

Pethybridge, H., Cossa, D. & Butler, E.C.V. 2010. Mercury in 16 demersal sharks from Southeast Australia: biotic and abiotic sources of variation and consumer health implications. *Marine Environmental Research,* 69:18-26.

Pethybridge, H.R., Parrish, C.C., Bruce, B.D., Young, J.W. & Nichols, P.D. 2014. Lipid, fatty acid and energy density profiles of white sharks: Insights into the feeding ecology and ecophysiology of a complex top predator. *PLoS ONE,* 9(5):e97877.

Plessl, C., Gilbert, B.M., Sigmund, M.F., Theiner, S., Avenant-Oldewage, A., Keppler, B.K. & Jirsa, F. 2019. Mercury, silver, selenium and other trace elements in three cyprinid fish species from the Vaal Dam, South Africa, including implications for fish consumers. *Science of the Total Environment,* 659:1158-1167.

Porter, S.N., Humphries, M.S., Buah-Kwofie, A. & Schleyer, M. 2018. Accumulation of organochlorine pesticides in reef organisms from marginal coral reefs in South Africa and links with coastal groundwater. *Marine Pollution Bulletin,* 137:295-305.

Przybyla, J., Wohlers, D. W., Roney, N., Barber, L., Abadin, H., Citra, M., Alman, B., Diamond, G.L., Szafran, B., Ingerman, L., Klotzbach, J.M. & Zaccaria, K. 2023. Toxicological profile for hexachlorocyclohexane (HCH): draft for public comment.

Quinn, L., De Vos, J., Fernandes-Whaley, M., Roos, C., Bouwman, H., Kylin, H., Pieters, R. & Van den Berg, J. 2011. Pesticide use in South African: one of the largest importers of pesticides in Africa. In: Stoytcheva, M. ed. *Pesticides in the Modern World – Pesticides Use and Management.* Croatia: InTech.

Ralston, N.V.C., Blackwell, J.L. & Raymond, L.J. 2007. Importance of molar ratios in selenium-dependent protection against methylmercury toxicity. *Biological Trace Element Research,* 119:255-268.

Ralston, N.V.C., Ralston, C.R., Blackwell, J.L. & Raymond, L.J. 2008. Dietary and tissue selenium in relation to methylmercury toxicity. *NeuroToxicology,* 29(5):802-811.

Ralston, N.V.C., Ralston, C.R. & Raymond, L.J. 2016. Selenium health benefit values: updated criteria for mercury risk assessments. *Biological Trace Element Research,* 171(2):262-269.

Ramalhosa, E., Pato, P., Monterroso, P., Pereira, E., Vale, C. & Duarte, A.C. 2006. Accumulation versus remobilization of mercury in sediments of a contaminated lagoon. *Marine Pollution Bulletin,* 52(3):353-356.

Rayman, M.P. 2000. The importance of selenium to human health. *The Lancet,* 356(9225):233-241.

Raymond, L.J. & Ralston, N.V.C. 2009. Selenium's importance in regulatory issues regarding mercury. *Fuel Processing Technology,* 90(11):1333-1338.

Reich, A.R., Perkins, J.L. & Cutter, G. 1986. DDT contamination of a north Alabama aquatic ecosystem. *Environmental Toxicology and Chemistry,* 5:725-736.

Rice, K.M., Walker Jr, E.M., Wu, M., Gillette, C. & Blough, E.R. 2014. Environmental mercury and its toxic effects. *Journal of Preventive Medicine and Public Health*, 47(2):74-83.

Risher, J. 2003. *Toxicological profile for selenium*. Georgia, Atlanta: Agency for Toxic Substances and Disease Registry

Rogers, P.J., Huveneers, C., Goldsworthy, S.D., Mitchell, J.G. & Seuront, L. 2013. Broad scale movements and pelagic habitat of the dusky shark *Carcharhinus obscurus* of Southern Australia determined using pop-up satellite archival tags. *Fisheries Oceanography,* 22:102-112.

Rosa, R., Baptista, M., Lopes, V.M., Pegado, M.R., Paula, J.R., Trübenbach, K., Leal, M.C., Calado, R. & Repolho, T. 2014. Early-life exposure to climate change impairs tropical shark survival. *Proceedings: Biological Sciences,* 281(1793):1-7.

Ruelas-Inzunza, J., Hernández-Osuna, J. & Páez-Osuna, F. 2011. Total and organic mercury in ten fish species for human consumption from the Mexican Pacific. *Bulletin of Environmental Contamination and Toxicology,* 86:679-683.

Ruelas-Inzunza, J., Amezcua, F., Coiraton, C. & Páez-Osuna, F. 2020. Cadmium, mercury and selenium in muscle of the scalloped hammerhead *Sphyrna lewini* from the tropical eastern Pacific: variation with age, molar ratios and human health risk. *Chemosphere,* 242:125180.

Rumbold, D., Wasno, R., Hammerschlag, N. & Volety, A. 2014. Mercury accumulation in sharks from the coastal waters of Southwest Florida. *Archives of Environmental Contamination and Toxicology*, 67:402-412.

Santos, S., Ungureanu, G., Boaventura, R. & Botelho, C. 2015. Selenium contaminated waters: An overview of analytical methods, treatment options and recent advances in sorption methods. *Science of the Total Environment*, *521*:246-260.

Schlenk, D., Sapozhnikova, Y. & Cliff, G. 2005. Incidence of organochlorine pesticides in muscle and liver tissues of South African great white sharks *Carcharodon carcharias*. *Marine Pollution Bulletin,* 50(2):208-211.

Schmeltz, D., Evers, D.C., Driscoll, C.T., Artz, R., Cohen, M., Gay, D., Haeuber, R., Krabbenhoft, D.P., Mason, R., Morris, K. & Wiener, J.G. 2011. MercNet: a national monitoring network to assess responses to changing mercury emissions in the United States. *Ecotoxicology,* 20:1713-1725.

Sereda, B.L. & Meinhardt, H.R. 2005. Contamination of the water environment in malaria endemic areas of KwaZulu-Natal, South Africa by DDT and its metabolites. *Bulletin of Environmental Contamination and Toxicology,* 75(3):538-545.

Shipley, O.N., Lee, C., Fisher, N.S., Sternlicht, J.K., Kattan, S., Staaterman, E.R., Hammerschlag, N. & Gallagher, A.J. 2021. Metal concentrations in coastal sharks from The Bahamas with a focus on the Caribbean Reef shark. *Scientific Reports,* 11(1):1-11.

Shiri, H.H., Godeto, T.W., Nomngongo, P.N. & Zinyemba, O. 2023. Selenium quantification in wastewaters from selected coal-fired power plants and river waters in South Africa using ICP-MS. *Water SA,* 49(3):291-300.

Sioen, I., Van Camp, J., Verdonck, F.A.M., Van Thuyne, N., Willems, J.L. & De Henauw, S.W.J. 2007. How to use secondary data on seafood contamination for probabilistic exposure assessment purposes? Main problems and potential solutions. *Human and Ecological Risk Assessment: An International Journal,* 13(3):632-657.

Smale, M.J., 1991. Occurrence and feeding of three shark species, *Carcharhinus brachyurus, C. obscurus* and *Sphyrna zygaena*, on the eastern Cape coast of South Africa*. South African Journal of Marine Science*, 11:31-42.

Smith-Dwoney, N.V., Sunderland, E.M. & Jacob, D.J. 2010. Anthropogenic impacts on global storage and emissions of mercury from terrestrial soils: Insights from a new global model. *Journal of Geophysical Research,* 115:G03008.

Soerensen, A.L., Sunderland, E.M., Holmes, C.D., Jacob, D.J., Yantosca, R.M., Skov, H., Christensen, J.H., Strode, S.A. & Mason, R.P. 2010. An improved global model for air-sea exchange of mercury: High concentrations over the North Atlantic. *Environmental Science & Technology,* 44(22):8574-8580.

South Africa. 2015. National Environmental Management: Biodiversity Act, Shark Biodiversity Management Plan. 2004 (Act NO. 10 OF 2004). (Notice 258). Government gazette, 38607:1, 25 March.

Stewart, J.D., Jaine, F.R.A., Armstrong, A.J., Armstrong, A.O., Bennet, M.B., Burgess, K.B., Couturier, L.I.E., Croll, D.A., Cronin, M.R., Deakos, M.H., Dudgeon, C.L., Fernando, D., Froman, N., Germanov, E.S., Hall, M.A., Hinojosa-Alvarez, S., Hosegoof, J.E., Kashiwagi, T., Laglbauer, B.J.L., Lezama-Ochoa, N., Marshall, A.D., McGregor, F., Notarbartolo di Sciara, G., Palacios, M.D., Peel, L.R., Richardson, A.J., Rubin, R.D., Townsend, K.A., Venables, S.K. & Stevens, G.M.W. 2018. Research priorities to support effective manta and devil ray conservation. *Frontiers in Marine Science,* 5:314.

Storelli, M.M., Ceci, E., Storelli, A. & Marcotrigiano, G.O. 2003. Polychlorinated biphenyl, heavy metal and methylmercury residues in hammerhead sharks: contaminant status and assessment. *Marine Pollution Bulletin,* 46(8):1035-1039.

Storelli, A., Barone, G., Garofalo, R., Busco, A. & Storelli, M.M. 2022. Determination of mercury, methylmercury and selenium in elasmobranch meat: fish consumption safety. *International Journal of Environmental Research and Public Health*, 19:788.

Suk, S. H., Smith, S. E. & Ramon, D. A. 2009. Bioaccumulation of mercury in pelagic sharks from the northeast Pacific Ocean. *CalCOFI Rep*, *50*:172-177.

Sun, T., Wu, H., Wang, X., Ji, C., Shan, X. & Li, F. 2020. Evaluation on the biomagnification or biodilution of trace metals in global marine food webs by meta-analysis. *Environmental Pollution,* 264:113856.

Sunderland, E.M., Krabbenhoft, D.P., Moreau, J.W., Strode, S.A. & Landing, W.M. 2010. Mercury sources, distribution, and bioavailability in the North Pacific Ocean: Insights from data and models. *Global Biogeochemical Cycles,* 23:GB2010.

Takahashi, K., Encinar, J.R., Costa-Fernández, J.M. & Ogra, Y. Distributions of mercury and selenium in rats ingesting mercury selenide nanoparticles. *Ecotoxicology and Environmental Safety,* 226:112867.

Takata, N., Myburgh, J., Botha, A. & Nomngongo, P.N. 2022. The importance and status of the micronutrient selenium in South Africa: a review. *Environmental Geochemistry and Health,* 44:3703-3723.

Taylor, J. & Wilson, J. D. 2002. Toxicological profile for hexachlorobenzene. Georgia, Atlanta: Agency for Toxic Substances and Disease Registry.

Teixeira, G., Raimundo, J., Goulart, J., Costa, V., Menezes, G. M., Caetano, M., Pacheco, M. & Martins, I. 2020. Hg and Se composition in demersal deep-sea fish from the North-East Atlantic. *Environmental Science and Pollution Research*, *27*:33649-33657.

Terrazas-López, R., Arreola-Mendoza, L., Galván-Magaña, F., Sujitha, S.B. & Jonathan, M.P. 2019. Understanding the antagonism of Hg and Se in two shark species from Baja California south, Mexico. *Science of the Total Environment,* 650:202-209.

Tiktak, G.P., Butcher, D., Lawrence, P.J., Norrey, J., Bradley, L., Shaw, K., Preziosi, R. & Megson, D. 2020. Are concentrations of pollutants in sharks, rays and skates (Elasmobranchii) a cause for concern? A systematic review. *Marine Pollution Bulletin,* 160:111701.

Tilami, S.K. & Samples, S. 2018. Nutritional value of fish: lipids, proteins, vitamins, and minerals. *Reviews in Fisheries Science and Aquaculture,* 26(2):243-253.

Tsydenova, O., Minh, T.B., Kajiwara, N., Batoev, V. & Tanabe, S. 2004. Recent contamination by persistent organochlorines in Baikal seal (*Phoca sibirica*) from Lake Baikal, Russia. *Marine Pollution Bulletin,* 48(7-8):749-758.

Ulusoy, S., Mol, S., Karakulak, F. & Kahraman, A.E. 2018. Selenium-mercury balance in commercial fish species from the Turkish waters. *Biological Trace Element Research,* 191(1):207-213.

United States Environmental Protection Agency (USEPA). 2005. Guidelines for carcinogenic risk assessment. https://www.epa.gov/sites/default/files/2013-09/documents/cancer_guidelines_final_3-25-05.pdf Date of access: 21 July 2023.

United States Environmental Protection Agency (USEPA). 2019. Integrated Risk Information System. https://www.epa.gov/iris Date of access: 5 August 2023.

Vélez, N., Bessudo, S., Barragán-Barrera, D.C., Ladino, F., Bustamante, P. & Luna-Acosta, A. 2021. Mercury concentrations and trophic relations in sharks of the Pacific Ocean of Colombia. *Marine Pollution Bulletin,* 173:113109.

Vinceti, M., Filippini, T. & Wise, L.A. 2018. Environmental selenium and human health: an update. *Current Environmental Health Reports,* 5464-485.

Volschenk, C.M., Gerber, R., Mkhonto, M.T., Ikenaka, Y., Yohannes, Y.B., Nakayama, S., Ishizuka, M., van Vuren, J.H.J., Wepener, V. & Smit, N.J. 2019. Bioaccumulation of persistent organic pollutants and their trophic transfer through the foodweb: Human health risks to the rural communities reliant on fish from South Africa's largest floodplain. *The Science of the Total Environment,* 685:1116-1126.

Walters, C.R., Somerset, V.S., Leaner, J.J. & Nel, J.M. 2011. A review of mercury pollution in South Africa: Current status. *Journal of Environmental Science and Health, Part A,* 46(10):1129-1137.

Wang, D., Yang, S., Wang, G., Gao, L., Wang, Y., Jiang, Q. & Chen, Y. 2016. Residues and distributions of organochlorine pesticides in China's Weihe River. *Polish Journal of Environmental Studies,* 25(3):1285-1292.

Watanabe, C., Yin, K., Kasanuma, Y. & Satoh, H. 1999. In utero exposure to methylmercury and Se deficiency converge on the neurobehavioral outcome in mice. *Neurotoxicology and Teratology,* 21(1):83-88.

Watanabe, T., Matsuda, R. & Uneyama, C. 2021. probabilistic estimation of dietary intake of methylmercury from fish in Japan. *Food Safety,* 9(1):1-9.

Watras, C.J. & Bloom, N.S. 1992. Mercury and methylmercury in individual zooplankton: Implications for bioaccumulation. *Limnology and Oceanography,* 37(6):1313-1318.

Weijs, L., Briels, N., Adams, D.H., Lepoint, G., Das, K., Blust, R. & Covaci, A. 2015. Bioaccumulation of organohalogenated compounds in sharks and rays from the southeastern USA. *Environmental Research,* 137:199-207.

Wepener, V. & Degger, N. 2019. South Africa. In Sheppard C. ed. *World Seas: An Environmental Evaluation Volume 2,* Amsterdam: Elsevier. pp. 101-119.

Wetherbee, B.M., Cortés, E. & Bizzarro, J.J. 2004. Food consumption and feeding habits. *Biology of sharks and their relatives*, United States, Broken Sound Parkway: CRC Press. pp. 225-246.

White, W. T., O'Neill, H. L. & Naylor, G. J. 2022. Taxonomy and diversity of extant elasmobranchs. In *Carrier, J., Simpfendorfer, C.A., Heithaus, M.R & Yopak, K.E. Biology of Sharks and Their Relatives.* Boca Raton: CRC Press. pp. 31-57.

Williams, C.R., Leaner, J.J., Nel, J.M. & Somerset, V.S. 2010. Mercury concentrations in water resources potentially impacted by coal-fired power stations and artisanal gold mining in Mpumalanga, South Africa. *Journal of Environmental Science and Health Part A,* 45:1363-1373.

Worm, B., Davis, B., Kettemer, L., ward-Paige, C.A., Chapman, D., Heithaus, M.R., Kessel, S.T. & Gruber, S.H. 2013. *Marine Policy,* 40(1):194-204.

Wourms, J.P. 1977. Reproduction and development in chondrichthyan fishes. *American Zoologist*, *17*(2):379-410.

Wyatt, C. J., Meléndez, J. M., Acuña, N. & Rascon, A. 1996. Selenium (Se) in foods in northern Mexico, their contribution to the daily Se intake and the relationship of Se plasma levels and glutathione peroxidase activity. *Nutrition Research*, *16*(6):949-960.

Yudovich, Y.E. & Ketris, M.P. 2006. Selenium in coal: A review. *International Journal of Coal Geology,* 67112-126.

Yohannes, Y. B., Ikenaka, Y., Nakayama, S. M., Saengtienchai, A., Watanabe, K. & Ishizuka, M. 2013. Organochlorine pesticides and heavy metals in fish from Lake Awassa, Ethiopia: Insights from stable isotope analysis. *Chemosphere*, *91*(6):857-863.

Zaera, D. & Johnsen, E. 2011. Foetal deformities in a smooth-hound shark, *Mustelus mustelus*, from an oil exploited area in Angola. *Cybium: International Journal of Ichthyology*, 35(3):231-236.

Zhang, G., Min, Y.S., Mai, B.X., Sheng, G.Y., Fu, J.M. & Wang, Z.S. 1999. Time trend of BHCs and DDTs in a sedimentary core in Macao estuary, Southern China. *Marine Pollution Bulletin,* 39:326-330.

Zhang, H., Feng, X., Chan, H.M. & Larssen, T. 2014. New insights into traditional health risk assessments of mercury exposure: Implications of selenium. *Environmental Science & Technology,* 48(2):1206-1212.

Zhou, R., Zhu, L., Yang, K. & Chen, Y. 2006. Distribution of organochlorine pesticides in surface water and sediments from Qiantang River, East China. *Journal of Hazardous Materials,* 137(1):68-75.

Appendix

Table S1. General information regarding the sampled elasmobranchs with Common name, sample name, biometrics, and sampling locations. Abbreviations: M = Male, F = Female, J = Juvenile, A = Adult.

Common name (species)	Sample Name	Gender	Length (cm)	Weight (g)	Sampling location
Shortfin devil ray (*Mobula kuhlii*)	KZN19-3	M (J)	102	15500	Karradene, KZN
Shortfin devil ray (*Mobula kuhlii*)	KZN20-5	F (J)	113	15700	Isipingo, KZN
Longhorn devil ray (*Mobula eregoodootenkee*)	KZN20-1	M (A)	106	12000	Zinkwazi, KZN
Longhorn devil ray (*Mobula eregoodootenkee*)	KZN20-15	F (A)	95	22000	Richards Bay, KZN
Longhorn devil ray (*Mobula eregoodootenkee*)	KZN20-20	F (A)	145	21500	Richards Bay, KZN
Bull ray (*Aetomylaeus bovinus*)	KZN19-17	F (A)	125	25400	Richards Bay, KZN
Bull ray (*Aetomylaeus bovinus*)	KZN19-18	M (A)	89	7500	Richards Bay, KZN
Bull ray (*Aetomylaeus bovinus*)	KZN20-12	F (A)	109	12900	Richards Bay, KZN
Bull ray (*Aetomylaeus bovinus*)	KZN20-13	F (A)	112.6	3400	Zinkwazi, KZN
Bull ray (*Aetomylaeus bovinus*)	KZN20-21	F (A)	187	28500	Richards Bay, KZN
Oman cownose ray (*Rhinoptera jayakari*)	KZN20-10	M (A)	92	5600	Scottburgh, KZN
Oman cownose ray (*Rhinoptera jayakari*)	KZN20-14	M (A)	143	28900	Richards Bay, KZN
Oman cownose ray (*Rhinoptera jayakari*)	KZN20-22	M (A)	167	25000	Richards Bay, KZN
Leopard catshark (*Poroderma pantherinum*)	HE18-1	M (J)	41.5	429	New Harbor, Hermanus WC
Leopard catshark (*Poroderma pantherinum*)	HE18-4	F (J)	61.5	1192	New Harbor, Hermanus WC
Leopard catshark (*Poroderma pantherinum*)	HE18-5	F (J)	45.6	465	New Harbor Hermanus, WC
Spotted skate (*Raja straeleni*)	HE18-15	M (J)	64.9	1900	Vermont Hermanus, WC
Puffadder shyshark (*Haploblepharus edwardsii*)	HE18-10	M (J)	45.3	286	Schulphoek Hermanus, WC
Brown shyshark (*Haploblepharus fuscus*)	HE18-6	M (J)	49.2	517	New Harbor Hermanus, WC
Brown shyshark (*Haploblepharus fuscus*)	HE18-7	F (J)	56	870	New Harbor Hermanus, WC
Dark shyshark (*Haploblepharus pictus*)	HE18-3	M (J)	55.7	719	Old Harbor Hermanus, WC
Smoothhound shark (*Mustelus mustelus*)	HE18-11	F (A)	104	4680	Vermont Hermanus, WC
Smoothhound shark (*Mustelus mustelus*)	HE18-13	F (J)	76.5	1823	Rietfontein Hermanus, WC

Table S1 (continued)

Smoothhound shark (*Mustelus mustelus*)	HE18-14	F (J)	68.4	1210	Rietfontein Hermanus, WC
Smoothhound shark (*Mustelus mustelus*)	HE18-16	M (A)	109.9	4860	Rietfontein Hermanus, WC
Smoothhound shark (*Mustelus mustelus*)	HE18-17	M (A)	103.5	4240	Rietfontein Hermanus, WC
Tiger shark (*Galeocerdo cuvier*)	KZN20-4	F (J)	116.2	17000	Umhlanga, KZN
Tiger shark (*Galeocerdo cuvier*)	KZN20-6	F	-	-	Umhlanga, KZN
Tiger shark (*Galeocerdo cuvier*)	KZN20-11	F (J)	173	34000	St. Michaels, KZN
Scalloped hammerhead shark (*Sphyrna lewini*)	KZN19-8	M (A)	289	146000	Zinkwazi, KZN
Scalloped hammerhead shark (*Sphyrna lewini*)	KZN19-11	M (A)	260	107500	Zinkwazi, KZN
Scalloped hammerhead shark (*Sphyrna lewini*)	KZN19-12	M (A)	239	76000	Zinkwazi, KZN
Scalloped hammerhead shark (*Sphyrna lewini*)	KZN19-14	M (A)	204	122000	Richards Bay, KZN
Scalloped hammerhead shark (*Sphyrna lewini*)	KZN19-15	M (A)	233	194000	Richards Bay, KZN
Scalloped hammerhead shark (*Sphyrna lewini*)	KZN20-19	M (A)	170	18300	Leisure Bay, KZN
Spinner shark (*Carcharhinus brevipinna*)	KZN20-9	M (A)	191	39000	Gln, KZN
Spinner shark (*Carcharhinus brevipinna*)	KZN20-17	M (A)	230	65000	Zinkwazi, KZN
Spinner shark (*Carcharhinus brevipinna*)	KZN20-18	F (A)	206	44500	Banana Beach, KZN
Spinner shark (*Carcharhinus brevipinna*)	KZN20-26	M (J)	145	14400	Umgaboba, KZN
Blacktip shark (*Carcharhinus limbatus*)	KZN19-9	M (A)	139	19500	Zinkwazi, KZN
Dusky shark (*Carcharhinus obscurus*)	KZN19-2	M (J)	90	4500	Durban, KZN
Dusky shark (*Carcharhinus obscurus*)	KZN20-2	M (J)	84	8900	Durban, KZN
Dusky shark (*Carcharhinus obscurus*)	KZN20-3	F	-	-	Durban, KZN
Dusky shark (*Carcharhinus obscurus*)	KZN20-27	M (J)	130	9400	Ballito Bay, KZN
Dusky shark (*Carcharhinus obscurus*)	KZN20-28	F (J)	131	10500	Durban, KZN

Table S1 (continued)

Smooth hammerhead shark (*Sphyrna zygaena*)	KZN20-25	M (J)	120	6000	Ramsgate, KZN
Angel shark (*Squatina africana*)	KZN19-1	M (A)	82	5100	Durban, KZN
Java shark (*Carcharhinus amboinensis*)	KZN19-10	F (J)	166	40500	Zinkwazi, KZN
Bull shark (*Carcharhinus leucas*)	KZN20-23	F (A)	194.8	75000	Zinkwazi, KZN
Ragged tooth shark (*Carcharhinus taurus*)	KZN20-24	F (A)	240	97000	Durban, KZN
Ragged tooth shark (*Carcharhinus taurus*)	KZN20-31	F	-	-	Richards Bay, KZN
Broadnose sevengill shark (*Notorynchus cepedianus*)	HE18-9	F (A)	235	98400	Schulphoek Hermanus, WC
Great white shark (*Carcharodon carcharias*)	DUR20-1	F	-	-	Leisure Bay, KZN
Great white shark (*Carcharodon carcharias*)	DUR20-2	-	-	-	St. Michaels, KZN
Great white shark (*Carcharodon carcharias*)	DUR20-4	M	-	-	Glendale Beach, KZN
Great white shark (*Carcharodon carcharias*)	DUR20-5	-	-	-	Umzumbe, KZN
Great white shark (*Carcharodon carcharias*)	DUR20-6	-	-	-	Ballito Bay, KZN
Great white shark (*Carcharodon carcharias*)	DUR20-7	-	-	-	Richards Bay, KZN
Great white shark (*Carcharodon carcharias*)	DUR20-9	-	-	-	St. Michaels, KZN

Table S2. Mean ± standard error and range (in parenthesis) of HCB and CHLs concentrations (ng/g lipid weight) in the muscle tissue samples of specified shark species.

Common name (species)	n	Location	HCB	Trans-chlordane	Cis-chlordane	Trans-nonachlor	∑CHL	Reference
Great white shark (*Carcharodon carcharias*)	1	Australia (New South Wales)	155.339	-	-	-	-	Cagnazzi *et al.,* 2019
Great white shark (*Carcharodon carcharias*)	2	South Africa (KwaZulu-Natal)	-	52.3±7.0	36.5±3.0	373.3±34.8	462.1±44.8	Beaudry *et al*., 2015
Dusky shark (Carcharhinus obscurus)	1	Australia (New South Wales)	6.06	-	-	-	-	Cagnazzi *et al.,* 2019
Dusky shark (*Carcharhinus obscurus*)	2	South Africa (KwaZulu-Natal)	-	47.1±9.5	25.8±6.4	133.1±26.4	206±42.3	Beaudry *et al.,* 2015
Great white shark (*Carcharodon carcharias*)	3	South Africa (Durban)	3.0±1.2	-	-	-	15.9±2.5	Schlenk *et al.,* 2005
Scalloped hammerhead (*Sphyrna lewini*)	20	Gulf of California, Mexico	0.02+0.1	-	-	-	-	Briones *et al.,* 2022
Smooth hammerhead shark (*Sphyrna zygaena*)	3	Korean coast	0.36+0.47	-	-	-	0.36±+0.62	Lee *et al.,* 2015
Ragged tooth shark (*Carcharhinus taurus*)	1	Australia (New South Wales)	7.37	-	-	-	-	Cagnazzi *et al.,* 2019
Bull shark (*Carcharhinus leucas*)	1	Australia (New South Wales)	11.94	-	-	-	-	Cagnazzi *et al.,* 2019
Bull shark (*Carcharhinus leucas*)	1	Australia (New South Wales)	4.94	-	-	-	-	Cagnazzi *et al.,* 2019
Great hammerhead shark (*Sphyrna mokarran*)	2	Australia (New South Wales)	8.3±1.8	-	-	-	-	Cagnazzi *et al.,* 2019

Table S2 (continued)

Blacktip shark (*Carcharhinus limbatus*)	7	Australia (New South Wales)	11.6±5.9	-	-	-	-	Cagnazzi *et al.,* 2019
Starspotted smoothhound shark (*Mustelus manazo*)	2	Korean coast	-	-	0.27±0.38	-	0.27±0.38	Lee *et al.,* 2015
Shortfin devil ray (*Mobula kuhlii*)	8	Australia (New South Wales)	8.9±5.0	-	-	-	-	Cagnazzi *et al.,* 2019
Australian cownose ray (*Rhinoptera neglecta*)	1	Australia (New South Wales)	8.92	-	-	-	-	Cagnazzi *et al.,* 2019
Shortfin devil ray (*Mobula kuhlii*)	2	Indian Ocean coast, South Africa	8.9±7.7	6.7±0.64	4.7±2.2	4.4±1.7	15.8±4.5	Current study
Longhorn devil ray (*Mobula eregoodootenkee*)	3	Indian Ocean coast, South Africa	5.5±2.1	7.7±3.6	4.0±2.1	2.3±2.6	18.0±8.3	Current study
Bull ray (*Aetomylaeus bovinus*)	5	Indian Ocean coast, South Africa	4.8±2.9	5.8±2.6	4.0±1.1	3.5±1.8	13.4±5.4	Current study
Oman cownose ray (*Rhinoptera jayakari*)	3	Indian Ocean coast, South Africa	22.2+27.6	27.4+35.0	16.0+19.8	16.0+21.3	59.3+76.0	Current study
Leopard catshark (*Poroderma pantherinum*)	3	Atlantic Ocean coast, South Africa	12.6±3.3	11.8±2.7	7.2±1.9	7.0±1.4	26.0±5.9	Current study
Spotted skate (*Raja straeleni*)	1	Atlantic Ocean coast, South Africa	3.199	6.5	3.1	3.4	13.1	Current study
Puffadder shyshark (*Haploplebharus edwardsii*)	1	Atlantic Ocean coast, South Africa	21.647	22.6	15.7	14.3	52.6	Current study
Brown shyshark (*Haploblepharus fuscus*)	2	Atlantic Ocean coast, South Africa	8.6±2.1	8.0±.08	5.5±0.01	4.6±0.14	18.4±1.1	Current study
Dark shyshark (*Haploblepharus pictus*)	1	Atlantic Ocean coast, South Africa	14.332	13.2	9.3	9.0	31.5	Current study
Smoothhound shark (*Mustelus mustelus*)	5	Atlantic Ocean coast, South Africa	6.8±6.2	4.9±2.0	3.5±1.8	6.2+7.2	14.6±9.8	Current study

Table S2 (continued)

Tiger shark (*Galeocerdo cuvier*)	3	Indian Ocean coast, South Africa	5.5±2.8	5.6±2.1	4.7±2.8	6.3±5.1	16.5±9.9	Current study
Scalloped hammerhead shark (*Sphyrna lewini*)	6	Indian Ocean coast, South Africa	9.7±4.2	7.2±2.3	5.5±2.0	5.4±2.1	18.0±5.8	Current study
Spinner shark (*Carcharhinus brevipinna*)	4	Indian Ocean coast, South Africa	5.1±2.0	6.5±2.0	4.3±2.3	4.2±1.3	14.9±5.5	Current study
Blacktip shark (*Carcharhinus limbatus*)	1	Indian Ocean coast, South Africa	7.847	4.4	3.1	3.0	10.4	Current study
Dusky shark (*Carcharhinus obscurus*)	5	Indian Ocean coast, South Africa	16.2±9.2	17.0±12.7	17.2+18.2	19.2±18.9	53.4±49.5	Current study
Smooth hammerhead shark (*Sphyrna zygaena*)	1	Indian Ocean coast, South Africa	2.011	2.8	2.2	1.8	6.8	Current study
African angel shark (*Squatina africana*)	1	Indian Ocean coast, South Africa	41.851	15.322	10.928	11.909	38.2	Current study
Java shark (*Carcharhinus amboinensis*)	1	Indian Ocean coast, South Africa	17.848	8.3	5.3	-	13.6	Current study
Bull shark (*Carcharhinus leucas*)	1	Indian Ocean coast, South Africa	6.114	9.7	7.2	4.5	21.4	Current study
Ragged tooth shark (*Carcharhias taurus*)	2	Indian Ocean coast, South Africa	5.9±0.43	9.4±0.36	6.6±0.59	7.2±1.4	23.2±2.4	Current study
Broadnose sevengill shark (*Notorynchus cepedianus*)	1	Atlantic Ocean coast, South Africa	3.18	3.0	3.6	7.2	13.8	Current study
Great white shark (*Carcharodon carcharias*)	7	Indian Ocean coast, South Africa	12.2+16.4	5.4±2.9	4.1±2.2	6.7±4.0	52.6	Current study

Table S3. Mean ± standard error and range (in parenthesis) of DDTs concentrations (ng/g lipid weight) in the muscle tissue samples of specified shark species.

Shark species	n	Location	p,p'-DDE	p,p'-DDD	p,p'-DDT	∑DDTs	Reference
Great **w**hite shark (*Carcharodon carcharias*)	2	Indian Ocean coast, South Africa	1802.9±339.2	-	18.2±3.2	1821.1±342.4	Beaudry *et al.,* 2015
Dusky shark (*Carcharhinus obscurus*)	2	Indian Ocean coast, South Africa	1114.3±302.7	-	35.8±17.1	1150.1±319.8	Beaudry *et al.,* 2015
Scalloped hammerhead (*Sphyrna lewini*)	2	Djibouti, Africa	-	-	857±18.5	857±18.5	Boldrocchi *et al.,* 2019
Scalloped hammerhead (*Sphyrna lewini*)	20	Gulf of california, Mexico	0.59±0.21	-	-	0.59±0.21	Briones *et al.,* 2022
Smooth hammerhead shark (*Sphyrna zygaena*)	3	Korean coast	-	-	-	8.38+12.8	Lee *et al.,* 2015
Starspotted smoothhound shark (*Mustelus manazo*)	2	Korean coast	-	-	-	1.59±+2.25	Lee *et al.,* 2015
Great **w**hite shark (*Carcharodon carcharias*)	3	South Africa (Durban)	15.9±2.5	51.1±13.1	17.5±7.7	126.6±53.8	Schlenk *et al.,* 2005
Great **w**hite shark (*Carcharodon carcharias*)	1	Australia (New South Wales)	-	-	-	1295.1	Cagnazzi *et al.,* 2019
Dusky shark (*Carcharhinus obscurus*)	1	Australia (New South Wales)	-	-	-	737.3	Cagnazzi *et al.,* 2019
Ragged tooth shark (*Carcharhinus taurus*)	1	Australia (New South Wales)				174.9	Cagnazzi *et al.,* 2019
Tiger shark (*Galeocerdo cuvier*)	21	Reunion Island, Indian Ocean	-	-	-	0.59±0.58	Chynel *et al.,* 2021
Bull shark (*Carcharhinus leucas*)	17	Reunion Island, Indian Ocean	-	-	-	0.58+0.65	Chynel *et al.,* 2021
Bull shark (*Carcharhinus leucas*)	2	Recife, Brazil	(2.16-3.63)	-	-	(2.16-3.63)	Afonso *et al.,* 2016
Bull shark (*Carcharhinus leucas*)	2	Australia (New South Wales)	-	-	-	483.9±39.5	Cagnazzi *et al.,* 2019

Table S3 (continued)

Great hammerhead shark (*Sphyrna mokarran*)	2	Australia (New South Wales)	-	-	-	195.2±66.5	Cagnazzi *et al.,* 2019
Blacktip shark (*Carcharhinus limbatus*)	9	Australia (New South Wales)	-	-	-	434.6+641.2	Cagnazzi *et al.,* 2019
Shortfin devil ray (*Mobula kuhlii*)	8	Australia (New South Wales)	-	-	-	452.5±232.7	Cagnazzi *et al.,* 2019
Australian cownose ray (*Rhinoptera neglecta*)	1	Australia (New South Wales)	-	-	-	262.4	Cagnazzi *et al.,* 2019
Shortfin devil ray (*Mobula kuhlii*)	2	Indian Ocean coast, South Africa	46.4±22.7	17.7±6.3	8.3±3.7	72.4±32.7	Current study
Longhorn devil ray (*Mobula eregoodootenkee*)	3	Indian Ocean coast, South Africa	232.5±211.6	31.4±28.2	12.3±11.0	92.1±83.6	Current study
Bull ray (*Aetomylaeus bovinus*)	5	Indian Ocean coast, South Africa	37.0±19.2	8.0±5.2	8.926	46.7±27.1	Current study
Oman cownose ray (*Rhinoptera jayakari*)	3	Indian Ocean coast, South Africa	265.5+407.1	66.6±91.2	42.1±54.0	360.2+543.6	Current study
Leopard catshark (*Poroderma pantherinum*)	3	Atlantic Ocean coast, South Africa	40.9±9.8	14.4±8.3	9.141	58.4±18.7	Current study
Spotted skate (*Raja straeleni*)	1	Atlantic Ocean coast, South Africa	24.0	10.8	2.7	37.5	Current study
Puffadder shyshark (*Haploblepharus edwardsii*)	1	Atlantic Ocean coast, South Africa	81.8	39.6	19.8	141.2	Current study
Brown shyshark (*Haploblepharus fuscus*)	2	Atlantic Ocean coast, South Africa	23.0±4.8	11.4±3.6	7.438	38.2±2.3	Current study

Table S3. (continued)

Dark shyshark (*Haploblepharus pictus*)	1	Atlantic Ocean coast, South Africa	38.3	17.8	12.9	68.9	Current study
Smoothhound shark (*Mustelus mustelus*)	5	Atlantic Ocean coast, South Africa	672.3+1219.8	45.6+74.2	6.4±3.3	721.7±1297.1	Current study
Tiger shark (*Galeocerdo cuvier*)	3	Indian Ocean coast, South Africa	122.5+124.9	11.9±5.1	6.3±4.2	138.6±120.8	Current study
Scalloped hammerhead shark (*Sphyrna lewini*)	6	Indian Ocean coast, South Africa	235.2±159.0	24.8±10.4	11.2±3.8	269.3±167.0	Current study
Spinner shark (*Carcharhinus brevipinna*)	4	Indian Ocean coast, South Africa	107.3±52.6	12.6±3.1	6.1±1.5	125.9±56.9	Current study
Blacktip shark (*Carcharhinus limbatus*)	1	Indian Ocean coast, South Africa	35.4	10.1	5.4	50.9	Current study
Dusky shark (*Carcharhinus obscurus*)	5	Indian Ocean coast, South Africa	705.8±690.5	51.0±46.3	21.6±13.9	774.0±749.4	Current study
Smooth hammerhead shark (*Sphyrna zygaena*)	1	Indian Ocean coast, South Africa	52.0	7.3	2.4	61.7	Current study
African angel shark (*Squatina africana*)	1	Indian Ocean coast, South Africa	242.0	46.3	20.4	308.8	Current study
Java shark (*Carcharhinus amboinensis*)	1	Indian Ocean coast, South Africa	58.4	34.4	9.7	102.5	Current study
Bull shark (*Carcharhinus leucas*)	1	Indian Ocean coast, South Africa	82.4	14.1	7.3	103.8	Current study
Ragged tooth shark (*Carcharias taurus*)	2	Indian Ocean coast, South Africa	218.5+221.5	21.3±10.9	10.4±4.6	250.2±237.0	Current study
Broadnose sevengill shark (*Notorynchus cepedianus*)	1	Atlantic Ocean coast, South Africa	506.8	-	-	506.8	Current study
Great white shark (*Carcharodon carcharias*)	7	Indian Ocean coast, South Africa	840.6±645.6	62.4±30.0	10.4±10.1	898.6±682.9	Current study

Table S4. Organochlorine compounds analysed for in elasmobranch muscle tissue.

	Detected	Not detected
HCB	x	
p,p'-DDD	x	
p,p'-DDE	x	
p,p'-DDT	x	
o,p'-DDD		x
o,p'-DDE		x
o,p'-DDT		x
Aldrin		x
Dieldrin		x
Endrin		x
α-HCH		x
β-HCH		x
δ-HCH		x
γ-HCH		x
Cis-Chlordane	x	
Cis-Nonachlor	x	
Oxy-Chlordane		x
Trans-Chlordane	x	
Trans-Nonachlor	x	
Heptachlor		x
Heptachlor-endo-epoxide		x
Heptachlor-exo-epoxide		x

Table S5. Lipid content percentages of the elasmobranchs sampled in this study.

	Male (%)	Female (%)
Shortfin devil ray (*Mobula kuhlii*)	0.08	0.21
Longhorn devil ray (*Mobula eregoodootenkee*)	0.13	0.18
Bull ray (*Aetomylaeus bovinus*)	0.09	0.22
Oman cownose ray (*Rhinoptera jayakari*)	0.12	-
Leopard catshark (*Poroderma pantherinum*)	0.08	0.08
Spotted skate (*Raja straeleni*)	0.21	-
Puffadder shyshark (*Haploblepharus edwardsii*)	0.04	-
Brown shyshark (*Haploblepharus fuscus*)	0.12	0.13
Dark shyshark (*Haploblepharus pictus*)	0.06	-
Smoothhound shark (*Mustelus mustelus*)	0.24	0.2
Tiger shark (*Galeocerdo cuvier*)	-	0.17
Scalloped hammerhead shark (*Sphyrna lewini*)	0.12	-
Spinner shark (*Carcharhinus brevipinna*)	0.15	0.19
Blacktip shark (*Carcharhinus limbatus*)	0.17	-
Dusky shark (*Carcharhinus obscurus*)	0.16	0.05
Smooth hammerhead shark (*Sphyrna zygaena*)	0.35	-
African angel shark (*Squatina africana*)	0.05	-
Java shark (*Carcharhinus amboinensis*)	-	0.15
Bull shark (*Carcharhinus leucas*)	-	0.11
Ragged tooth shark (*Carcharias taurus*)	-	0.1
Broadnose sevengill shark (*Notorynchus cepedianus*)	-	0.38
Great white shark (*Carcharodon carcharias*)	0.28	0.1

Table S6. Mean ± standard error of mercury (Hg) and selenium (Se) concentrations (mg/kg wet weight) in the muscle tissue samples of specified shark species.

Common name (species)	**n**	**Location**	**Mercury**	**Selenium**	**Reference**
Shortfin devil ray (*Mobula kuhlii*)	2	Indian Ocean coast, South Africa	0.05±0.001	0.18±0.15	Current study
Longhorn devil ray (*Mobula eregoodootenkee*)	3	Indian Ocean coast, South Africa	0.09±0.02	0.23±0.09	Current study
Bull ray (*Aetomylaeus bovinus*)	5	Indian Ocean coast, South Africa	0.26±0.14	0.55±0.2	Current study
Oman cownose ray (*Rhinoptera jayakari*)	3	Indian Ocean coast, South Africa	0.22±0.13	0.6±0.52	Current study
Leopard catshark (*Poroderma pantherinum*)	3	Atlantic Ocean coast, South Africa	0.26±0.14	0.24±0.07	Current study
Spotted skate (*Raja straeleni*)	1	Atlantic Ocean coast, South Africa	0.13	0.37	Current study
Puffadder shyshark (*Haploblepharus edwardsii*)	1	Atlantic Ocean coast, South Africa	0.19	0.27	Current study
Brown Shyshark (*Haploblepharus fuscus*)	2	Atlantic Ocean coast, South Africa	0.22+0.22	0.25+0.29	Current study
Dark shyshark (*Haploblepharus pictus*)	1	Atlantic Ocean coast, South Africa	0.07	0.21	Current study
Smoothhound shark (*Mustelus mustelus*)	4	Atlantic Ocean coast, South Africa	0.21±0.03	0.34±0.1	Current study
Tiger shark (*Galeocerdo cuvier*)	3	Indian Ocean coast, South Africa	0.98±0.27	0.2±0.17	Current study
Scalloped hammerhead shark (*Sphyrna lewini*)	6	Indian Ocean coast, South Africa	4.0±1.56	0.52±0.07	Current study
Spinner shark (*Carcharhinus brevipinna*)	4	Indian Ocean coast, South Africa	0.67±0.34	0.29±0.08	Current study
Blacktip shark (*Carcharhinus limbatus*)	1	Indian Ocean coast, South Africa	0.39	0.85	Current study
Dusky shark (*Carcharhinus obscurus*)	5	Indian Ocean coast, South Africa	0.55±0.33	0.38±0.29	Current study
Smooth hammerhead shark (*Sphyrna zygaena*)	1	Indian Ocean coast, South Africa	0.59	0.47	Current study

Table S6. (continued)

African angel shark (*Squatina africana*)	1	Indian Ocean coast, South Africa	0.49	0.24	Current study
Java shark (*Carcharhinus amboinensis*)	1	Indian Ocean coast, South Africa	1.1	0.51	Current study
Bull shark (*Carcharhinus leucas*)	1	Indian Ocean coast, South Africa	3.2	0.57	Current study
Ragged tooth shark (*Carcharias taurus*)	1	Indian Ocean coast, South Africa	2.6	0.22	Current study
Broadnose sevengill shark (*Notorynchus cepedianus*)	1	Atlantic Ocean coast, South Africa	1.1	0.14	Current study
Great white shark (*Carcharodon carcharias*)	7	Indian Ocean coast, South Africa	0.57±0.17	0.72±0.17	Current study

Table S7. Mean ± standard error of mercury (Hg) and selenium (Se) concentrations (mg/kg wet weight) in the muscle tissue samples of specified shark species.

Common name (species)	**n**	**Location**	**Mercury**	**Selenium**	**Reference**
Shortfin devil ray (*Mobula kuhlii*)	9	Pacific Ocean coast, Australia	(0.04-1.58)	-	Cagnazzi *et al.,* 2019
Longhorn devil ray (*Mobula eregoodootenkee*)	9	Pacific Ocean coast, Australia	(0.04-1.58)	-	Cagnazzi *et al.,* 2019
Thornback ray (*Raja clavata*)	41	Mediterranean Sea, Italy	0.65±0.02	0.6±.02	Storelli *et al.,* 2022
Brown ray (*Raja miraletus*)	45	Mediterranean Sea, Italy	0.64±0.02	0.5±0.03	Storelli *et al.,* 2022
Sandy ray (*Leucoraja circularis*)	48	Mediterranean Sea, Italy	0.58±0.03	0.43±0.03	Storelli *et al.,* 2022
Bull ray (*Aetomylaeus bovinus*)	1	Eastern Mediterranean	2.7	0.8	Giovos *et al.,* 2022
Picked dogfish (*Squalus acanthias*)	38	Mediterranean Sea, Italy	1.03±0.02	0.49±0.03	Storelli *et al.,* 2022
Starry smoothhound shark (*Mustelus asterias*)	30	Mediterranean Sea, Italy	0.73±0.03	0.39±0.02	Storelli *et al.,* 2022
Smoothhound shark (*Mustelus mustelus*)	12	Atlantic Ocean coast, South Africa	1.1±0.2	-	Bosch *et al.,* 2013
Smoothhound shark (*Mustelus mustelus*)	30	Atlantic Ocean coast, South Africa	0.96±0.69	0.7±0.44	Bosch *et al.* 2016
Smoothhound shark (*Mustelus mustelus*)	9	Atlantic Ocean coast, South Africa	0.03	-	Zaera and Johnsen, 2011
Smoothhound shark (*Mustelus mustelus*)	32	Mediterranean Sea	1.0±0.02	0.49±0.03	Storelli *et al.,* 2022
Smoothhound shark (*Mustelus mustelus*)	18	Eastern Mediterranean Sea	0.39±0.37	-	Kousteni *et al.,* 2016
Smoothhound shark (*Mustelus mustelus*)	1	Eastern Adriatic Sea	0.003	0.003	Grgec *et al.* 2020
Brown smoothhound shark (*Mustelus henlei*)	6	Gulf of California, Mexico	0.18±0.1	-	Garcia-Hernandez *et al.,* 2007
Brown smoothhound shark (*Mustelus henlei*)	83	Mexican Pacific	0.02±0.02	0.2±0.1	Pantoja-Echevarría *et al.* 2021
Brown smoothhound shark (*Mustelus henlei*)	22	Northern Mexican Pacific	0.12+0.15	0.02±0.01	Medina-Morales *et al.,* 2020
Tiger shark (*Galeocerdo cuvier*)	41	Pacific Ocean coast, Japan	0.77±0.25	-	Endo *et al.* 2008
Tiger shark (*Galeocerdo cuvier*)	112	Pacific Ocean coast, Japan	0.86±0.34	-	Endo *et al.* 2015
Tiger shark (*Galeocerdo cuvier*)	8	Gulf of Mexico, USA	0.37±0.3	-	Rumbold *et al.* 2014
Tiger shark (*Galeocerdo cuvier*)	18	Indian Ocean coast, South Africa	1.0±0.11	-	McKinney *et al.* 2016
Tiger shark (*Galeocerdo cuvier*)	20	Indian Ocean coast, La Réunion Island	0.76±0.3	-	Le Croizier *et al.* 2020
Tiger shark (*Galeocerdo cuvier*)	7	The Bahamas	1.1±0.39	-	Shipley *et al.,* 2021

Table S7. (continued)

Scalloped hammerhead shark (*Sphyrna lewini*)	22	Gulf of California, Mexico	1.1±0.95	-	García-Hernández *et al.* 2007
Scalloped hammerhead shark (*Sphyrna lewini*)	34	Indian Ocean coast, South Africa	2.7±0.4	-	McKinney *et al.* 2016
Scalloped hammerhead shark (*Sphyrna lewini*)	6	Indian Ocean coast, Madagascar	1.4±0.66	-	Kiszka *et al.* 2015
Scalloped hammerhead shark (*Sphyrna lewini*)	44	Indian Ocean coast, Madagascar	0.66±0.48	-	Le Bourg *et al.* 2019
Scalloped hammerhead shark (*Sphyrna lewini*)	12	Gulf of California, Mexico	0.82±0.33	-	Hurtado-Banda *et al.* 2012
Scalloped hammerhead shark (*Sphyrna lewini*)	20	Pacific Ocean coast, Colombia	0.81±0.73	-	Vélez *et al.* 2021
Scalloped hammerhead shark (*Sphyrna lewini*)	40	Gulf of California, Mexico	0.63±0.04	1.2±0.1	Bergés-Tiznado *et al.* 2015
Scalloped hammerhead shark (*Sphyrna lewini*)	116	Pacific Ocean coast, Mexico	0.37±0.36	0.32±0.22	Ruelas-Inzunza *et al.* 2020
Scalloped hammerhead shark (*Sphyrna lewini*)	10	Caribbean Sea, Trinidad and Tobago	1.0±0.89	-	Mohammed and Mahammed, 2017
Scalloped hammerhead shark (*Sphyrna lewini*)	13	Global FAO regions	1.09±0.66	0.86±0.38	Amezcua *et al.* 2022
Hammerhead shark (*Sphyrna spp.*)	9	Atlantic Ocean, Brazil	0.234	0.501	Mirlean *et al.* 2019
Spinner shark (*Carcharhinus brevipinna*)	19	Indian Ocean coast, South Africa	0.56±0.1	-	McKinney *et al.* 2016
Blacktip shark (*Carcharhinus limbatus*)	16	Gulf of California, Mexico	0.51±0.31	-	García-Hernández *et al.* 2007
Blacktip shark (*Carcharhinus limbatus*)	5	Pacific Ocean coast, Canada	1.9±0.56	-	Forsyth *et al.* 2004
Blacktip shark (*Carcharhinus limbatus*)	23	Gulf of Mexico, USA	3.2±1.12	-	Matulik *et al.* 2017
Blacktip shark (*Carcharhinus limbatus*)	28	Gulf of Mexico, USA	2.7±0.9	-	Rumbold *et al.* 2014
Blacktip shark (*Carcharhinus limbatus*)	32	Indian Ocean coast, South Africa	2.2±0.23	-	McKinney *et al.* 2016
Blacktip shark (*Carcharhinus limbatus*)	7	Pacific Ocean coast, Australia	0.58±0.67	-	Cagnazzi *et al.* 2019
Dusky shark (*Carcharhinus obscurus*)	1	Gulf of California, Mexico	1.16	-	García-Hernández *et al.* 2007
Dusky shark (*Carcharhinus obscurus*)	64	Indian Ocean coast, South Africa	1.4±0.14	-	McKinney *et al.* 2016
Dusky shark (*Carcharhinus obscurus*)	12	Pacific Ocean coast, Australia	2.0±0.34	-	Gilbert *et al.* 2015

Table S7. (continued)

Smooth hammerhead shark (*Sphyrna zygaena*)	15	Indian Ocean coast, South Africa	0.54±0.04	-	McKinney *et al.* 2016
Smooth hammerhead shark (*Sphyrna zygaena*)	31	Pacific Ocean coast, Mexico	0.98±0.92	-	Maz-Courrau *et al.* 2012
Smooth hammerhead shark (*Sphyrna zygaena*)	4	Gulf of California, Mexico	8.3±9.1	-	García-Hernández *et al.* 2007
Smooth hammerhead shark (*Sphyrna zygaena*)	37	Pacific Ocean coast, Mexico	0.73±0.48	0.34±0.27	Escobar-Sánchez *et al.* 2010
Smooth hammerhead shark (*Sphyrna zygaena*)	18	Pacific Ocean coast, Mexico	0.13±0.04	0.09±0.06	Lara *et al.,* 2022
Smooth hammerhead shark (*Sphyrna zygaena*)	13	Peru	0.25	-	Gonzalez-Pestana *et al.,* 2017
Smooth hammerhead shark (*Sphyrna zygaena*)	5	Atlantic Ocean coast, Brazil	0.44±0.3	-	Márprevisico *et al.* 2007
Smooth hammerhead shark (*Sphyrna zygaena*)	16	Pacific Ocean coast, Mexico	0.13±0.04	-	Lara *et al.* 2022
Smooth hammerhead shark (*Sphyrna zygaena*)	48	Pacific Ocean coast, Mexico	4.3±1.4	-	Terrazas-López *et al.* 2019
Smooth hammerhead shark (*Sphyrna zygaena*)		Mediterranean Sea	12.2±4.6	0.78±0.0.09	Storelli *et al.,* 2003
Java shark (*Carcharhinus amboinensis*)	9	Indian Ocean coast, South Africa	1.9±0.25	-	McKinney *et al.* 2016
Bull shark (*Carcharhinus leucas*)	11	Indian Ocean coast, South Africa	1.2±0.11	-	McKinney *et al.* 2016
Bull shark (*Carcharhinus leucas*)	1	Pacific Ocean coast, Mexico	0.62	-	Ruelas-Inzunza *et al.* 2011
Bull shark (*Carcharhinus leucas*)	7	Gulf of Mexico, USA	4.0±1.3	-	Matulik *et al.* 2017
Bull shark (*Carcharhinus leucas*)	7	Gulf of Mexico, USA	1.5±1.2	-	Rumbold *et al.* 2014
Bull shark (*Carcharhinus leucas*)	11	Indian Ocean coast, Madagascar	0.52±0.35	-	Le Bourg *et al.* 2019
Bull shark (*Carcharhinus leucas*)	20	Indian Ocean coast, La Réunion Island	1.0±0.74	-	Le Croizier *et al.* 2020
Bull shark (*Carcharhinus leucas*)	2	Pacific Ocean coast, Australia	4.0	-	Cagnazzi *et al.* 2019
Bull shark (*Carcharhinus leucas*)	1	The Bahamas	1.6	-	Shipley *et al.,* 2021
Ragged tooth shark (*Carcharias taurus*)	30	Indian Ocean coast, South Africa	3.1±0.26	-	McKinney *et al.* 2016
Ragged tooth shark (*Carcharias taurus*)	1	Pacific Ocean coast, Australia	0.87	-	Cagnazzi *et al.* 2019
Broadnose sevengill shark (*Notorynchus cepedianus*)	1	Pacific Ocean coast, USA	0.48	-	Suk *et al.* 2009
Broadnose sevengill shark (*Notorynchus cepedianus*)	2	Tasman Sea, Australia	1.4±0.21	-	Pethybridge *et al.* 2010
Great white shark (*Carcharodon carcharias*)	33	Indian Ocean coast, South Africa	2.5±0.17	-	McKinney *et al.* 2016
Great white shark (*Carcharodon carcharias*)	30	Pacific Ocean coast, USA	1.2±0.2	-	Lyons *et al.* 2013
Great white shark (*Carcharodon carcharias*)	20	Southern California	2.8-3.3	-	Mull *et al.,* 2012

Table S8. Selenium health benefit from international literature.

Common name (species)	**n**	**Location**	**HBV_{Se}**	**Reference**
Scalloped hammerhead shark (*Sphyrna lewini*)	116	Pacific Ocean coast, Mexico	1.48	Ruelas-Inzunza *et al.,* 2020
Smoothhound shark (*Mustelus mustelus*)	1	Eastern Adriatic Sea	8.11	Grgec *et al.,* 2020
Hammerhead shark (*Sphyrna spp.*)	9	Atlantic Ocean, Brazil	6.1	Mirlean *et al.,* 2019
Shortfin mako shark (*Ishurus oxyrinchus*)	9	Atlantic Ocean, Brazil	4.6	Mirlean *et al.,* 2019
Smoothhound shark (*Mustelus mustelus*)	32	Mediterranean Sea	1.96	Storelli *et al.,* 2022
Sharks from different FAO regions	65	Global	3.06±13.84	Amecuza *et al.,* 2022
Birdbeak dogfish (*Deania calcea*)	2	North-East Atlantic	-14.56	Teixeira *et al.,* 2020
Shortfin mako shark (*Ishurus oxyrinchus*)	10	Central North Pacific	-16.4	Ralston *et al.,* 2016
Brown smoothhound shark (*Mustelus henlei*)	22	Northern Mexican Pacific	0.08	Medina-Morales *et al.,* 2020